



Universiteit  
Leiden

The Netherlands

## **Influence of central neuraxial blockade on anesthetic pharmacology and brain function**

Sitsen, M.E.

### **Citation**

Sitsen, M. E. (2023, January 10). *Influence of central neuraxial blockade on anesthetic pharmacology and brain function*. Retrieved from <https://hdl.handle.net/1887/3505777>

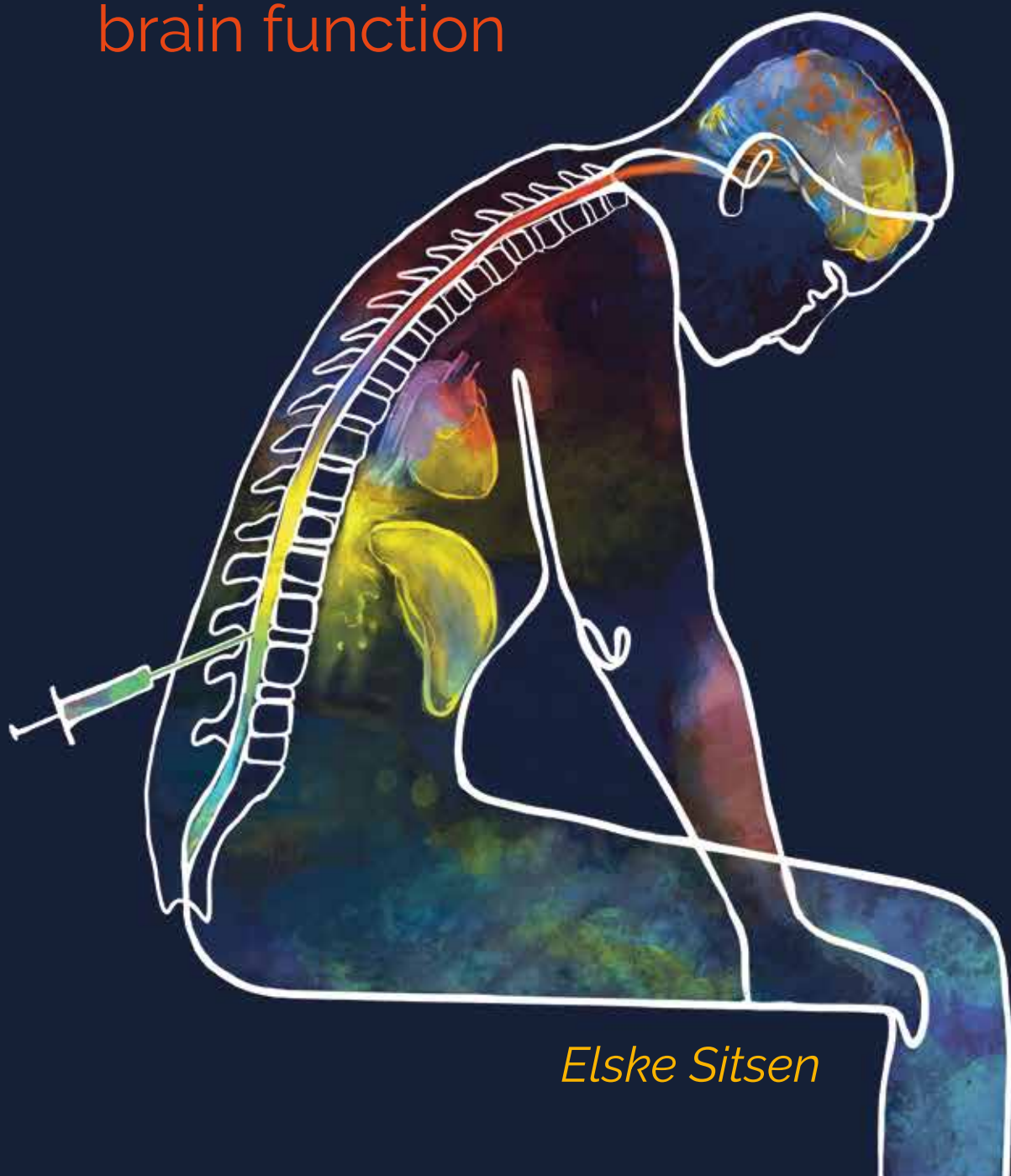
Version: Publisher's Version

License: [Licence agreement concerning inclusion of doctoral thesis in the Institutional Repository of the University of Leiden](#)

Downloaded from: <https://hdl.handle.net/1887/3505777>

**Note:** To cite this publication please use the final published version (if applicable).

# Influence of Central Neuraxial blockade on anesthetic pharmacology and brain function



*Elske Sitsen*

# Influence of Central Neuraxial blockade on anesthetic pharmacology and brain function

Marianne Elisabeth Sitsen

©M.E. Sitsen, Voorschoten, the Netherlands

*Printing of this thesis was financially supported by:*

*Pajunk Medical Produkte GmbH*

*B. Braun Medical BV*

*Cover design: Sieben Medical Art; [www.annasieben.com](http://www.annasieben.com)*

*Printed by Puntgaaf drukwerk, Leiden, the Netherlands*

*ISBN: 9789090368269*

# PROEFSCHRIFT

*ter verkrijging van  
de graad van Doctor aan de Universiteit Leiden,  
op gezag van Rector Magnificus prof.dr.ir. H. Bijl  
volgens besluit van het College voor Promoties  
te verdedigen op 10 januari 2023  
klokke 15:00*

*door*

*Elske Sitsen*

*geboren te Harderwijk*

*Promotor: prof. dr. A. Dahan*  
*Copromotor: dr J. Vuijk*  
*dr. M. Niesters*  
*Leden promotiecommissie: prof. dr. E.Y. Sarton*  
*prof. dr. L. Aarts*  
*prof. dr. R.J. Stolker*  
*prof. dr. M.J.P. van Osch*  
*prof. dr. L. Reneman*  
*prof. dr. G.G. Groeneveld*  
*dr. M. van Velzen*

# Table of contents

Chapter 1	Introduction	7
<b>PART 1</b>	<b><i>Pharmacology of epidural analgesia</i></b>	
Chapter 2	Chapter 2 Postoperative epidural analgesia after total knee arthroplasty with sufentanil 1 mcg/mL combined with ropivacaine 0.2%, ropivacaine 0.125%, or levobupivacaine 0.125%: a randomized, double-blind comparison	15
Chapter 3	Epidural blockade affects the pharmacokinetics of propofol in surgical patients	25
Chapter 4	No interactive effect of lumbar epidural blockade and target-controlled infusion of propofol on mean arterial pressure, cardiac output and bispectral index; <i>A randomised controlled and pharmacodynamic modelling study</i>	49
<b>PART 2</b>	<b><i>Spinal anesthesia, pain perception and functional magnetic resonance imaging (fMRI) of the brain</i></b>	
Chapter 5	Spinal anesthesia-induced deafferentation; resting-state functional brain connectivity and pain perception	67
Chapter 6	Hyperalgesia and reduced offset analgesia during spinal anesthesia	85
Chapter 7	Effect of spinal anesthesia-induced deafferentation on pain processing in healthy male volunteers: a task-related fMRI study	97
<b>PART 3</b>	<b><i>Synthesis</i></b>	
Chapter 8	Summary, conclusions and future perspectives	131
Chapter 9	Nederlandse samenvatting en conclusies	139
Addenda		147
	Curriculum vitae	148
	List of publications	149
	Abbreviations	151





# *Chapter 1*

## **Introduction**

## Introduction

Central neuraxial blockade is the injection of local anesthetics (with or without an opioid) around the nerves that exit the spinal cord. In modern clinical practice, neuraxial blockade is an essential part of the armamentarium of the anesthesiologist in providing safe and effective anesthesia. There are several techniques for neuraxial blockade including spinal injection of local anesthetics into the intrathecal space, epidural injection into the (lumbar or thoracic) epidural space, combined spinal-epidural and caudal injections, and finally continuous or patient-controlled epidural administration of local anesthetics. All techniques are applicable in different clinical settings.

The principle of central neuraxial blockade was first described by James Leonard Corning (1855–1923). In 1884, he injected cocaine between the spinous processes of the lower lumbar vertebrae, in a dog and later in a healthy human volunteer.<sup>1</sup> The surgeon August Bier performed the first surgery under spinal anesthesia in 1899.<sup>2</sup> In 1921, Spanish military surgeon Fidel Pagés (1886–1923) developed the modern technique of lumbar epidural anesthesia.<sup>3</sup> No publicity was given to this revolutionary anesthetic technique at that time. Dogliotti first utilized the epidural technique in 1931.<sup>4</sup> He advocated its use and wrote a book, which was later translated into English. The first lumbar continuous anesthesia was performed by Manuel Martinez Curbelo in 1947.<sup>5</sup> Since these early years, techniques have been developed further and new anesthetics have been registered for use in neuraxial anesthesia and analgesia.

The discovery of local anesthetics goes back to the Middle Ages, Calatayud et al. did a thorough search of the first use of coca leaves and the first documentation of its anesthetic and adverse effects.<sup>6</sup> They discovered that the isolation of cocaine out of coca leaves was a joint venture of Austrian naturalist Carl von Scherzer (1821-1903) and German chemist Albert Niemann (1834-1861).<sup>7,8</sup> From here steps were taken to apply it as a local anesthetic. Niemann reported numbness of the tongue caused by this new alkaloid, cocaine.<sup>7</sup> In the mid and late 19<sup>th</sup> century, the first experimental studies on cocaine were published. They described injection of cocaine solutions causing insensitivity in rats, pigeons and frogs. Basil von Anrep, a Russian aristocrat, performed experiments on animals and experimented on himself. A solution of cocaine injected under the skin resulted in insensitivity of the area.<sup>9</sup> It was the Viennese ophthalmologist Carl Koller (1857-1944), who experimented with cocaine solutions for surgery first on animals and performed the first operation using this local anesthetic on a patient with glaucoma.<sup>10</sup> The news and use as an anesthetic for surgery spread quickly, the increase in usage coincided with its alarming side effects, one of them was abuse and addiction to cocaine. This and other side effects resulted in an ongoing search for new local anesthetic drugs. In 1905 novocaine, invented by Alfred Einhorn, was the first to replace cocaine as a local anesthetic.<sup>11</sup> The urge to search for better and safer local anesthetics maintained and led to the development and clinical introduction in 1948 of lidocaine by Nils Löfgren and Bengt Lundquist.<sup>12</sup> The first amide-type local anesthetics, mepivacaine and bupivacaine, were

developed by Ekenstam et al.<sup>13</sup> Bupivacaine, on the market since 1965, is still one of the most intensively used local anesthetics despite the presence of neurological and cardiovascular toxicity at high dose. Several experiments were carried out to determine the cause of toxicity and to improve our understanding of how local anesthetics work. As a result, two amide local anesthetics, ropivacaine and levobupivacaine were developed with less cardiotoxicity compared to bupivacaine. The clinical use and pharmacology of these long acting local anesthetics since their introduction in late 20<sup>th</sup> century is one of the topics in this thesis.

Today, central neuraxial blockade is one of the most used stand-alone anesthesia techniques or is combined with general anesthesia to reduce opioid consumption during surgery and can provide effective postoperative pain relief. Additionally, the epidural analgesia has been widely accepted as an effective method of pain relief during labor and childbirth. Although the use of local anesthetics and central neuraxial blockade is widely studied, several issues remain still unknown, such as:

(1) What is the effect of the (transient) state of deafferentation induced by the neuraxial blockade on pain perception of the non-deafferented part of the body? Deafferentation is the disruption of afferent and efferent signals between the central and peripheral nervous system and occurs albeit transiently during neuraxial blockade. When peripheral input to supra-spinal areas of the central nervous system (CNS) is lost, various changes occur within the brain including behavioral changes. For example, patients experience illusionary changes of the affected limbs during spinal and epidural anesthesia. Another observation is an improvement of function of contralateral or adherent limbs during temporary deafferentation. Also pain perception may change.<sup>14,15</sup> How this relates to changes within brain networks remains unknown but may be studied using functional magnetic resonance imaging (*fMRI*). Generally, there are two approaches, task-based *fMRI* and resting state *fMRI* (*RS-fMRI*). Task-based *fMRI* is frequently utilized to identify brain regions that are functionally involved in a given task performance. *RS-fMRI* is used to investigate the fundamentally functional segregation or specialization of brain areas and brain networks. Different resting state networks have been discovered by studying functional brain connectivity in the state of rest, each of which depicts unique functions and spatia. This relative new technique is noninvasive and easy to perform and needs no cooperation of patient or subject.

(2) Epidural (and spinal) anesthesia is often combined with general anesthesia. How these two anesthetic states interact on various endpoints is poorly studied. We know, for example, that the state of deafferentation from neuro-axial blockade affects the level of hypnosis induced by general anesthetics. Importantly, these two states negatively affect hemodynamics either through pharmacokinetic or pharmacodynamic interactions, or both. Such issues are best addressed by performing pharmacokinetic-pharmacodynamic modeling studies.

(3) Finally, although various local anesthetics are available, we remain uninformed on their efficacy in terms of anesthesia, analgesia and adverse effects. Three long acting local anesthetics are currently available for use in epidural anesthesia. Long acting local anesthetics, bupivacaine, ropivacaine and levobupivacaine differ in potency, efficacy and central nervous system (CNS) and cardiovascular (CV) toxicity. The difference in toxicity of these long acting local anesthetics implies a possible preferred application in anesthetic practice. Comparisons, particularly when these local anesthetics are combined with an opioid in general practice are needed.

The aim of this thesis was to address these issues by gaining more insight in the pharmacodynamics and pharmacokinetics of central neuraxial blockade and to explore the effect of spinal anesthesia on brain networks and pain perception using fMRI.

In Chapter 2, the efficacy of epidural postoperative analgesia using levobupivacaine and ropivacaine was evaluated in postoperative patients in a randomized and double-blind study. The anesthetics were evaluated at two concentrations in combination with the opioid sufentanil.

In Chapter 3, the effect of epidural analgesia with ropivacaine on the pharmacokinetics of propofol was studied in a double-blind, placebo-controlled study. The data were analyzed using a population pharmacokinetic modeling approach in NONMEM.

In Chapter 4, we examined the effect of epidural analgesia with ropivacaine during propofol sedation on cardiac output, mean arterial pressure and bispectral index. The data were analyzed using a population pharmacodynamic modeling approach in NONMEM. The goal of both chapters was to identify whether possible interaction between neuraxial blockade and general anesthesia are pharmacokinetic or pharmacodynamic in nature or have components from both.

In Chapter 5, we examined whether spinal anesthesia changes pain perception in non-deafferented skin areas. Pain sensitivity and offset analgesia (a form of endogenous pain modulation) were tested in healthy volunteers at dermatomes above the level of deafferentation during spinal versus sham anesthesia.

In Chapter 6, the influence of spinal anesthesia on resting state fMRI brain networks was tested in healthy volunteers using 10 predefined networks, generally accepted and pain sensitivity on non-deafferented body parts were evaluated. In Chapter 7, to further identify the effect of deafferentation on pain areas in the brain, we explored the effect of spinal anesthesia on brain functionality using (pain) task-related functional magnetic resonance imaging.

## Reference list

1. Corning J. Spinal anesthesia and local medication of the cord. *New York Medical Journal*, 1885(42): p. 483-485.
2. Bier A. Versuche über Cocainisierung des Rückenmarkes. *Deutsche Zeitschrift für Chirurgie*, 1889. 51(3-4): p. 361-9.
3. Pages F. Anestesia metamérica. *Rec de la sanidad militar*, 1921. 11: p. 351-65.
4. Dogliotti A.M. Segmental peridural spinal anesthesia: A new method of block anesthesia. *The American Journal of Surgery*, 1933. 20(1): p. 107-118.
5. Martinez Curbelo M. Continuous peridural segmental anesthesia by means of a ureteral catheter. *Curr Res Anesth Alg*, 1949. 28(1): p. 13-23.
6. Calatayud, J and Gonzalez A. History of the development and evolution of local anesthesia since the coca leaf. *Anesthesiology*, 2003. 98(6): p. 1503-8.
7. Niemann A. Ueber eine neue organische Base en den Cocablättern. *Arch Pharm*, 1860. 153: p. 129-55, 291-308.
8. Buhler A. Erforschung des Kokagenusses. *Ciba Z*, 1944(8): p. 3353-9.
9. von Anrep B. Ueber die physiologische Wirkung des Cocain. *E Pfluger Arch Ges Physiol*, 1880. 21: p. 38-77.
10. Fink BR. Leaves and needles: the introduction of surgical local anesthesia. *Anesthesiology*, 1985. 63(1): p. 77-83.
11. Link WJ, Alfred Einhorn, SD. Inventor of novocaine. *Dent Radiog Photog*, 1959(32): p. 1-20.
12. Löfgren N. Studies on local anesthetics. *Svensks Kem Tidskr*, 1946(58): p. 206-17.
13. Ekenstam B, Pettersson G. Local anesthetics: I. N-alkyl pyrrolidine and N-alkyl piperidine carboxylic acid amides. *Acta Chem Scand*, 1957(11): p. 1183-90.
14. Bjorkman A, Rosen B, and Lundborg G. Enhanced function in nerve-injured hands after contralateral deafferentation. *Neuroreport*, 2005. 16(5): p. 517-9.
15. Werhahn KJ. Cortical excitability changes induced by deafferentation of the contralateral hemisphere. *Brain*, 2002. 125(Pt 6): p. 1402-13.



Part 1

# Pharmacology of epidural analgesia





## *Chapter 2*

# **Postoperative epidural analgesia after total knee arthroplasty with sufentanil 1 mcg/mL combined with ropivacaine 0.2%, ropivacaine 0.125%, or levobupivacaine 0.125%: a randomized, double-blind comparison**

Elske Sitsen, M.D., Frans van Poorten, M.D., Wim van Alphen, M.D.,  
Lili Rose, M.D., Albert Dahan, M.D., Ph.D., and Rudolf Stienstra, M.D., Ph.D.

*Regional Anesthesia and Pain Medicine, Vol 32, No 6 (November - December),  
2007: pp 475 - 480*

## Introduction

Patient-controlled epidural analgesia (PCEA) is used to provide postoperative analgesia for painful orthopedic procedures. Its benefits are avoidance of overdose, involvement of the patient in his/her own analgesic regimen, and reduction of the waiting time and “peaks and valleys” compared with physician-administered analgesics.<sup>1</sup> Several different amide-type local anesthetics are currently available to provide satisfactory postoperative analgesia via the epidural route. Racemic bupivacaine has traditionally been the most widely used local anesthetic for this purpose.<sup>2,3</sup> Ropivacaine is now frequently used as an alternative to bupivacaine. It is structurally closely related to bupivacaine and is supplied as the pure S-enantiomer.

It possesses a more favorable toxicity profile than bupivacaine, with higher thresholds for cardiotoxicity and central nervous system toxicity.<sup>4,5</sup> Additionally, ropivacaine tends to produce less motor blockade<sup>6,7</sup> which is a benefit during postoperative recovery. Levobupivacaine is the pure S-enantiomer of bupivacaine and was recently introduced into clinical practice. Preclinical studies demonstrated that both enantiomers of bupivacaine exhibit anesthetic activity, but the S-enantiomer is associated with less toxicity.<sup>8,9</sup> Levobupivacaine has been compared with ropivacaine and bupivacaine in epidural analgesia, but only in the perioperative and direct postoperative phase, where they produced adequate pain relief after major orthopedic surgery, with similar preservation of motor function.<sup>10</sup> In parturient epidural studies designed to compare the minimal effective local anesthetic concentration (MLAC), ropivacaine was determined to be 40% less potent than racemic bupivacaine.<sup>11,12</sup> However, controversy exists as to whether this potency difference may be extrapolated to the high end of the dose-response curve. The aim of this study is to compare the efficacy of levobupivacaine and ropivacaine in combination with sufentanil in prolonged postoperative patient-controlled epidural analgesia. The null hypothesis is the absence of a potency difference between levobupivacaine and ropivacaine at the high end of the dose response curve. An alternative hypothesis is a potency difference in favor of levobupivacaine. To explore the possible 40% potency difference suggested by previous authors, 3 different mixtures were compared: levobupivacaine 0.125%/sufentanil 1 µg/mL, ropivacaine 0.2%/sufentanil 1 µg/mL, and ropivacaine 0.125%/sufentanil 1 µg/mL.

## Methods

The study was approved by the Medical Ethics Committees of the Leiden University Medical Center and the Reiner de Graaf Hospital, Delft, The Netherlands, and written informed consent was obtained from all patients. The study design was a multicenter randomized prospective double-blind comparison of ropivacaine 0.2% (group 1), ropivacaine 0.125% (group 2) and levobupivacaine 0.125% (group 3), all in combination with sufentanil 1 µg/mL.

Sixty-three patients, ASA (American Society of Anesthesiologists) Classification I to III, aged over 18 years, scheduled for total knee replacement under combined spinal-epidural anesthesia

were studied. Exclusion criteria were known hypersensitivity to amide-type local anesthetics, known hypersensitivity to opioids, known history of severe cardiovascular, renal, hepatic, neurological or psychiatric disease as judged by the investigator, known history of peripheral neuropathies, those receiving chronic analgesic therapy, any contraindication for epidural analgesia (e.g., clotting disorders, history of lumbar surgery), inability to perform a pain score, and pregnancy or lactation. After instituting routine ASA monitoring and intravenous access, the patient was placed in the sitting position and a 17-gauge epidural needle (Becton & Dickinson, Drogheda, Ireland) was introduced into the epidural space via the third lumbar interspace using the loss of resistance to saline technique. The third lumbar interspace was identified as the interspace superior to Tuffier's line (the line connecting the superior borders of the left and right crista iliaca). After identifying the epidural space, a 27-gauge Whitacre spinal needle (Becton & Dickinson) was introduced into the subarachnoid space through the epidural needle and a subarachnoid dose of 10 mg plain bupivacaine (Marcaine® 0.5% spinal [bupivacaine 20 mg/4 mL] AstraZeneca, Zoetermeer, The Netherlands) was administered. The spinal needle was then removed and an epidural catheter inserted 5 cm into the epidural space through the epidural needle. After removal of the epidural needle, the patient was placed supine. Sensory block (loss of sensation to temperature) was assessed in the anterior axillary line at 5 minute intervals using a bottle containing a frozen salt solution until the maximum level of sensory block (MLSB) had been established. MLSB was defined as no further increase during 3 consecutive measurements and >20 minutes after subarachnoid injection. Motor blockade of the lower limbs was scored on a 12 point scale, where each joint of the lower limbs (hip, knee, ankle) was scored from 0 to 2 (0, no motor block; 1, partial motor block; 2, complete motor block). Partial motor block was defined as the possibility to move the joint, but not sustainable against manual counter pressure. Motor block scores (MBS) were evaluated at 5-minute intervals until maximum motor block had been established or until 30 minutes after subarachnoid injection. After obtaining successful spinal anesthesia, a bladder catheter was inserted and surgery was allowed to proceed. Patients were randomly allocated to 1 of 3 study groups of 21 patients each using sealed envelopes and a computer-generated randomization list. During surgery patients received additional intravenous midazolam upon request, remaining easily arousable at all times. One hour after the subarachnoid dose and with the MLSB at or below T<sub>4</sub>, patients received an epidural loading dose and the time was designated as T = 0. If sensory block was above T<sub>4</sub>, sensory block was checked every 10 minutes and the epidural loading dose postponed until the block had regressed to at or below T<sub>4</sub>. Patients in groups 1 and 2 received an epidural loading dose of 10 mL ropivacaine 0.75%; patients in group 3 received 10 mL levobupivacaine 0.75%. After completion of the epidural loading dose, a PCEA device (Gemstar, Hospira, Hoofddorp, The Netherlands) with a blinded cassette was connected to the epidural catheter and started with a background infusion of 6 mL/hour, a bolus dose of 2 mL, a lock-out period of 10 minutes and a maximum of 3 bolus doses per hour. Patients in group 1 received a mixture of ropivacaine 0.2% with sufentanil 1 µg/mL, patients in group 2 received a mixture of ropivacaine 0.125% with sufentanil 1 µg/mL, and patients in group 3

received a mixture of levobupivacaine 0.125% with sufentanil 1 µg/mL. At the time of inclusion, all patients were made familiar with the PCEA device and instructed to titrate themselves to adequate pain relief (numerical rating score [NRS] of 3 or less on a scale from 0 [no pain] to 10 [intolerable pain]). The administration of the epidural loading dose and connection of the patient to the PCEA device was performed by an investigator who was not involved in subsequent data collection. NRS and MBS were recorded at 6, 12, 24, and 48 hours after administration of the epidural loading dose by blinded observers. At the same time intervals, patient satisfaction was measured using an 11 point numerical rating scale ranging from 0 (dissatisfied) to 10 (satisfied). In case of insufficient analgesia, an epidural rescue dose of 75 mg ropivacaine (groups 1 and 2) or levobupivacaine (group 3) was administered by an investigator who was aware of the treatment schedule but not involved in data collection.

Outcome variables were NRS for pain and patient satisfaction, MBS, time to first demand (TFD) of the PCEA device, bolus/demand ratio (number of granted requests/number of requests of the PCEA device), and average hourly consumption of local anesthetic and sufentanil. Average hourly local anesthetic consumption was calculated using data from the PCEA device (total infusion time and infused volume), the epidural loading dose at T = 0 plus additional top-ups administered during the study period. On the given time intervals (6, 12, 24, and 48 hours) patients were interviewed for side effects (nausea and/or vomiting and pruritus).

In the absence of relevant data, the sample size was estimated assuming 40% variability (coefficient of variation) in the number of patient-controlled requests for medication. With this assumption the sample size required to have an 80% probability of detecting a clinically relevant (40%) difference between group means (level of significance 0.05) was 21 patients per group. Sensory and motor block data, and NRS scores are reported as median (range); patient age, height and weight, TFD, bolus/demand ratio, and local anesthetic and sufentanil consumption are expressed as mean ± SD. Gender, ASA Classification, and side effects are reported as proportions.

Data were analyzed using the GraphPad InStat v.3.06 package (GraphPad Software Inc, San Diego, CA). The 2 test was used for comparison of proportions. Continuous data were analyzed using one-way analysis of variance (ANOVA) or the Kruskal-Wallis test, as appropriate. The level of significance was set at 0.05.

## Results

Sixty-three patients were studied, 21 in each group. Thirty-nine patients were studied in the Reinier de Graaf Gasthuis, 24 patients at the Leiden University Medical Center. One patient in group 3 ended the study prematurely because of catheter leakage; the data of this patient was evaluated for the first 24 hours only. Demographics of the patients were similar and are presented in Table 1.

Table 1. Patient demographics

	Group 1 Ropivacaine 0.2 % Sufentanil 1 µg/mL (n = 21)	Group2 Ropivacaine 0.125 % Sufentanil 1 µg/mL (n = 21)	Group3 Levobupivacaine 0.125 % Sufentanil 1 µg/mL (n = 21)	P
Age (years)	68,5 ± 11,9	69 ± 12,5	71,7 ± 6,9	NS
Sex (M/F)	6/15	6/15	4/17	NS
ASA Class (1/2/3)	4/15/2	3/15/3	2/15/4	NS
Weight (kg)	84,5 ± 17,7	83,8 ± 12,6	83 ± 11,7	NS
Height (cm)	166,2 ± 10,4	168 ± 8,9	165,8 ± 6,8	NS

Data are mean ± SD or number of patients. NS= no statistically significant difference. TFD averaged 7.7 ± 4.2 hours in group 1 (ropivacaine 0.2%), 8.8 ± 5.5 hours in group 2 (ropivacaine 0.125%), and 8.3 ± 6.3 hours in group 3 (levobupivacaine 0.125%), the difference not being statistically significant. There were no significant differences between the 3 groups regarding NRS for pain and patient satisfaction, bolus/demand ratio, and MBS at any of the time intervals (Table 2).

Table 2. Pain, satisfaction, motor block scores and Bolus/Demand Ratio

	Group 1 Ropivacaine 0.2 % Sufentanil 1 µg/mL (n = 21)	Group 2 Ropivacaine 0.125 % Sufentanil 1 µg/mL (n = 21)	Group 3 Levobupivacaine 0.125 % Sufentanil 1 µg/mL (n = 21)	P
<b>NRS Pain</b>				
T = 6	0 (0-5)	0 (0-7)	0 (0-5)	NS
T = 12	2 (0-7)	1 (0-7)	1 (0-9)	NS
T = 24	2 (0-10)	2 (0-7)	2 (0-5)	NS
T = 48	2 (0-8)	3 (0-6)	2 (0-7)	NS
<b>NRS Satisfaction</b>				
T = 6	10 (7-10)	10 (6-10)	10 (8-10)	NS
T = 12	9 (2-10)	10 (6-10)	10 (3-10)	NS
T = 24	9 (1-10)	10 (4-10)	10 (3-10)	NS
T = 48	9 (1-10)	10 (4-10)	10 (6-10)	NS
<b>Bolus/Demand Ratio</b>	0.84 ± 0.17	0.84 ± 0.14	0.87 ± 0.22	NS
<b>MBS</b>				
T = 6	6 (0-12)	2 (0-12)	9 (0-12)	NS
T = 12	0 (0-8)	0 (0-4)	0 (0-12)	NS
T = 24	0 (0-8)	0 (0-4)	0 (0-4)	NS
T = 48	0 (0-8)	0 (0-4)	0 (0-4)	NS

NRS Pain = Numerical rating scale score for pain (ranging from 0 = no pain to 10 = very painful). NRS Satisfaction = Numerical rating scale score for patient satisfaction (ranging from 0 = highly dissatisfied to 10 = highly satisfied). Bolus/Demand Ratio: The number of granted PCEA bolus doses/bolus requests during the 48 h study period. MBS = Motor block score of the lower

limbs (ranging from 0 = no motor block to 12 = complete motor block). Data are expressed as median (range) or mean  $\pm$  SD. T = 6, 12, 24 or 48: 6, 12, 24 or 48 h after administration of the epidural loading dose. NS = no statistically significant difference.

The average hourly sufentanil consumption was similar among groups. Patients in group 1 used significantly more local anesthetic as compared with patients in groups 2 and 3. Results are summarized in Table 3.

Table 3. Average local anesthetic and sufentanil consumption during 48 h

	Group 1 Ropivacaine 0.2 % Sufentanil 1 $\mu$ g/mL (n = 21)	Group2 Ropivacaine 0.125 % Sufentanil 1 $\mu$ g/mL (n = 21)	Group3 Levobupivacaine 0.125 % Sufentanil 1 $\mu$ g/mL (n = 21)	P
Sufentanil $\mu$ g/h	6.8 $\pm$ 0.7	7.1 $\pm$ 0.6	6.6 $\pm$ 0.8	NS
Local anesthetic mg/h	15.5 $\pm$ 2.0 *	10.3 $\pm$ 1.0	10.0 $\pm$ 1.6	P < 0.001

Data are mean  $\pm$  SD. \* Group 1 significant versus groups 2 and 3. NS: no statistically significant difference

Episodes of nausea were recorded in 43% of the patients in group 1, 38% in group 2, and 43% in group 3. Pruritus occurred in 43% of the patients in groups 1 and 2, and in 52% of the patients in group 3. Symptoms of pruritus and nausea were mild, the majority of patients requiring no treatment. Results are summarized in Table 4.

Table 4. Postoperative Nausea and vomiting (PONV) and pruritus

	Group 1 Ropivacaine 0.2 % Sufentanil 1 $\mu$ g/mL (n = 21)	Group2 Ropivacaine 0.125 % Sufentanil 1 $\mu$ g/mL (n = 21)	Group3 Levobupivacaine 0.125 % Sufentanil 1 $\mu$ g/mL (n = 21)	P
PONV	9 (43 %)	8 (38 %)	9 (43 %)	NS
PONV M/F	2/7	1/7	2/7	NS
Pruritus	9 (43 %)	9 (43 %)	11 (52%)	NS

Data are expressed as number of patients and proportions

## Discussion

This study was designed to determine the efficacy of levobupivacaine and ropivacaine in combination with sufentanil for prolonged postoperative PCEA. Under the conditions of this study all 3 combinations provided good postoperative analgesia and there were no significant differences in the outcome parameters with the exception of local anesthetic consumption. Whereas sufentanil consumption was similar, the consumption of ropivacaine was significantly higher in patients receiving ropivacaine 0.2% (group 1). The higher concentration

of ropivacaine did not result in better analgesia or a reduction in sufentanil consumption, indicating that postoperative analgesia in this setting was primarily determined by sufentanil.

Our results are in agreement with Kampe et al.<sup>13</sup> who found no difference in efficacy between ropivacaine 0.1% and ropivacaine 0.2%, both combined with sufentanil 1 µg/mL for postoperative analgesia after total knee replacement. Kampe et al. used a continuous epidural infusion and observed that 8 hours after initiation of the epidural infusion, patients were unable to achieve sufficient pain relief. In addition, the sample size of their study groups was small. In the present study, larger groups and PCEA technology as opposed to continuous infusion was used in an attempt to decrease sufentanil consumption with higher ropivacaine concentrations as well as evaluating the previously suggested potency difference between ropivacaine and levobupivacaine. While we did not find insufficient analgesia after 8 hours or at any other time interval, our results confirm Kampe's conclusion that when using sufentanil 1 µg/mL, an increase in ropivacaine concentration only leads to increased consumption of local anesthetic without reducing sufentanil consumption or improving the quality of analgesia. There is controversy regarding the relative potencies of ropivacaine and levobupivacaine in MLAC studies. While some observed that there is no difference in potency between levobupivacaine and racemic bupivacaine<sup>14</sup> others showed that ropivacaine is 40% less potent.<sup>11,12</sup> With these results in mind, a similar potency difference would be expected between levobupivacaine and ropivacaine. However, a recent MLAC study found levobupivacaine and ropivacaine to be equipotent.<sup>15</sup> This raises questions about the reliability of MLAC studies to compare potencies of local anesthetics, and about the validity of extrapolating MLAC results to the high end of the dose-response curve. We did not find a potency difference between ropivacaine and levobupivacaine. However, in view of our observation that under the conditions of our study postoperative pain relief was predominantly determined by sufentanil, it is likely that a possible potency difference has been masked by the presence of sufentanil in the epidural mixture. Adding sufentanil to a local anesthetic enhances the potency of the latter. In a labor analgesia study the MLAC of ropivacaine and levobupivacaine was decreased with 78% by adding sufentanil 0.75 µg/mL.<sup>16</sup> In this study, sufentanil was used in a concentration of 1 µg/mL, which previous authors have shown effective with local anesthetics in epidural analgesia.<sup>13,17-20</sup> Postoperative epidural regimens aim to minimize motor block by reducing the amount of local anesthetic. Motor blockade of the lower limbs is not only a nuisance for the patient, it also interferes with early mobilization, which accelerates postoperative recovery and reduces hospital stay. In a study comparing different concentrations of ropivacaine and fentanyl, Liu et al. found that motor block was significantly more frequent with ropivacaine 0.2%<sup>21</sup>. By contrast, we observed no significant difference in motor block scores between the 3 groups. All of our patients were able to mobilize on the first postoperative day. Epidural sufentanil may contribute to postoperative nausea and vomiting (PONV), although Brodner et al. observed no increase in the incidence of PONV with increasing sufentanil doses.<sup>22</sup> The incidence of PONV reported by others using sufentanil 1 µg/mL in

combination with a local anesthetic varies from 10% to 20%.<sup>19,22,23</sup> We found a higher incidence (range 38% to 43%). This may be explained on methodological grounds: we recorded every patient mentioning 1 or more episodes of nausea and/or vomiting as PONV positive. Similarly, the incidence of pruritus in our study is higher than that reported by others. However, the severity of postoperative nausea and/or vomiting and pruritus was mild, requiring no treatment in the majority of patients.

In conclusion, all 3 solutions provided adequate postoperative pain relief. Increasing the concentration of ropivacaine from 0.125% to 2% resulted in an increase in local anesthetic consumption without improving analgesia or reducing the consumption of sufentanil. Under the conditions of our study, postoperative analgesia was predominantly determined by sufentanil.



## References

1. Liu SS, Allen HW, Olsson GL. Patient-controlled epidural analgesia with bupivacaine and fentanyl on hospital wards: Prospective experience with 1,030 surgical patients. *Anesthesiology* 1998;88:688-695.
2. McCaughey W, Mirakhor RK. Drugs in anaesthetic practice and analgesia. In: *Speight TM, ed. Avery's Drug Treatment. 4th ed. Yardley, PA: Adis International, Lim*
3. Albaladejo P, Bouaziz H, Benhamou D. Epidural analgesics: How can safety and efficacy be improved? *CNS Drugs* 1998;10:91-104.
4. Santos AC, Arthur GR, Wlody D, de Armas P, Morishima HO, Finster M. Comparative systemic toxicity of ropivacaine and bupivacaine in nonpregnant and pregnant ewes. *Anesthesiology* 1995;82:734-740.
5. Reiz S, Haggmark S, Johansson G, Nath S. Cardiotoxicity of ropivacaine—a new amide local anaesthetic agent. *Acta Anaesthesiol Scand* 1989;33:93-98.
6. Brockway MS, Bannister J, McClure JH, McKeown D, Wildsmith JA. Comparison of extradural ropivacaine and bupivacaine. *Br J Anaesth* 1991;66:31-37.
7. Morrison LM, Emanuelsson BM, McClure JH, Pollok AJ, McKeown DW, Brockway M, Jozwiak H, Wildsmith JA. Efficacy and kinetics of extradural ropivacaine: Comparison with bupivacaine. *Br J Anaesth* 1994;72:164-169.
8. Foster RH, Markham A. Levobupivacaine: A review of its pharmacology and use as a local anaesthetic. *Drugs* 2000;59:551-579.
9. Mazoit JX, Boico O, Samii K. Myocardial uptake of bupivacaine: II. Pharmacokinetics and pharmacodynamics of bupivacaine enantiomers in the isolated perfused rabbit heart. *Anesth Analg* 1993;77:477-482.
10. Casati A, Santorsola R, Aldegheri G, Ravasi F, Fanelli G, Berti M, Frascini G, Torri G. Intraoperative epidural anesthesia and postoperative analgesia with levobupivacaine for major orthopedic surgery: A double-blind, randomized comparison of racemic bupivacaine and ropivacaine. *J Clin Anesth* 2003;15:126-131.
11. Capogna G, Celleno D, Fusco P, Lyons G, Columb M. Relative potencies of bupivacaine and ropivacaine for analgesia in labour. *Br J Anaesth* 1999;82:371-373.
12. Polley LS, Columb MO, Naughton NN, Wagner DS, van de Ven CJ. Relative analgesic potencies of ropivacaine and bupivacaine for epidural analgesia in labor: Implications for therapeutic indexes. *Anesthesiology* 1999;90:944-950.
13. Kampe S, Diefenbach C, Kanis B, Auweiler M, Kiencke P, Cranfield K. Epidural combination of ropivacaine with sufentanil for postoperative analgesia after total knee replacement: A pilot study. *Eur J Anaesthesiol* 2002;19:666-671.
14. Lyons G, Columb M, Wilson RC, Johnson RV. Epidural pain relief in labour: Potencies of levobupivacaine and racemic bupivacaine. *Br J Anaesth* 1998;81:899-901.
15. Polley LS, Columb MO, Naughton NN, Wagner DS, van de Ven CJ, Goralski KH. Relative analgesic potencies of levobupivacaine and ropivacaine for epidural analgesia in labor. *Anesthesiology* 2003;99:1354-1358.

16. Buyse I, Stockman W, Columb M, Vandermeersch E, Van de Velde M. Effect of sufentanil on minimum local analgesic concentrations of epidural bupivacaine, ropivacaine and levobupivacaine in nullipara in early labour. *Int J Obstet Anesth* 2007;16:22-28.
17. Wiebalck A, Brodner G, van Aken H. The effects of adding sufentanil to bupivacaine for postoperative patient-controlled epidural analgesia. *Anesth Analg* 1997;85:124-129.
18. Kampe S, Weigand C, Kaufmann J, Klimek M, Konig DP, Lynch J. Postoperative analgesia with no motor block by continuous epidural infusion of ropivacaine 0.1% and sufentanil after total hip replacement. *Anesth Analg* 1999;89:395-398.
19. Kampe S, Randebrock G, Kiencke P, Hunseler U, Cranfield K, Konig DP, Diefenbach C. Comparison of continuous epidural infusion of ropivacaine and sufentanil with intravenous patient-controlled analgesia after total hip replacement. *Anaesthesia* 2001;56: 1189-1193.
20. Lorenzini C, Moreira LB, Ferreira MB. Efficacy of ropivacaine compared with ropivacaine plus sufentanil for postoperative analgesia after major knee surgery. *Anaesthesia* 2002;57:424-428.
21. Liu SS, Moore JM, Luo AM, Trautman WJ, Carpenter RL. Comparison of three solutions of ropivacaine/ fentanyl for postoperative patient-controlled epidural analgesia. *Anesthesiology* 1999;90:727-733.
22. Brodner G, Mertes N, van Aken H, Mollhoff T, Zahl M, Wirtz S, Marcus MA, Buerkle H. What concentration of sufentanil should be combined with ropivacaine 0.2% Wt/Vol for postoperative patient-controlled epidural analgesia? *Anesth Analg* 2000;90:649-657.
23. Debon R, Allaouchiche B, Duflo F, Boselli E, Chassard D. The analgesic effect of sufentanil combined with ropivacaine 0.2% for labor analgesia: A comparison of three sufentanil doses. *Anesth Analg* 2001; 92:180-183.

# Chapter 3

## Epidural blockade affects the pharmacokinetics of propofol in surgical patients

Elske Sitsen, MD, Erik Olofsen, MSc, Agnes Lesman, MD, Albert Dahan, MD, PhD,  
and Jaap Vuyk, MD, PhD

*Anesthesia & Analgesia* Volume 122; Number 5; May 2016; pp 1341-1349

## Introduction

Epidural anesthesia provides surgical analgesia and reduces postoperative pain. Intraoperatively, epidural anesthesia is often used in combination with general anesthesia to reduce anesthetic requirements. Neuraxial blockade has been shown to affect the dose requirements of hypnotic agents required to achieve a given sedative or anesthetic effect.<sup>1</sup> In the presence of epidural blockade, the dose of midazolam and propofol needed to induce loss of consciousness was reduced by up to 25%.<sup>1,2</sup> A similar reduction in dose requirement has been described for volatile anesthetics in the presence of epidural anesthesia.<sup>3</sup> In addition to an hypnotic sparing effect, the sensory blockade from spinal anesthesia itself has been associated with a sedative effect.<sup>4</sup> Lastly, Doherty et al. found that intravenous lidocaine decreased the MAC of halothane in a dose dependent manner in animals, suggesting that the systemic effects of local anesthetics may have direct sedative effects.<sup>5,6</sup>

Epidural blockade, through sympathetic output reduction and the direct vasodilating and myocardial depressant effect of local anesthetics,<sup>7,8</sup> may cause hemodynamic depression. Because sedative agents affect the hemodynamics as well, it is of importance to determine the interaction between epidural blockade and sedative agents, to allow analgesia and sedation in the presence of optimal hemodynamic stability.

The mechanism and the magnitude of the sedative sparing effect of central neuraxial blockade is unclear. The pharmacokinetics of intravenous sedatives may be affected by epidural induced changes in cardiac output and regional blood flow. For example, reductions in liver blood flow reduce propofol clearance, as a consequence of its high extraction ratio.

We hypothesized that epidural blockade affects the pharmacokinetics of propofol due to the hemodynamic alterations that result from epidural blockade. We therefore studied the influence of epidural blockade on the pharmacokinetics of propofol in a double-blind randomized manner.

## Materials and Methods

### Subjects

After obtaining approval of the Medical Ethics Committee of the Leiden University Medical Centre, registration in National Ethics Registry CCMO, NL32295.058.10 and written informed consent,<sup>28</sup> American Society of Anesthesiologists status I or II patients, aged 18-65 years, scheduled for surgical procedures requiring epidural anesthesia, participated in the study. All patients were within 30% of ideal body weight, had no history of cardiac, hepatic or renal disease and were allowed to take their usual medication up until the day before the investigation. Patients taking  $\beta$ -blocking agents and patients taking chronic pain medication were excluded from the study. All patients denied smoking or consumption of more than 20 g of alcohol per day. The study was conducted in an operating room and was completed before the start of the surgical procedure.

The study was powered at 80% to detect a difference of 15% in the blood propofol concentration associated with a level of (un)consciousness equal to a BIS of 60 between epidural ropivacaine doses of 0 and 150 mg with 28 patients. Patients who dropped out would be replaced.

### Study design

This was a randomized double-blind study. The 28 patients were randomly assigned to one of four study groups of 7 patients. The randomization and preparation of the study medication was performed by the hospital pharmacist, who took no further part in the study. Randomization was performed in blocks of 4 by a computerized randomization program. Patients were allocated to sequentially numbered boxes. The study medication was delivered in a closed box. The ropivacaine dose was taken out of the box and administered via the epidural catheter to the patient by a qualified anesthesia nurse, who took no further part in the study. This anesthesia nurse then signed the medication form and returned the, again closed, box to the hospital pharmacist.

After arrival in the operating room the un-premedicated patients received the standard perioperative monitoring including the electrocardiogram, end-tidal carbon dioxide, peripheral oxygen saturation, bispectral index, and intra-arterial blood pressure. These were monitored continuously throughout the study. An intravenous cannula was inserted into a large forearm vein for the infusion of propofol. An intra-arterial cannula was placed in the radial artery for continuous hemodynamic monitoring and blood sampling. Following placement of monitors patients were moved to a sitting position for placement of the epidural catheter. After skin infiltration with lidocaine patients received a lumbar epidural catheter at the L2-L3 or L3-L4 level, placed 5 cm in the epidural space.

Following placement of the epidural catheter cardiac output was determined using the pulse-contour methodology on the basis of the intra-arterial blood pressure curve with the Vigileo (Edwards Life sciences). A preload of 500 mL of Voluven® was given in 15 min. before the epidural medication was given.

### Drug administration

After the gathering of baseline measurements, an anesthesia nurse not otherwise involved in the study administered the study medication of 10 ml NaCl 0.9%, ropivacaine 50 mg (7.5 mg/ml), ropivacaine 100 mg (7.5 mg/ml) or ropivacaine 150 mg (7.5 mg/ml) via the epidural catheter, according to the randomization protocol. After aspiration, a test dose of 2 ml of the blinded medication was given to exclude a spinal position of the catheter. Then, 3 minutes thereafter, in the absence of significant sensory or motor blockade, the remaining dose was given. The study nurse had no further involvement in the study to maintain the double blinding of the patient and investigators.

Patients in groups 1, 2, 3, and 4 received an epidural dose of 10 ml of NaCl 0.9%, 50 mg of ropivacaine 7.5 mg/ml (6.7 ml), 100 mg of ropivacaine 7.5 mg/ml (13.3 ml), and 150 mg of ropivacaine 7.5 mg/ml (20 ml), respectively. Assessments of the epidural blockade level were performed every 5 minutes during the first 30 min after epidural administration. Hypotension defined as greater than a 30% decrease in systolic blood pressure compared to control, was treated with phenylephrine 100 µg, intravenously. Bradycardia defined as a heart rate less than 40 beats/min was treated with atropine 0.5 mg intravenously.

The propofol infusion was started 30 min after epidural study medication administration using the target controlled infusion pump of Fresenius Vial Infusion Technology; called the Base Primea® using the propofol pharmacokinetic parameters reported by Marsh et al<sup>10</sup>. Patients received a target-controlled infusion with propofol with an initial target concentration of 1 µg/ml. After 6, 12 and 18 minutes this target propofol concentration was increased to 2.5 µg/ml, 4 µg/ml, and 6 µg/ml, respectively. The target-controlled infusion of propofol was terminated 24 min after its initiation. During the propofol infusion all patients received 100 % oxygen through a non-rebreathing mask.

After termination of the study, 120 minutes after cessation of the propofol infusion, the level of epidural blockade was determined again and an additional epidural dose of ropivacaine was given as required to assure adequate sensory blockade for surgery.

### **Assessment of clinical response**

The level of sensory loss was determined by loss of cold sensation bilateral in the anterior axillary line. All patients were tested in a supine position; the upper and lower limits of the blockade were registered. A stable level of sensory loss was defined as an unchanged upper blockade level during two consecutive 5 min assessments. Motor function loss was scored using the Bromage scale (0 = no motor function loss, 1 = patient is able to flex the ankle and knee, 2 = patient is able to flex the ankle, 3 = complete motor loss).

### **Arterial blood samples and assays**

A blank blood sample (10 ml) was obtained for calibration purposes prior to propofol administration. Arterial blood samples for blood propofol concentration determination were taken at 3, 6, 9, 12, 15, 18, 21 and 24 min after the start of the target controlled propofol infusion (the 6-, 12-, 18- and 24-minutes samples were taken just before the change in target concentration), and at 2, 5, 10, 20, 30, 60, 90, 120 and 150 min after termination of the propofol infusion. Blood samples were collected in potassium-oxalate coated syringes and stored at 4 °C. Propofol assays were carried out within 12 weeks in our laboratory. Propofol concentrations in blood were measured by HPLC-fluorescence at an excitation wavelength of 276 nm with emission wavelength of 310 nm.<sup>11</sup> The intra- and inter-assay coefficients of variation were 4.3% and 3.7% for propofol in blood in the concentration range of 0.06 – 14.0 µg/mL.

### Pharmacokinetic modelling and covariate selection

The target-controlled infusion regimens of the individual patients were used as the input (“the dose”) in the pharmacokinetic analysis. The TCI log files of the Base Primea® TCI pump in combination with simulations using Marsh’s model<sup>10</sup> allowed for an accurate representation of the individual infusion rates over time in each individual patient.

The pharmacokinetics were based on a 3-compartment mammillary model. The parameters were estimated using the measured blood propofol concentration time-data alone (without covariates) of the 28 sessions. This model was parameterized using volumes and clearances. These included three volumes,  $V_1$ ,  $V_2$ , and  $V_3$ , describing the central volume of distribution, and the shallow and deep volumes of distribution, and three clearances,  $Cl_1$ ,  $Cl_2$ , and  $Cl_3$ , describing elimination clearance, clearance to the shallow compartment, and clearance to the deep compartment.

Weight, sex, ropivacaine dose, and number of blocked segments were tested as possible covariates improving the model (see statistical analysis). We first estimated the volumes and clearances without covariates. We then added weight as a covariate. Weight was incorporated in the model by multiplying volumes and clearances by factors  $WT/70$  and  $(WT/70)^{0.75}$ , respectively.<sup>12</sup> These powers were tested for significant differences from 1 and 0.75 for volumes and clearances, respectively. Then, sex was added as covariate so that the pharmacokinetic parameters could have different values for males and females. This was tested for significant improvement versus the same value for males and females. Lastly, the dose of ropivacaine and number of blocked segments were evaluated simultaneously. The ropivacaine dose was incorporated by multiplying the pharmacokinetic parameters by factors  $e^{((DOSE/75^{-1})^{\alpha})}$ . The number of blocked segments (NBS) was incorporated by multiplying the pharmacokinetic parameters by factors  $e^{((NBS/10^{-1})^{\alpha})}$ . Parameter alpha denotes covariate coefficients that characterize how strongly the six pharmacokinetic parameters are influenced by the covariate (ropivacaine dose or NBS). These were tested for significant difference from zero.

To determine whether to incorporate a covariate in the model, each of the 64 possible combinations was evaluated ( $64 = 2^6$ , 2 referring to the presence or absence of the covariate, 6 referring to the 6 possible pharmacokinetic parameters).

### Statistical Analysis

Data are described as mean + standard error unless stated otherwise. The pharmacokinetic models were fit to the data using NONMEM<sup>13</sup> (version 7.2.0 ADVAN 6). The pharmacokinetic parameters were assumed to be lognormally distributed across the population. Constant relative and/or additive residual error models were tested. Model discrimination was done using the Bayesian Information Criterion.<sup>14</sup> All possible subsets were sequentially tested for covariates weight, sex, ropivacaine dose and the number of blocked segments.

The predictive accuracy of the Base Primea® TCI pump at various target concentration levels was compared between the epidural dose groups (0, 50 mg, 100 mg and 150 mg ropivacaine) with the multi-sample median test followed by a Mann-Whitney U test.

A visual prediction-corrected predictive check<sup>15</sup> was constructed by simulating the designed TCI drug administration schedule for 28 x 357 subjects; 28 equals the number of subjects in the study and their values of the covariates were retained. From the 9996 simulated concentration versus time profiles, 95% prediction intervals were calculated. The prediction-corrected predictive check was required because not all patients received the same dosing regimen.

The standard error of clearance as a function of the number of blocked segments (Abstract and Results section) was assessed by calculating the standard deviation of (1,000,000) simulated values based on the population clearance and covariate coefficient estimates and standard errors, assuming the estimates are normally distributed. In plots of clearance versus covariates, 95% confidence intervals were plotted based on the interindividual variability estimate ( $w^2$ ) of the population clearance.

A cross-validation method using the “leave-one-out” procedure, as described by Fiset et al.<sup>16</sup>, was used to determine the predictive power of the model. In short, a population model is constructed from N-1 patients by leaving patient i out, and used to predict the concentration-time data of the i-th patient. This is repeated for all N patients. This procedure provides almost unbiased estimates of the performance of the population model. From the measured and predicted data, the median and 95% relative prediction error interval were calculated. The software to automate covariate selection and the jackknife procedure was written by one of the authors (E.O.).

### **Computer simulations.**

The influence of the significant covariates (weight, sex and ropivacaine dose or number of blocked segments) on propofol pharmacokinetics was explored by computer simulation using NONMEM. The final model as displayed in Table 1 was used for this purpose in a typical patient receiving a propofol regimen of 2 mg/kg bolus followed by a continuous infusion of 8 mg.kg<sup>-1</sup>.h<sup>-1</sup> for 120 min.

## **Results**

The patients were recruited between December 2010 and February 2012. All 28 patients (17 males, 11 females) completed the study without adverse events. The patients were (mean + SD) aged 44.9 + 15.1 yrs., with a body weight of 77.9 + 10.6 kg, a height of 177.6 + 11.1 cm and a BMI of 24.8 + 2.9. All patients were classified as American Society of Anesthesiologists class I or II.

In 3 patients hypotension was treated in total 8 times with intravenous phenylephrine, 100 µg.



In 2 patients intravenous atropine, 0.5 mg, was given to treat bradycardia during the insertion of the epidural catheter. In 5 patients in the 150 mg ropivacaine group, the highest target propofol concentration of 6 µg/ml was not reached due to a combination of deep sedation and hemodynamic depression. The TCI of propofol therefore was terminated at a maximum target concentration of 2.5 µg/ml in 1 patient and at a maximum target concentration of 4.0 µg/ml in 4 patients. In all other patients the 4 targets of propofol were maintained for 6 min each, and a total propofol dose of 400-500 mg was given in 24 min. All patients maintained spontaneous ventilation during the study. Patients returned to consciousness  $16.3 \pm 5.2$  min after termination of the propofol TCI.

With the ropivacaine dose increasing from 0 to 50, 100 and 150 mg, the number of blocked segments (median and (range)) increased from 0 (0-3) to 9 (3-15), 12 (9-14) and 15.5 (6-21), respectively (Figure 1). In 2 of the 7 patients who received 0 mg ropivacaine, 1 or more blocked dermatomes were recorded in the 30 min after the epidural administration of 10 ml of NaCl 0.9%, suggestive of an epidural induced placebo effect but which we consider a measurement error.

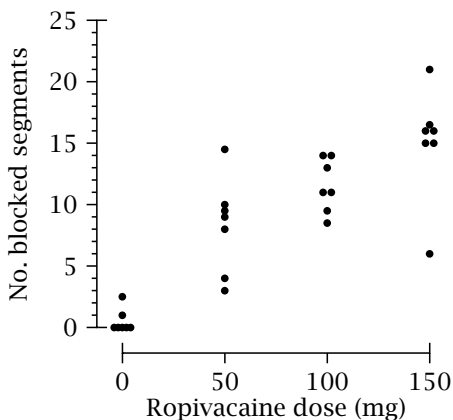


Fig. 1: The number of blocked segments of the individual patients in the 4 groups receiving 0, 50, 100 and 150 mg of ropivacaine in the epidural space.

In the 28 sessions a total of 472 blood samples were drawn for blood propofol concentration determination. With the ropivacaine dose increasing from 0 to 50, 100 and 150 mg (with increasing number of blocked segments) the measured blood propofol concentration increasingly exceeded that predicted by the

Base Primea® TCI pump that based its predictions on the Marsh pharmacokinetics<sup>17</sup>. The bias (= median performance error; MDPE (25th - 75th %)) increased in the patients that had received a ropivacaine dose of 0, 50, 100 and 150 mg from 1% (-10 to 16%), to 13% (-9 to 30%), 13% ((2 to 27%),  $P = 0.001$  compared to placebo) and 32% ((6 - 62%), significantly different from placebo ( $P < 0.0001$ ), 50 mg ( $P = 0.003$ ) and 100 mg ( $P = 0.018$ )). The inaccuracy (median absolute performance error: MDAPE (25th - 75th %)) increased from 12% (6 to 22%) to 19% (11 to 31%) ( $P = 0.003$  compared to placebo), 18% (9 to 32%), ( $P = 0.033$  compared to placebo) and 37% (19 to 62%), ( $P < 0.0001$  compared to placebo) respectively, in these patients. The influence of epidural ropivacaine on the bias and inaccuracy of the Base Primea® TCI pump is indicative of a pharmacokinetic interaction between the ropivacaine dose and the corresponding level of epidural blockade and the pharmacokinetics of propofol (Figure 2).

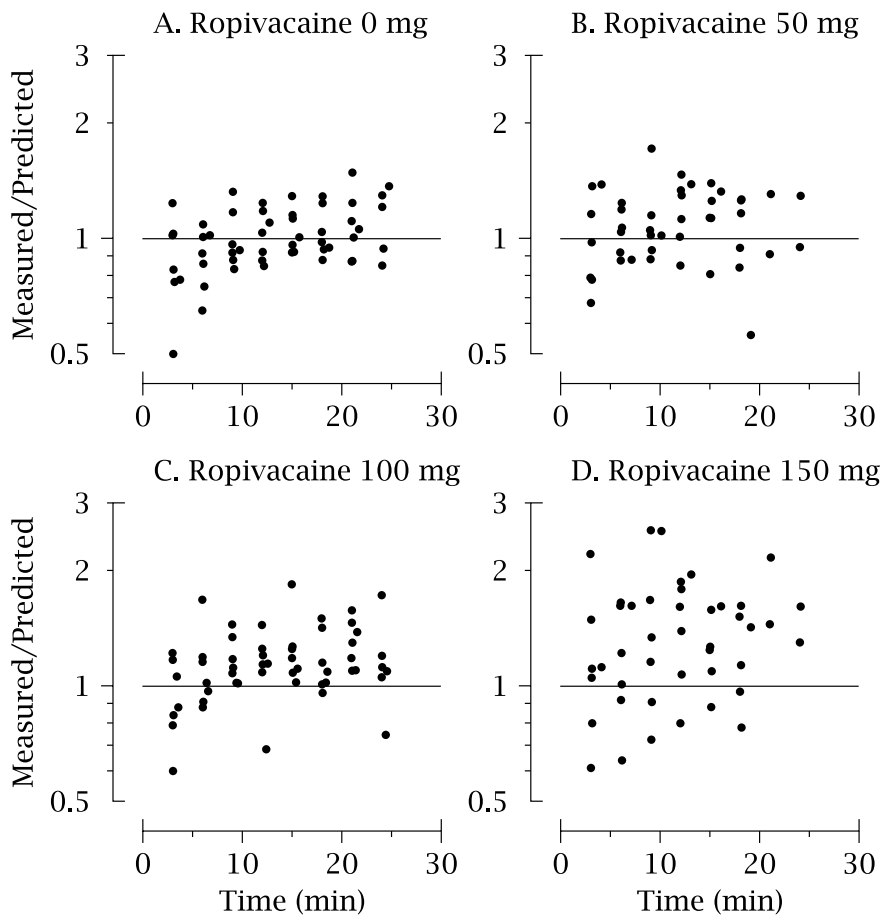


Fig. 2: The measured versus predicted propofol ratio's during a TCI of propofol using the Marsh parameter set in the patients of the 4 groups receiving 0, 50, 100 and 150 mg of epidural ropivacaine. The MDPE in patients of group A (1%) who received no epidural ropivacaine, increased to 13%, 13% and 29% in the patients of group B, C and D who received 50, 100 and 150 mg of epidural ropivacaine.

This then was confirmed in the pharmacokinetic analysis. A 3-compartment model adequately fitted the data. Figure 3 presents the measured blood propofol concentrations in 3 patients, the best, median, and worst fit of the data, the final model fit of this study and the predicted propofol concentration by the Base Primea® TCI pump as based on the Marsh pharmacokinetics.

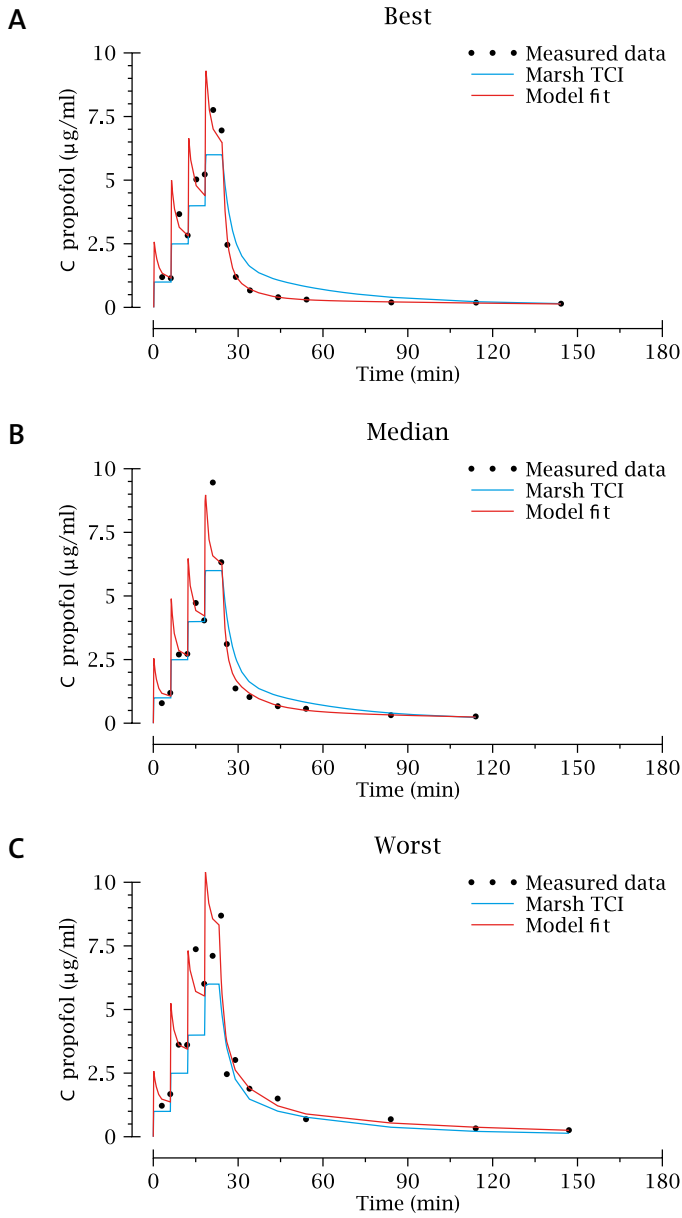


Fig. 3: The measured blood propofol concentrations in time in 3 patients that represent the best (panel A), median (panel B) and worst (panel C) fitted data according to the individual objective function values. The dots represent the measured blood propofol concentrations, the solid red line represents the final model fit; the solid blue line represents the propofol concentration as predicted on the basis of the pharmacokinetics of Marsh et al. as used in the TCI device in this study.

Our initial model was a conventional mammillary 3 compartment model with no covariates. This model had an objective function value of -483.876. We then added weight using an allometric approach, multiplying volumes by  $(WT/70)^1$ , and clearances by  $(WT/70)^{0.75}$ , respectively. We tested the volume exponent of 1 and the clearance exponent of 0.75 to see if other exponents provided better fits. Other values for these exponents did not improve the goodness of fit, so in the final model weight is scaled by  $WT/70$ , and clearances are scaled by  $(WT/70)^{0.75}$ . This model an objective function value of -495.466, demonstrating that our data significantly support scaling propofol pharmacokinetics by weight.

Sex was added as covariate to have different values for males and females. This resulted in a decrease in the objective function value to -512.742. Dose of ropivacaine and number of blocked segments were introduced concurrently in the analysis. The number of blocked segments (NBS) as covariate reduced the objective function value to -526.464. The ropivacaine dose as covariate resulted in a slightly less decrease in the objective function value to -523.496. We therefore selected number of blocked segments as the covariate for the model, recognizing that the high correlation between dose and blocked segments precludes assigning the effect of epidural blockade definitively to either dose or number of blocked segments.

Table 1 presents the base model (objective function -483.876), the model with weight, sex and dose as covariates, and the final model with weight, sex and number of blocked segments as covariates. The full equations of the final model for all volumes and clearances are for women:  $V_1 (L) = 5.98 \cdot (WT/70)$ ,  $V_2 (L) = 4.19 \cdot (WT/70)$ ,  $V_3 (L) = 65.8 \cdot (WT/70)$ ,  $Cl_1 (L/min) = 2.22 \cdot e^{(-0.173 \cdot (NBS/10-1))}$ ,  $(WT/70)^{0.75}$ ,  $Cl_2 (L/min) = 0.724 \cdot (WT/70)^{0.75}$  and  $Cl_3 (L/min) = 1.13 \cdot (WT/70)^{0.75}$ . Males and females have different typical values for  $V_2$  and  $Cl_2$ , see Table 1.

Table 1. Pharmacokinetic parameters of propofol of the base model without covariates, model with weight, gender and dose as covariates and model with weight, gender and number of epidural ropivacaine-blocked segments as covariates.

Base Model	Typical value	SEE	$\omega^2$	SEE
$V_1$ (L)	6.23	0.297	-	-
$V_2$ (L)	6.53	0.790	-	-
$V_3$ (L)	70.0	5.58	0.0581	0.0203
$Cl_1$ (L/min)	2.45	0.0797	0.0307	0.00758
$Cl_2$ (L/min)	1.21	0.128		
$Cl_3$ (L/min)	1.27	0.0894	-	-
SDE	0.197	0.00995	0.104	0.0320
Dose Model	Typical value	SEE	$\omega^2$	SEE
$V_1$ (L/70 kg)	6.00	0.124	-	-
$V_{2M}$ (L/70 kg)	8.72	0.303	-	-
$V_{2F}$ (L/70 kg)	4.21	0.929	-	-
$V_3$ (L/70 kg)	65.8	3.08	0.0781	0.0193
$Cl_1$ (L/(70 kg) <sup>0.75</sup> /min)	2.27	0.0559	0.0164	0.00369
$Cl_{2M}$ (L/(70 kg) <sup>0.75</sup> /min)	1.43	0.106	-	-
$Cl_{2F}$ (L/(70 kg) <sup>0.75</sup> /min)	0.720	0.143	-	-
$Cl_3$ (L/(70 kg) <sup>0.75</sup> /min)	1.13	0.0654	0.0915	0.0311
SDE	0.192	0.00939		
$\alpha$ DOSE	-0.129	0.0269		
Blocked Segments Model	Typical value	SEE	$\omega^2$	SEE
$V_1$ (L/70 kg)	5.98	0.446	-	-
$V_{2M}$ (L/70 kg)	8.71	0.906	-	-
$V_{2F}$ (L/70 kg)	4.19	0.974	-	-
$V_3$ (L/70 kg)	65.8	5.93	0.0853	0.0223
$Cl_1$ (L/(70 kg) <sup>0.75</sup> /min)	2.22	0.0558	0.0142	0.00397
$Cl_{2M}$ (L/(70 kg) <sup>0.75</sup> /min)	1.42	0.162	-	-
$Cl_{2F}$ (L/(70 kg) <sup>0.75</sup> /min)	0.724	0.168	-	-
$Cl_3$ (L/(70 kg) <sup>0.75</sup> /min)	1.13	0.0814	0.0893	0.0302
SDE	0.192	0.00899		
$\alpha$ NBS	-0.173	0.0367		

$V_1$ : central volume of distribution,  $V_2$ : shallow peripheral volume of distribution,  $V_3$ : deep peripheral volume of distribution,  $Cl_1$ : elimination clearance,  $Cl_2$ : rapid distribution clearance and  $Cl_3$ : slow distribution clearance. M: male and F: female. SEE: standard error of the estimate in the preceding column; SDE: standard deviation of relative residual error (absolute error was not significant); -: not estimable;  $\omega^2$ : interindividual variance (of log normally distributed parameters);  $\alpha$ DOSE: covariate coefficient for dose ropivacaine.  $\alpha$ NBS: covariate coefficient for number of blocked segments. The clearance and volume values for the dose model and the blocked segments model are standardized for a ropivacaine dose of 75mg or standardized NBS of 10.

An example of how the parameters of the final model may be calculated for a female patient with a weight of 80 kg and 8 blocked segments is as follows:

$$V_1 = 5.98 \cdot (80/70) = 6.83 \text{ L}; V_2 = 4.19 \cdot (80/70) = 4.79 \text{ L}; V_3 = 65.8 \cdot (80/70) = 75.2 \text{ L}$$

$$Cl_1 = 2.22 \cdot e^{(-0.173 \cdot (8/10-1))} \cdot (80/70)^{0.75} = 2.54 \text{ L/min}; Cl_2 = 0.724 \cdot (80/70)^{0.75} = 0.80 \text{ L/min}; Cl_3 = 1.13 \cdot (80/70)^{0.75} = 1.25 \text{ L/min}.$$

With the epidural blockade increasing from 0 to 20 blocked segments the metabolic clearance of propofol was reduced from 2.64 + 0.12 to 1.87 + 0.08 L/min (Figure 4B).

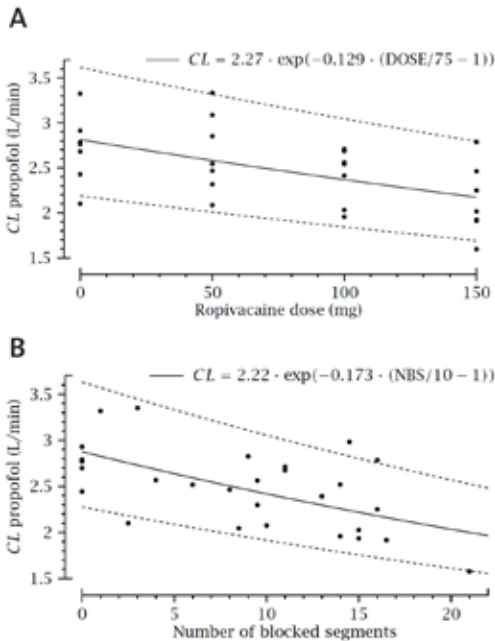


Fig 4: The influence of dose (Panel A) and the number of blocked segments (Panel B) on the clearance of propofol according to the final model fit. An epidural dose of 150 mg ropivacaine decreases the clearance from 2.58 to 2.0 L/min, 20 blocked segments reduces the clearance of propofol from 2.64 to 1.87 L/min. The discontinuous line shows the 95% confidence intervals as based on the interindividual variability estimate ( $\omega^2$ ) of the population clearance. The dots are the empirical Bayesian estimates of clearance for each patient.

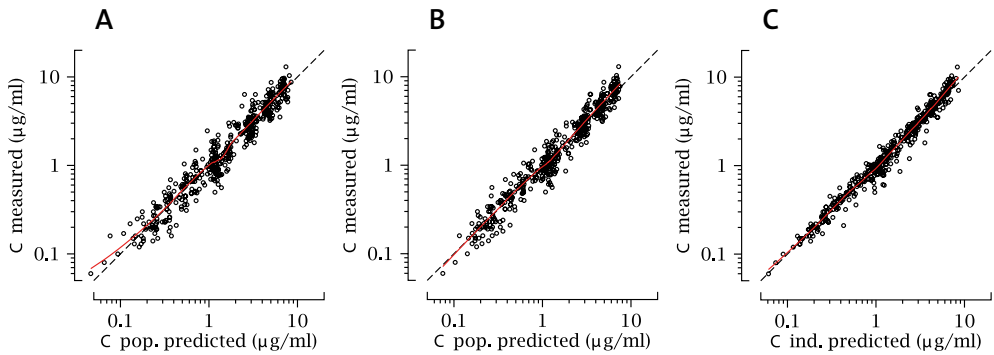


Fig 5: The measured versus population predicted blood propofol concentrations of the model without covariates (Panel A). The measured versus population predicted blood propofol concentrations of the final model including the covariates weight, sex and number of blocked segments (Panel B). The measured versus the individual predicted blood propofol concentrations of the final model including the covariates weight, sex and number of blocked segments (Panel C). The dashed lines represent the line of identity ( $Y=X$ ), the red lines represent the supersmoother through the data.

Figure 5A displays the measured versus population predicted blood propofol concentrations without covariates and figure 5B displays the measured versus population predicted blood propofol concentrations with covariates. Figure 5C displays the measured versus the individual predicted blood propofol concentrations. These figures show that less variability remains after the inclusion of the 3 covariates, weight, sex and number of blocked segments. Also the super smoother more closely corresponds to the line of identity of the final model after inclusion of the 3 significant covariates.

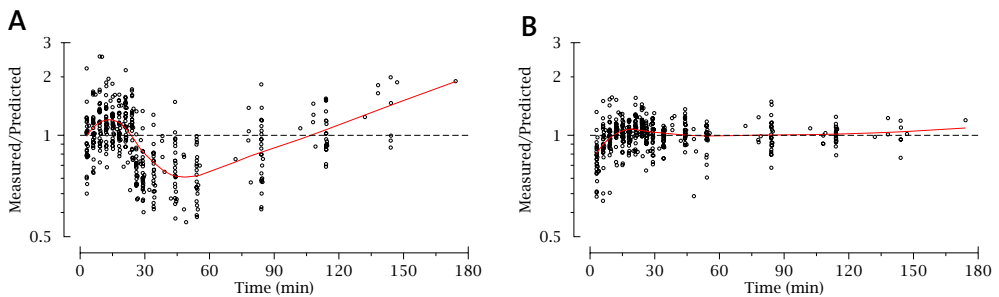


Fig 6: The performance error versus time of all measured blood propofol concentrations as based on the pharmacokinetics of Marsh et al., used in the TCI device in this study (Performance error; panel A) and on the basis of the model fit including weight, sex and number of blocked segments (Performance error; panel B). In red the median performance error (MDPE) is presented as a continuous line.

Figure 6 represents the MDPE over time of the model used in the TCI device by Marsh et al. (Panel A) and our final model based on the population values (Panel B). Compared to the prediction from the TCI device, the final model has a narrower error window and is stable over time.

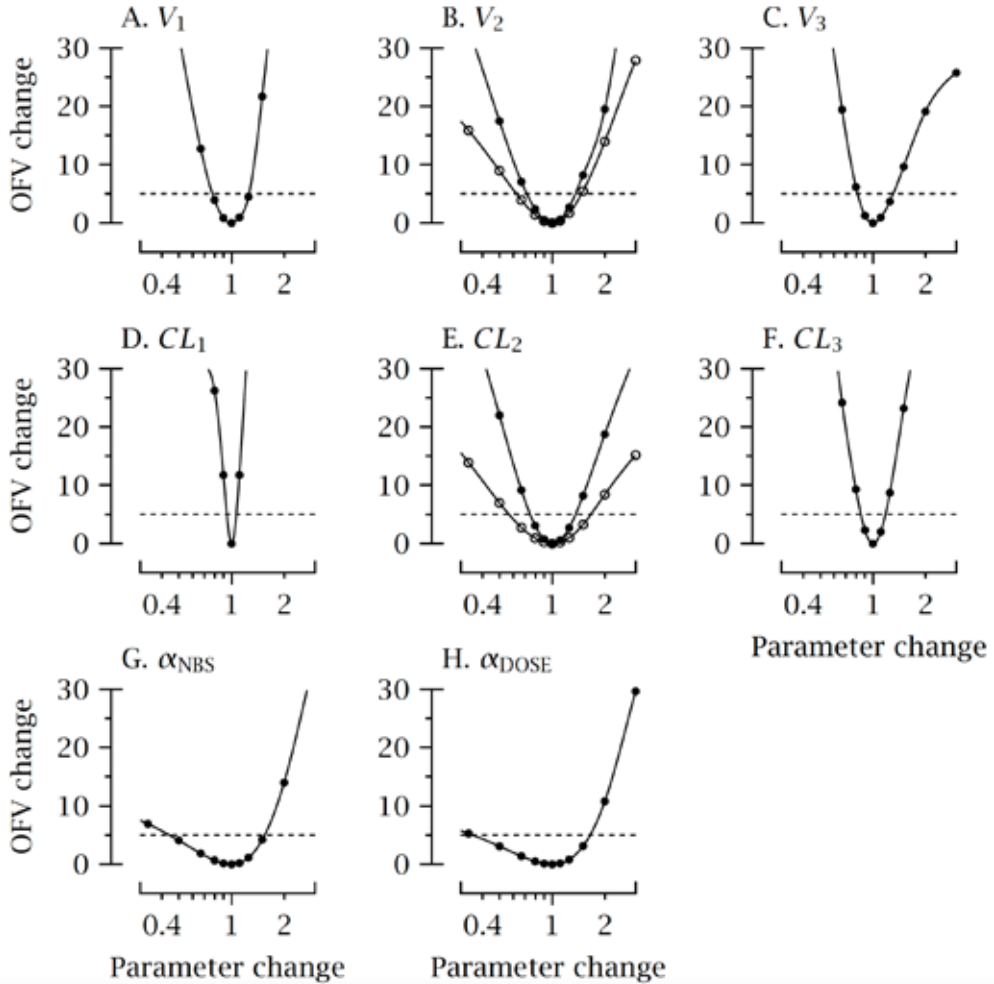


Figure 7: Likelihood profiles showing the change in objective function versus a relative change in the denoted parameter (A-H) while estimating the remaining parameters. The dashed line denotes a change of 5.02 points in objective function, indicating the  $p = 0.025$  level. The crossings of the likelihood profiles with the dashed lines give a parameter range corresponding to a 95% confidence interval. For  $V_2$  and  $CL_2$  de closed and open dots denote the profiles for males and females, respectively.

Figure 7 gives the log-likelihood profiles of the model parameters. The objective function is most sensitive to changes in the structural parameters (volume and clearances A-F), and less sensitive to changes in the covariate coefficients (females B, E) and effect of ropivacaine on



propofol clearance (G, H). The crossings of the likelihood profiles with the dashed lines give a parameter range corresponding to a 95% confidence interval (note that a 99% interval would not include zero for these parameters).

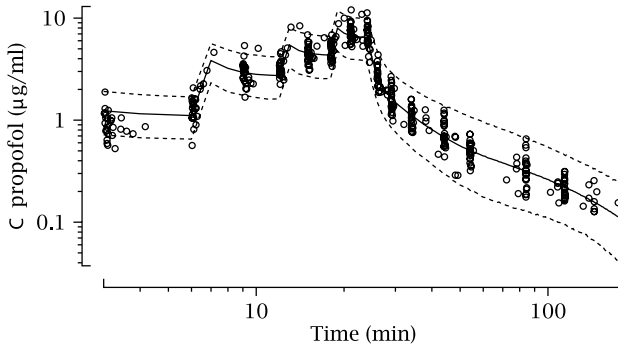
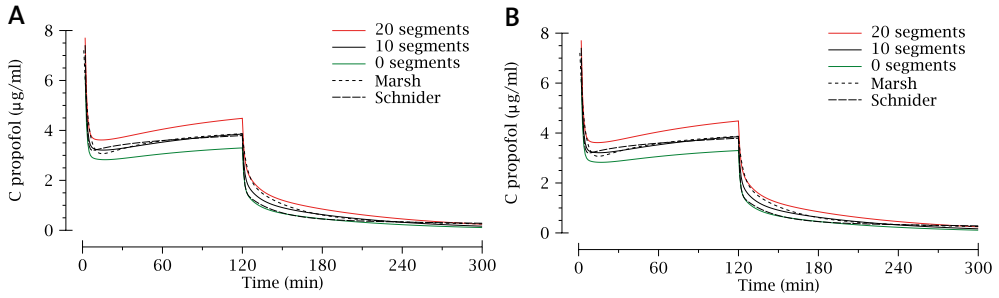


Fig 8: The prediction-corrected Visual Predictive Check of 28 patients. The dashed lines represent the 95% prediction interval

Figure 8 shows the prediction-corrected Visual Predictive Check of all patients as described in the methods section. To test the power of the study a leave-one-out procedure was performed, the median prediction error from the leave-one-out procedure (95% prediction error interval) was -10% (-48 to 54) %.

### Computer simulation

As visible in the raw data, the computer simulations with the final model also revealed (figure 9A) that increasing the level of epidural blockade increased blood propofol concentration up to 30% after a standard propofol administration regimen (propofol bolus of 2 mg/kg followed by 8 mg.kg<sup>-1</sup>.h<sup>-1</sup> for 120 min). Figure 9B shows the influence of body weight on the pharmacokinetics when the propofol dosing scheme is not weight corrected. Obviously, when a 90 kg and 50 kg patient receive a similar propofol dose, the resulting blood propofol concentration is significantly lower in the 90 kg patient (weight affected all parameters).



**Fig 9A:** Computer simulation of the blood propofol concentration in the presence of 0 (green), 10 (black) and 20 (red) blocked segments with a propofol infusion scheme of 2 mg/kg administered in 1 min, followed by 8 mg.kg<sup>-1</sup>.h<sup>-1</sup> for 119 min, using the final model. The discontinuous lines represent the blood propofol concentration as predicted on the basis of the pharmacokinetics of Marsh et al. and Schneider et al.

**Fig 9B:** Computer simulation of the blood propofol concentration using the final pharmacokinetic model in a patient with a weight of 50, 70 and 90 kg with a propofol infusion scheme of 140 mg administered in 1 min, followed by 560 mg.h<sup>-1</sup> for 119 min.

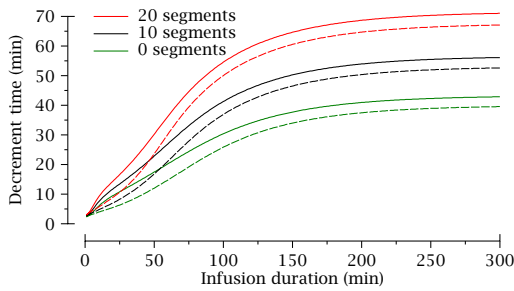


**Fig 10:** The 50% decrement time (= context-sensitive half-time) of propofol in the presence of 0, 10 and 20 blocked segments based on the final model fit for male (continuous lines) and female (discontinuous lines) subjects.

Figure 10 shows the 50% plasma decrement time (*i.e.*, the context sensitive half-time) of propofol in the presence of an epidural blockade of 0, 10 or 20 segments. From this one may conclude that epidural blockade significantly increases the 50% decrement time of propofol. This suggests, that blood propofol concentrations will remain longer at higher levels after termination of the propofol infusion, in the presence of epidural blockade. The figure also suggests that the decrement time is smaller in women compared to men.

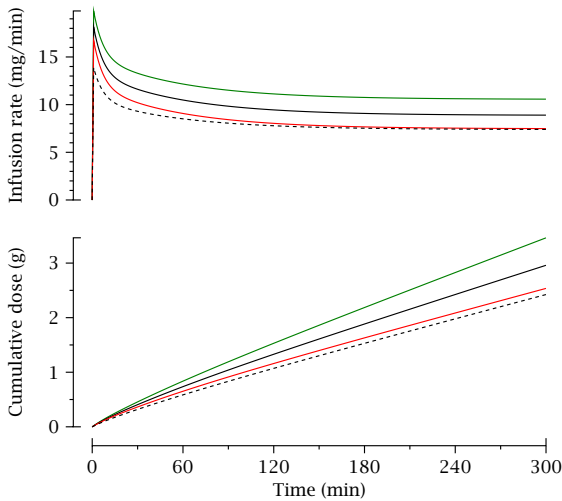


Fig 11: Computer simulation of the propofol infusion rate (upper panel) and cumulative propofol dose (lower panel) required to maintain a constant blood propofol concentration of  $4 \mu\text{g/ml}$  in the presence of 0 (green), 10 (black) and 20 (red) blocked segments using the final model in a 70 kg female.

In figure 11 the required propofol infusion rate (mg/min) and cumulative propofol dose (g) to maintain a constant blood propofol concentration of  $4 \mu\text{g/ml}$  are shown in time, in the presence of 0, 10 and 20 blocked segments. In the presence of 20 blocked segments an approximately 30% lower propofol infusion rate and equivalently lower total propofol dose are required to assure the same blood propofol concentration when no epidural block is present.

## Discussion

We studied the influence of epidural blockade on the pharmacokinetics of propofol. The results of this study confirm our hypothesis that epidural blockade affects propofol pharmacokinetics. In the presence of an epidural blockade of 20 segments blood propofol concentrations are elevated by about 30% due to a reduced propofol elimination clearance. After exploring multiple models sex was found to affect  $V_2$  and  $Cl_2$ . Sex and weight further improved the model fit.

Recent reports on the effect of neuraxial blockade on propofol pharmacology suggest that neuraxial blockade mainly affects the pharmacodynamics of propofol. This study, however, shows that epidural blockade affects the pharmacokinetics of propofol through a reduction in propofol clearance.

We successfully fitted a 3-compartment model to the data. Covariates were included in the model based on the Bayesian Information Criterion (BIC), evaluated for every possible combination of influence of a covariate on any of the six pharmacokinetic parameters. With our data set, the BIC required a change in NONMEM's objective function value of 6.03 points, close to the 6.63 required for a p-value of 0.01 for a single test. The probability to find an effect on any of the six parameters is

larger than 0.01 due to multiplicity, so likely close to the standard value of 0.05. A standard forward inclusion/backward elimination procedure would have resulted in the same final model (based on inspection of all objective function values). Significant covariates were weight, sex and number of blocked segments (fig. 5A and 5B). Figures 6A and 6B show the reduction in error and stability of model performance with the final model, in comparison with the time-varying error seen with the predictions on the basis of Marsh et al. Note however that our data is best described by our model by definition, and that any other model is bound to have a larger prediction error.

The likelihood profiles (Figure 7) show that the elimination clearance of propofol is estimated most accurately as becomes clear from the steep and narrow shaped likelihood profile. This, while still some unexplained variability exists regarding the influence of number of blocked segments and ropivacaine dose as is represented by the more shallow and wider shaped likelihood profiles. Further studies are needed to gain insight on this variability and obtain a more precise estimate of the effect of central neuraxial blockade (CNB) on propofol pharmacokinetics. Lastly, the wider likelihood profile for women for  $V_2$  and  $Cl_2$  compared to men probably results from the smaller number of women included.

The mechanism through which epidural blockade affects propofol's elimination clearance probably is related to the epidurally induced hemodynamic alterations. Epidural blockade reduces systemic vascular resistance resulting from the blockade of the sympathetic nervous system. The consecutive venous pooling of blood results in a reduced preload and thus reduced cardiac output. As a result of the reduced cardiac output and the altered mesenteric blood flow, epidural blockade is associated with a reduction in hepatic blood flow.<sup>18,19</sup> Because propofol has a high hepatic extraction ratio, changes in hepatic blood flow may readily produce changes in propofol elimination clearance. It may therefore well be that the epidural anesthesia-induced reduction in propofol elimination clearance that we observed, is the result of a reduction in hepatic blood flow.

In comparison to the pharmacokinetics by Marsh et al<sup>10</sup> and Schnider et al.<sup>20</sup>, the shallow and deep peripheral volumes of distribution in our parameter set are relatively small. This probably is due to the relatively short period of propofol infusion and the fact that in our study setting blood samples were only taken until 120 minutes after termination of the propofol infusion. The elimination clearance we found exceeds hepatic blood flow, thus confirming that propofol is cleared also at extrahepatic sites like the kidney.<sup>21</sup> Hiraoka et al<sup>22</sup> determined in patients undergoing cardiac surgery the elimination of propofol in other organs and found a renal extraction ratio of  $0.70 \pm 0.13$ . The renal blood flow and thus renal clearance may be influenced by epidural induced sympathetic blockade just as hepatic clearance may be affected, although renal autoregulation may interfere in this and maintain renal blood flow constant in the presence of a decreasing cardiac output.

With an increase in the epidural dose of ropivacaine from 0 to 150 mg, the elimination clearance of propofol was reduced from 2.58 to 2.0 L/min (Figure 4A). With inclusion of the number of blocked segments as an individual covariate instead of the epidural ropivacaine dose, the elimination clearance of propofol decreased significantly from 2.64 to 1.87 L/min (from 0 to 20 blocked segments) Fig. 4B, objective function decreased from -512.742 to -526.464). In the final model we included number of blocked segments as an independent covariate. The better fit of number of blocked segments as a covariate is explained by the fact that the hemodynamic response to epidural blockade probably is the driving force behind the influence of epidural blockade on propofol pharmacokinetics, and this is more closely related to the number of blocked segments than to the ropivacaine dose.

Figure 9A includes simulations based on our final model as well as on the PK set by Marsh<sup>17</sup> as based on Gepts<sup>23</sup> and Schnider et al.<sup>20</sup> In the time frame of this study and with the characteristics of this study population the Schnider parameter set and Marsh parameter set produce results that are comparable. Both run parallel to the predictions based on our model with 10 blocked segments. In the absence of epidural blockade, like the situation in the patients of the Schnider population, our simulation overestimates the blood propofol concentration by about 15% compared to that by Schnider et al. In the presence of an epidural blockade of 10 segments our simulation closely corresponds to that by Marsh et al. that was based on the data by Gepts et al. who studied patients who received in a majority of cases propofol in the presence of locoregional blockade.

Pharmacokinetic interaction studies of propofol with opioids and other sedatives have shown an increase in the blood propofol concentration by up to 25% after combined administration of propofol with opioids or sedatives.<sup>24,25</sup> The pharmacokinetic interactions between propofol and these opioids or sedatives are, just as we find in this study, predominantly the result of hemodynamic alterations that cause reductions in hepatic blood flow and/or reductions in peripheral propofol distribution. The elimination, rapid and slow distribution clearances ( $Cl_{1-3}$ ) of propofol are reduced in the presence of midazolam.<sup>26</sup> Similarly, the rapid and slow distribution and elimination of propofol are decreased in combination with alfentanil.<sup>25</sup> In conclusion, the mechanism of action and magnitude of the effect of epidural blockade on the pharmacokinetics of propofol resembles the effect of opioids and other sedatives on propofol pharmacokinetics. Both are the result of hemodynamic alterations, both induce blood propofol concentration elevations by about 25-30%.

### Conclusions

Epidural blockade affects the predictive accuracy of a TCI of propofol. With an increasing epidural blockade from 0 to 20 blocked segments, the measured blood propofol concentrations exceed those predicted by the Marsh pharmacokinetic parameter set 10 from 1% to 32%.

Epidural blockade affects the pharmacokinetics of propofol such that with an increasing epidural blockade from 0-20 blocked segments the elimination clearance decreases from 2.64 to 1.87 L/min. In the presence of high epidural blockade propofol dose may be reduced by about 30% to assure a similar blood propofol concentration as compared to when epidural blockade is absent.

### **Acknowledgments**

We thank René Mooren for the analysis of the blood samples of propofol.

## References

1. Tverskoy M, Fleyshman G, Bachrak L, Ben-Shlomo I. Effect of bupivacaine-induced spinal block on the hypnotic requirement of propofol. *Anaesthesia* 1996; 51:652-653.
2. Tverskoy M, Shifrin V, Finger J, Fleyshman G, Kissin I. Effect of epidural bupivacaine block on midazolam hypnotic requirements. *Reg Anesth* 1996; 21:209-213.
3. Yang MK, Kim JA, Ahn HJ, Choi DH. Influence of the baricity of a local anaesthetic agent on sedation with propofol during spinal anaesthesia. *Br J Anaesth* 2007; 98:515-518.
4. Senturk M, Gucyetmez B, Ozkan-Seyhan T et al. Comparison of the effects of thoracic and lumbar epidural anaesthesia on induction and maintenance doses of propofol during total i.v. anaesthesia. *Br J Anaesth* 2008; 101:255-260.
5. Agarwal A, Pandey R, Dhiraaj S et al. The effect of epidural bupivacaine on induction and maintenance doses of propofol (evaluated by bispectral index) and maintenance doses of fentanyl and vecuronium. *Anesth Analg* 2004; 99:1684-1688, table of contents.
6. Dumans-Nizard V, Le Guen M, Sage E, Chazot T, Fischler M, Liu N. Thoracic Epidural Analgesia With Levobupivacaine Reduces Remifentanyl and Propofol Consumption Evaluated by Closed-Loop Titration Guided by the Bispectral Index: A Double-Blind Placebo-Controlled Study. *Anesth Analg* 2017; 125:635-642.
7. Xiang Y, Chen CQ, Chen HJ, Li M, Bao FP, Zhu SM. The effect of epidural lidocaine administration on sedation of propofol general anesthesia: a randomized trial. *J Clin Anesth* 2014; 26:523-529.
8. Ozkan-Seyhan T, Sungur MO, Senturk E et al. BIS guided sedation with propofol during spinal anaesthesia: influence of anaesthetic level on sedation requirement. *Br J Anaesth* 2006; 96:645-649.
9. Valverde A, Doherty TJ, Hernandez J, Davies W. Effect of lidocaine on the minimum alveolar concentration of isoflurane in dogs. *Vet Anaesth Analg* 2004; 31:264-271.
10. Foffani G, Humanes-Valera D, Calderon-Munoz F, Oliviero A, Aguilar J. Spinal cord injury immediately decreases anesthetic requirements in rats. *Spinal Cord* 2011; 49:822-826.
11. Pollock JE, Neal JM, Liu SS, Burkhead D, Polissar N. Sedation during spinal anesthesia. *Anesthesiology* 2000; 93:728-734.
12. Antognini JF, Jinks SL, Atherley R, Clayton C, Carstens E. Spinal anaesthesia indirectly depresses cortical activity associated with electrical stimulation of the reticular formation. *Br J Anaesth* 2003; 91:233-238.
13. Doufas AG, Wadhwa A, Shah YM, Lin CM, Haugh GS, Sessler DI. Block-dependent sedation during epidural anaesthesia is associated with delayed brainstem conduction. *Br J Anaesth* 2004; 93:228-234.
14. Lanier WL, Iazzo PA, Milde JH, Sharbrough FW. The cerebral and systemic effects of movement in response to a noxious stimulus in lightly anesthetized dogs. Possible modulation of cerebral function by muscle afferents. *Anesthesiology* 1994; 80:392-401.
15. Sitsen E, Olofsen E, Lesman A, Dahan A, Vuyk J. Epidural Blockade Affects the Pharmacokinetics of Propofol in Surgical Patients. *Anesth Analg* 2016; 122:1341-1349.

16. Marsh B, White M, Morton N, Kenny GN. Pharmacokinetic model driven infusion of propofol in children. *Br J Anaesth* 1991; 67:41-48.
17. Ishiyama T, Kashimoto S, Oguchi T, Yamaguchi T, Okuyama K, Kumazawa T. Epidural ropivacaine anesthesia decreases the bispectral index during the awake phase and sevoflurane general anesthesia. *Anesth Analg* 2005; 100:728-732, table of contents.
18. Hodgson PS, Liu SS. Epidural lidocaine decreases sevoflurane requirement for adequate depth of anesthesia as measured by the Bispectral Index monitor. *Anesthesiology* 2001; 94:799-803.
19. Zhang J, Zhang W, Li B. The effect of epidural anesthesia with different concentrations of ropivacaine on sevoflurane requirements. *Anesth Analg* 2007; 104:984-986.
20. Aguilar J, Humanes-Valera D, Alonso-Calvino E et al. Spinal cord injury immediately changes the state of the brain. *J Neurosci* 2010; 30:7528-7537.
21. Niesters M, Sitsen E, Oudejans L et al. Effect of deafferentation from spinal anesthesia on pain sensitivity and resting-state functional brain connectivity in healthy male volunteers. *Brain Connect* 2014; 4:404-416.
22. Bjorkman A, Rosen B, van Westen D, Larsson EM, Lundborg G. Acute improvement of contralateral hand function after deafferentation. *Neuroreport* 2004; 15:1861-1865.
23. Bjorkman A, Rosen B, Lundborg G. Acute improvement of hand sensibility after selective ipsilateral cutaneous forearm anaesthesia. *Eur J Neurosci* 2004; 20:2733-2736.
24. Flor H, Nikolajsen L, Staehelin Jensen T. Phantom limb pain: a case of maladaptive CNS plasticity? *Nat Rev Neurosci* 2006; 7:873-881.
25. Kazama T, Ikeda K, Morita K et al. Comparison of the effect-site  $k(eO)s$  of propofol for blood pressure and EEG bispectral index in elderly and younger patients. *Anesthesiology* 1999; 90:1517-1527.
26. Masui K, Kira M, Kazama T, Hagihira S, Mortier EP, Struys MM. Early phase pharmacokinetics but not pharmacodynamics are influenced by propofol infusion rate. *Anesthesiology* 2009; 111:805-817.
27. Masui K, Upton RN, Doufas AG et al. The performance of compartmental and physiologically based recirculatory pharmacokinetic models for propofol: a comparison using bolus, continuous, and target-controlled infusion data. *Anesth Analg* 2010; 111:368-379.
28. Eleveld DJ, Colin P, Absalom AR, Struys M. Pharmacokinetic-pharmacodynamic model for propofol for broad application in anaesthesia and sedation. *Br J Anaesth* 2018; 120:942-959.







# Chapter 4

**No interactive effect of lumbar epidural blockade and target-controlled infusion of propofol on mean arterial pressure, cardiac output and bispectral index;  
*A randomised controlled and pharmacodynamic modelling study***

Elske Sitsen, Erik Olofsen, Albert Dahan and Jaap Vuyk

*Eur J Anaesthesiol* 2021; 38:1-9

## Introduction

Epidural blockade is offered to patients to provide intra- and postoperative analgesia. In the presence of a neuraxial blockade the intraoperative intravenous hypnotic and volatile anaesthetic agent dose requirements for adequate anaesthesia or sedation are reduced by about 25-62%.<sup>1-9</sup> In prior research a higher level of blocked segments induced by spinal or epidural anaesthesia results in a lower induction and maintenance dose of propofol to reach a certain level of sedation guided by the bispectral index monitor.<sup>1, 3, 5, 7, 8</sup> In animal experiments a transection of the spinal cord resulted in a decrease in anaesthetic requirements.<sup>10</sup> The general proposed explanation is a pharmacodynamic effect of epidural or spinal anaesthesia at supraspinal brain sites, whereby the reduction of afferent sensory input to the central nervous system, also known as deafferentation, is thought to mitigate this hypnotic-sparing effect.<sup>11-14</sup>

We recently studied the influence of epidural blockade on the pharmacokinetics of propofol. We hypothesized that the hemodynamic alterations associated with epidural blockade may affect the distribution, redistribution or clearance of propofol, a drug known for its lipophilicity and high hepatic extraction ratio. At an epidural ropivacaine dose that blocks up to 20 spinal segments, the propofol dosage for adequate hypnosis was reduced by 30% compared to a condition in which no epidural blockade was present. This is mainly the result of an epidural-induced reduction in propofol clearance from 2.6 to 1.9 L/min and consequently higher propofol concentrations in plasma. The reduction of hepatic and renal blood flow by the epidural anaesthetic best explains this pharmacokinetic interaction.<sup>15</sup>

Apart from a pharmacokinetic interaction, an additive pharmacodynamic interaction between epidural anaesthesia and propofol is also plausible, in line with prior research and the concept of spinal epidural-induced deafferentation. In the current analysis, we therefore quantified the influence of epidural blockade on propofol-induced changes in arousal state (as measured by bispectral index) and haemodynamics (mean arterial pressure and cardiac output). We hypothesize that, apart from the above mentioned pharmacokinetic effect, epidural anaesthesia will affect propofol pharmacodynamics.

## Materials and Methods

### Subjects

Ethical approval for this study (Ethical Committee Leiden P10.087) was provided by the Ethical Committee of Leiden University Medical Centre, Leiden, The Netherlands (Chairperson Prof. R. Willemze) on 28 July 2010. Written informed consent was obtained from all subjects participating in the trial. Twenty-eight American Society of Anaesthesiologists status I or II patients, aged 18-65 years, scheduled for elective surgical procedures that required epidural anaesthesia, participated in this study, as previously described<sup>15</sup>. This is a secondary analysis of an earlier published data set on the pharmacokinetic interactive effects of lumbar epidural anaesthesia and propofol TCI.<sup>15</sup>

### Study design

The study had a randomized, double-blind, parallel design. The 28 patients were randomly assigned to one of four study groups of 7 patients each. None of the patients received preoperative premedication. An intravenous line was placed in the forearm for administration of medication and fluids, and a second line for the infusion of propofol. Apart from standard monitoring, which included bispectral index monitoring (BIS VISTA) using a head electrode as specified by the manufacturer, an arterial line was placed in the left or right radial artery for blood sampling and continuous measurement of blood pressure. Furthermore, the cardiac output was calculated using the pulse-contour methodology from the intra-arterial blood pressure curve using the Vigileo device (Edwards Life Sciences, USA).

A lumbar epidural catheter was inserted at spinal level L2-L3 or L3-L4; the catheter was placed 5 cm into the epidural space. After baseline data were collected, the study drug was injected through the epidural catheter. Patients were randomized according to a computer-generated randomization list to receive placebo or one of three doses of the study drug (ropivacaine 7.5 mg/mL): Group 1, placebo (10 ml NaCl 0.9%); group 2, ropivacaine 50 mg; Group 3 ropivacaine 100 mg, Group 4 ropivacaine 150 mg. The study drug was administered by an anaesthesia nurse who took no further part in the study. After epidural anaesthetic level had stabilized, propofol was infused using a Base Primea® TCI system (Fresenius Vial Infusion Technology, France). The infusion algorithm was based on the propofol pharmacokinetic parameters reported by Marsh et al<sup>6</sup>. The initial propofol plasma concentration target was 1 µg/mL. After 6, 12 and 18 min the target concentration was increased to 2.5 µg/mL, 4 µg/mL and 6 µg/mL. The propofol infusion ended 24 min after its start. During the study period, 1-min averages of the three study endpoints, mean arterial pressure, bispectral index and cardiac output, were collected from baseline (prior to the epidural injection) until 2 hours after the start of the propofol infusion and stored in the patient data monitoring system (Metavision, iMD-Soft, Netherlands) for later analysis. Surgery started after the patients finished the study.

Arterial blood samples for blood propofol concentration measurement were taken at 3, 6, 9, 12, 15, 18, 21 and 24 min after the start of the propofol infusion, and at 2, 5, 10, 20, 30, 60, 90, 120 and 150 min after infusion ended. A blank blood sample (10 ml) was first obtained and used for calibration purposes. Propofol concentrations in blood were measured as described previously.<sup>15</sup>

### Pharmacodynamic modelling and covariate selection

The data were analysed using NONMEM version 7.4.1 (Icon plc., Gaithersburg, MD, USA) using the First-Order Conditional Estimation with Interaction method. Blood concentration versus time profiles were calculated for each subject using the empirical Bayesian parameter estimates from the earlier published pharmacokinetic study.<sup>15</sup> These were linked to the sedative and hemodynamic parameters using a sigmoid- $E_{MAX}$  model of the form:

$$\text{Effect}(t) = \text{BLN} + (E_{\text{MAX}} - \text{BLN}) \times [C_E(t)^{\gamma} / (C_{50}^{\gamma} + C_E(t)^{\gamma})]$$

where BLN is the effect at baseline,  $E_{MAX}$  the maximum predicted effect,  $C_{50}$  the concentration where the effect is halfway between BLN and  $E_{MAX}$ , and  $\gamma$  a steepness parameter. Relative to the plasma propofol concentration, the effect-site concentration  $C_E(t)$  was assumed to be delayed with half-life factor  $t_{1/2}k_{eo}$ , i.e. the blood-effect site half-life. Because of effects on haemodynamics of waking up, hemodynamic data were excluded when BIS exceeded baseline minus one.

The influence of two covariates was explored: the ropivacaine dose (ROPI), and the number of blocked segments (NBS). These were assumed to possibly affect parameters  $C_{50}$ , BLN,  $E_{MAX}$ , or shift the curve (affecting both BLN and  $E_{MAX}$ ) by multiplying these parameters by factors  $\exp(\alpha*(NBS/10-1))$  or  $\exp(\alpha*(ROPI/75-1))$ , where  $\alpha$  is a covariate coefficient measuring the strength of the covariate influence. A change in the minimum value of the objective function (MVOF) of 6.61 was required for a covariate coefficient to have statistically significant influence (corresponding to  $P < 0.01$ ).

### Simulations

The influence of epidural blockade on the effect of propofol on mean arterial pressure and bispectral index was explored by simulating a single intravenous bolus dose of 2 mg/kg propofol, and a propofol bolus dose (2 mg/kg) followed by a 120 min propofol infusion of 8 mg.kg<sup>-1</sup>.h<sup>-1</sup> for a 70 kg patient.

### Results

The patients were recruited between December 2010 and February 2012. All 28 patients (17 men, 11 women) completed the study without adverse events and surgery started after the study period. The patients were aged  $44.9 \pm 15.1$  years (mean  $\pm$  SD), with body weight of  $77.9 \pm 10.6$  kg, height of  $177.6 \pm 11.1$  cm and body mass index of  $24.8 \pm 2.9$  kg/m<sup>2</sup>. All patients were classified as American Society of Anaesthesiologists class I or II. With the epidural ropivacaine dose increasing from 0 to 150 mg, the number of blocked segments (median [range]) increased from 0 [0-3] after placebo to 9 [3-15] after 50 mg ropivacaine, 12 [9-14] after 100 mg ropivacaine and 15.5 [6-21] after 150 mg ropivacaine. In Figure 1 the individual data of the effect of propofol on mean arterial pressure, cardiac output and bispectral index without epidural anaesthesia (panels A-C), following epidural injection of 50 mg ropivacaine (panels D-F), following epidural injection of 100 mg ropivacaine (panels G-I) and following epidural injection of 150 mg ropivacaine (panels J-L) are given. Prior to propofol infusion, the epidural blockade reduced mean arterial pressure from  $103 \pm 17$  mmHg (0 mg ropivacaine) to  $76 \pm 18.7$  mmHg (150 mg ropivacaine), without affecting bispectral index and cardiac output (Fig. 1 panels D-L,  $t = -30$  to 0 min). In patients that received placebo rather than ropivacaine, propofol reduced the bispectral index from  $97.6 \pm 0.5$  to  $25.7 \pm 7.5$ , mean arterial pressure from  $100 \pm 20.8$  to  $59 \pm 10.1$  mmHg, and cardiac output from  $9.8 \pm 2.7$  to  $5.65 \pm 2.1$  L/min (Fig. 1A-C). We compared the decrease of the mean of CO, MAP and BIS values of the 4 groups from reference value before epidural injection till end of propofol infusion. The ropivacaine dose does not significantly influence the final decrease.

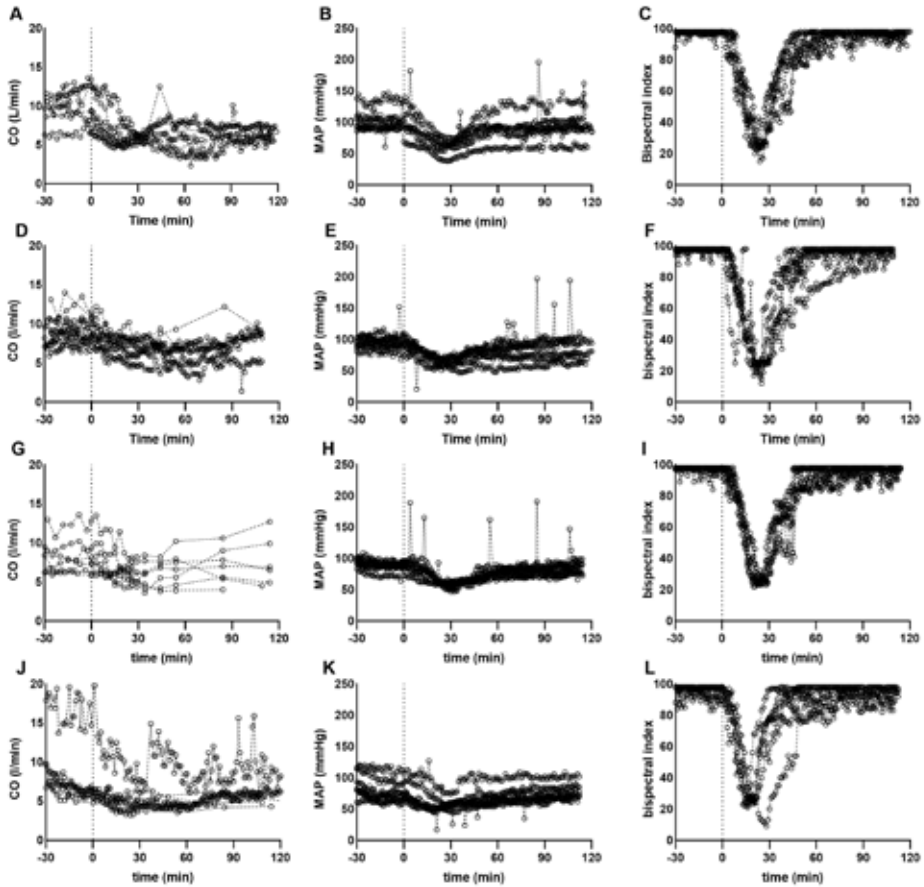


Figure 1. Individual 1-min averages of cardiac output (CO), mean arterial pressure (MAP) and bispectral index following epidural placebo (A-C), 50 mg epidural ropivacaine (D-F), 100 mg ropivacaine (G-I) and 150 mg ropivacaine (J-L).

### Pharmacodynamic model analyses

Best, median and worst data fits of three patients are given in Figure 2, based upon the coefficient of determination ( $R^2$ ) obtained from mean arterial pressure. Goodness of fit plots are given in Figure 3. Based upon the data fits and goodness of fit plots we conclude that all three endpoints were well described by the pharmacodynamic models. Table 1 gives the pharmacodynamic model estimates. For mean arterial pressure, adding covariates NBS or ROPI resulted in a decrease of the objective function value by 17 and 13 points, respectively. The best model was obtained with covariate NBS affecting BLN and  $E_{MAX}$  simultaneously with  $\alpha = -0.17 \pm 0.03$  (Table 1); combining NBS and ROPI did not further improve the model. This indicates that the epidural blockade caused a downward shift of the propofol concentration-mean arterial pressure data without affecting propofol potency parameter  $C_{50}$ . Similarly, the two covariates had no effect on propofol  $C_{50}$  for bispectral index or cardiac output.  $C_{50}$  values

for bispectral index and mean arterial pressure were of the same order of magnitude, while the effect of propofol on cardiac output was more potent ( $C_{50}$  value about one-fifth of the values of bispectral index and mean arterial pressure). The absence of significant interactions between epidural anaesthesia and propofol pharmacodynamics is further illustrated by the response surfaces analyses (Figure 4). Finally, epidural blockade had no effect on the effect-site equilibration half-life of propofol for its hemodynamic effects ( $t_{1/2}k_{eo} = 11.5 \pm 0.5$  min), nor for its effects on the bispectral index ( $t_{1/2}k_{eo} = 4.6 \pm 0.4$  min).

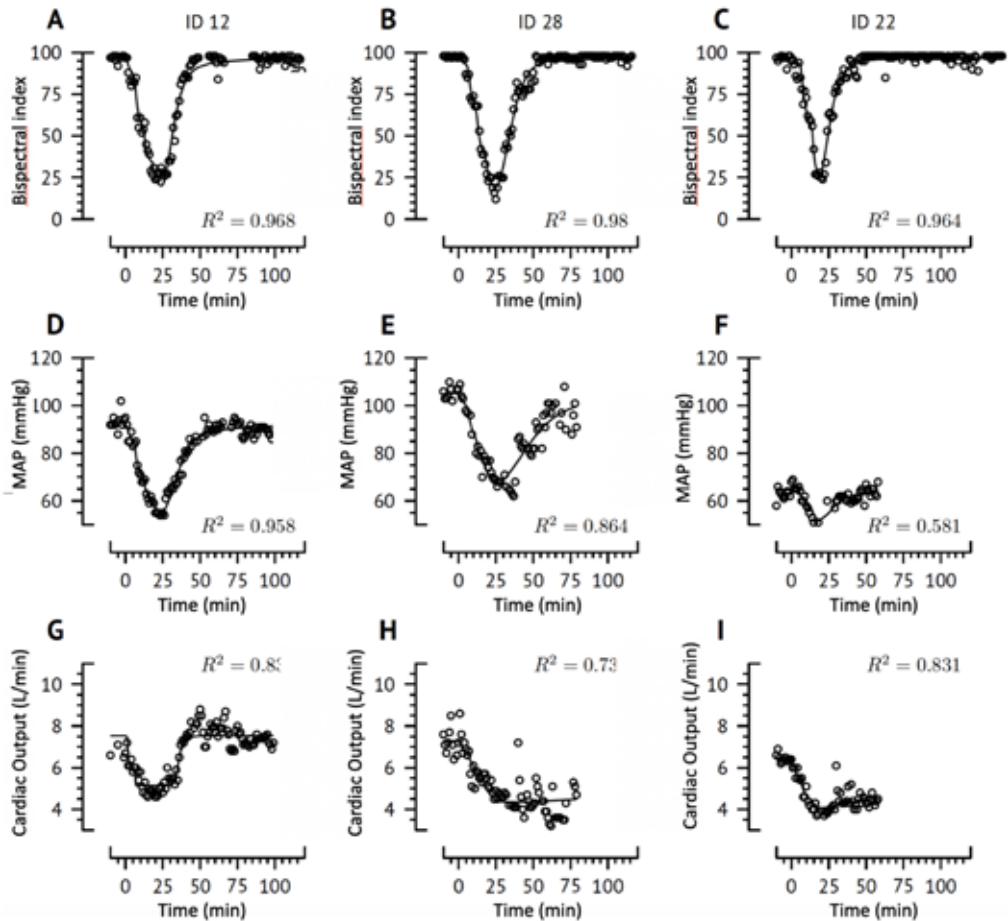


Figure 2. Best, median and worst data fits as determined by the coefficient of variation ( $R^2$ ) of three patients. A-C: bispectral index, D-F: mean arterial pressure (MAP) and G-I cardiac output. The goodness of fit was determined based on the  $R^2$  for mean arterial pressure. For bispectral index and cardiac output, the data are presented of the same patients as for mean arterial pressure. The dots represent the individual measured data, the solid lines represent the final model fits.



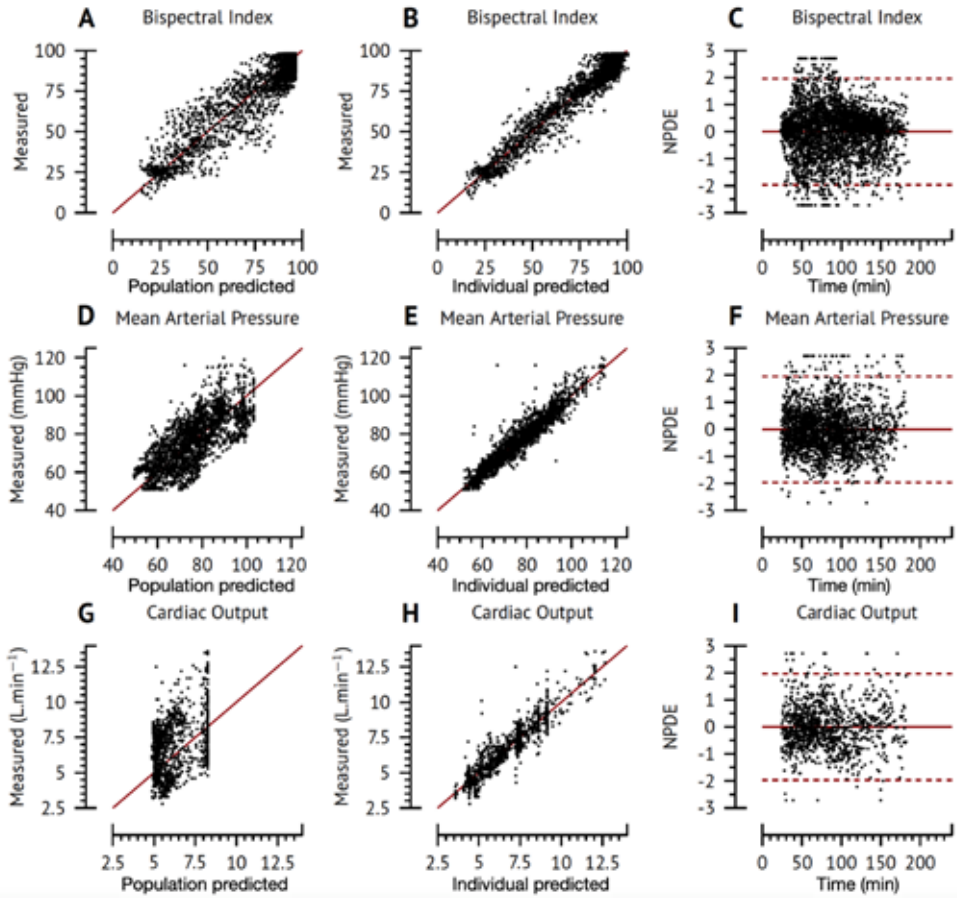


Figure 3. Goodness of fit plots for bispectral index (A-C), mean arterial pressure (D-F) and cardiac output (G-I). A, D and G: measured data versus population predicted data; B, E and H: measured versus individual predicted data; C, F and I: normalized prediction distribution errors (NPDE) versus time. The solid red lines are the lines of identity.

Table 1. Pharmacodynamic parameters of propofol with respect to its effect on bispectral index, mean arterial pressure and cardiac output.

<b>Bispectral Index</b>				
	Estimate	SEE	$\omega^2$	SEE
BLN	96.6	0.46	0.0006	0.0002
Emax	0	#		
C <sub>50</sub>	2.92	0.10	0.04	0.01
t <sub>½</sub> k <sub>eo</sub> (min)	4.63	0.38	0.17	0.06
$\gamma$	1.97	0.11	0.07	0.04
<b>Mean arterial pressure</b>				
	Estimate	SEE	$\omega^2$	SEE
BLN	87.5	0.90	0.008	0.002
Emax	43.1	3.64	0.06	0.03
C <sub>50</sub>	2.12	0.20	0.08	0.04
t <sub>½</sub> k <sub>eo</sub> (min)	11.5	0.50	0.33	0.08
$\gamma$	1.49	0.12	0.29	0.09
$\alpha$	-0.17	0.03		
<b>Cardiac output</b>				
	Estimate	SEE	$\omega^2$	SEE
BLN	8.27	0.37	0.06	0.02
Emax	4.57	0.18	0.17	0.13
C <sub>50</sub>	0.64	0.02	0.18	0.19
t <sub>½</sub> k <sub>eo</sub> (min)	29.8	0.82	1.82	0.59
$\gamma$	1.73	0.14	1.31	0.56

BLN = baseline value, Emax = maximal effect, C<sub>50</sub> = 50% of maximal effect, t<sub>½</sub>k<sub>eo</sub> = blood-effect site equilibration half-life,  $\gamma$  = parameter defining the steepness of the Emax curve,  $\alpha$  = interaction parameter characterizing the influence of epidural blocked segments, SEE = standard error of the estimate.  $\omega^2$  = between-subject variability.

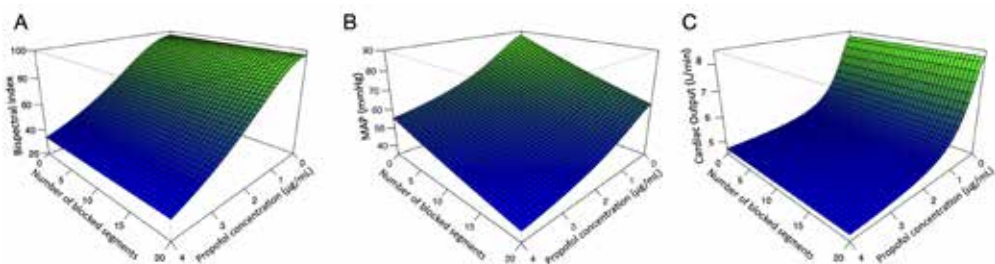


Figure 4. Response surfaces determined from the pharmacokinetic-pharmacodynamic analyses visualizing the interaction between the number of blocked segments (z-axis, NBS) and the measured propofol concentration (x-axis) for bispectral index (A), mean arterial pressure (MAP) (B) and cardiac output (C).

The results of the simulations of a propofol bolus and a bolus following by a 2 h infusion on propofol pharmacokinetics and pharmacodynamics (bispectral index and mean arterial

pressure) at 0, 10 and 20 blocked dermatomes are given in Figures 5. Following a propofol bolus, the epidural anaesthetic intensifies the effect of propofol on both endpoints (Fig. 5A-C). The epidural effect on bispectral index is probably due to the reduced clearance of propofol and thus the higher plasma propofol concentrations. The epidural effect on mean arterial pressure is related to the shift of the concentration-effect response (which is best explained by an epidural anaesthetic-induced reduction in sympathetic tone) and the higher plasma propofol concentrations. This same pattern becomes clear when propofol is given as bolus and continuous infusion (Fig. 5D-F). Bispectral index values are lower in the presence of an epidural block. Similarly, the epidural block causes a significant further reduction in mean arterial pressure, which only recovers slowly and partially after termination of propofol infusion.

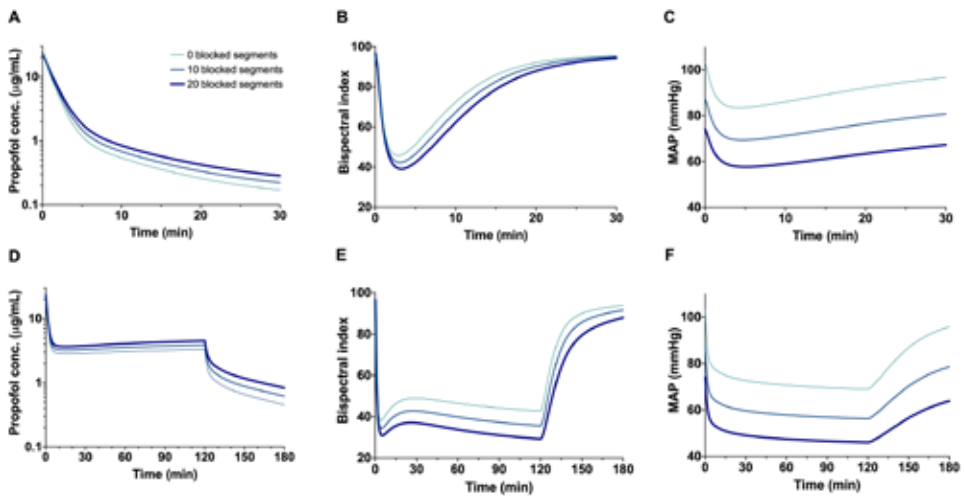


Figure 5. A-C. Simulations of the influence of 2 mg/kg intravenous bolus administration at 0, 10 and 20 blocked spinal segments. D-F. Simulations of the influence of 2 mg/kg intravenous bolus administration followed by a 2 hour infusion of  $8 \text{ mg} \cdot \text{kg}^{-1} \cdot \text{h}^{-1}$  at 0, 10 and 20 blocked spinal segments. Thin light green lines: 0 blocked segments, thin blue lines: 10 blocked segments, and thick blue lines 20 blocked segments. A. Propofol concentration; B. Bispectral index; C. mean arterial pressure (MAP).

## Discussion

We quantified the interaction of epidural anaesthesia and intravenous propofol by population pharmacokinetic-pharmacodynamic analyses before scheduled surgery (*i.e.* the study was performed without nociceptive stimuli). Epidural anaesthesia, up to 20 blocked dermatomes, did not affect propofol sensitivity (as determined by potency parameter  $C_{50}$ ) for mean arterial pressure, bispectral index or cardiac output and therefore had no significant pharmacodynamic interaction with propofol. We therefore refute the hypothesis that epidural anaesthesia changes propofol sensitivity for sedation, as measured by bispectral index. Any effect of epidural anaesthesia on the three studied endpoints is best explained by a pharmacokinetic epidural-propofol interaction.<sup>15</sup>

Several earlier studies showed that epidural anaesthesia is associated with the reduction of volatile agent concentration and propofol requirement for sedative endpoints. For example, these studies showed that in the presence of epidural anaesthesia, the dose of propofol required to reach a certain predetermined BIS level is reduced by up to 64%.<sup>4,5,7</sup> A similar reduction in dose requirements was found for volatile anaesthetics.<sup>17-19</sup> In these studies effective analgesia by spinal anaesthesia resulted in a reduction of propofol requirements during surgery but the haemodynamic values were kept in a predetermined range.<sup>3,8</sup> In other studies that were executed during surgery, in case of insufficient analgesia, opioids were subsequently added. In these cases, nociception with hemodynamic responses were present and also kept within predefined ranges. Also under these circumstances significant less hypnotics were necessary to maintain predefined BIS values.<sup>4-6</sup>

These studies do not allow separation of the underlying cause, *i.e.* we remain uninformed whether the observed reduced anaesthetic requirements are related to epidural anaesthesia-induced changes in anaesthetic pharmacokinetics or pharmacodynamics. The idea that a neuraxial blockade enhances the pharmacodynamic effects of anaesthetics is related to the observation that deafferentation or the disruption of afferent and efferent signals between the central and peripheral nervous system is associated with detectable functional changes at cortical and subcortical sites.<sup>12,14</sup> For example spinal cord injury produces abrupt irreversible deafferentation of cortical circuits leading to cortical reorganization.<sup>20</sup> These changes occur rapidly upon the induction of deafferentation and are related to neuronal adaptation and plasticity from rebalancing of excitatory and inhibitory neuronal processes upon the loss of afferent input. For example, spinal deafferentation is associated with a reduced pain threshold above the level of the anaesthetic block,<sup>21</sup> improved sensory or motor performance and, in case of maladaptive plasticity, phantom limb pain.<sup>22-24</sup> In case of epidural anaesthesia, *e.g.* temporary deafferentation, it was hypothesized that central changes in response to epidural deafferentation are responsible for enhanced anaesthetic sensitivity.

An earlier analysis of the current data set showed that epidural anaesthesia changed propofol pharmacokinetics with a 30% reduction of propofol elimination clearance. In the current analysis that focused on the interaction between epidural anaesthesia and propofol pharmacodynamics, the only significant finding was that epidural blockade lowers mean arterial pressure with increasing numbers of blocked segments and thereby aggravates the subsequent cardiovascular depression by propofol. No effect of epidural anaesthesia was observed on propofol sensitivity for its effect on mean arterial pressure, bispectral index or cardiac output. Consequently, we conclude that in our study epidural deafferentation (or any other central effect of epidural anaesthesia) is not causally related to the observation that anaesthetic requirement is reduced during epidural anaesthesia.

Our estimated pharmacodynamic parameters closely correspond with earlier findings.<sup>25-27</sup> In agreement with Kazama et al. the effect-site equilibration half-life of propofol for its effect on mean arterial pressure is considerably longer than for its effect on the bispectral index (11.5 versus 4.6 min). This suggests that after induction of anaesthesia the peak hemodynamic depression is delayed compared to the peak depressant effect of propofol on bispectral index. According to our simulations this delay in the peak depression in mean arterial pressure versus bispectral index is clinically negligible. In contrast, in the recovery phase, the bispectral index rapidly approaches baseline values, whereas mean arterial pressure remains depressed for a prolonged period of time, even at plasma propofol concentrations at which patient may be expected to have regained consciousness. This is partially explained by the prolonged effect-site equilibration half-life for mean arterial pressure depression, but may also related to the small difference in  $C_{50}$  between mean arterial pressure and bispectral index (2.12  $\mu\text{g}/\text{mL}$  versus 2.92  $\mu\text{g}/\text{mL}$ , Table 1). Figure 5 furthermore show that this prolonged depression of mean arterial pressure after propofol induction is aggravated by the epidural blockade of 10 and 20 blocked segments. In clinical practice, it is therefore expected that hemodynamic depression will persist even after return of consciousness and that this especially holds true in the presence of epidural blockade.

Our results have an important consequence for the performance of target-controlled infusion systems during epidural anaesthesia. When propofol is infused by TCI, the change in propofol concentration is easiest captured after a long infusion period, when distribution kinetics are no longer relevant and the infusion just compensates the clearance. In that case, the steady-state concentration equals infusion/clearance. The steady-state concentration is equal to the target concentration setting of the TCI system ( $C_{\text{Target}}$ ) when the clearance is as expected *i.e.*, without epidural anaesthesia. Substituting the covariate equation for the clearance from our pharmacokinetic study, we have:

$$C(\text{NBS}) = \text{infusion} / [2.22 \times \exp(-0.173 \times (\text{NBS}/10-1))],$$

with  $C_{\text{Target}}$  equals the propofol plasma concentration when there is no epidural blockade,  $C(\text{NBS}=0)$ . This may be rewritten as

$$C(\text{NBS}) = C_{\text{Target}} \times \exp(0.173 \times (\text{NBS}/10)).$$

So, with increasing numbers of blocked segments, the attained propofol concentration is increasingly higher than expected based on the TCI setting. At 20 blocked segments, the plasma concentration is 41% greater than expected.

Eleveld et al developed a pharmacokinetic/dynamic model based on a wide range of data from 30 studies, using BIS as endpoint. Local regional or regional techniques were present in 2 of the 30 included studies. The concomitant use of local anaesthetics can differ certain parameters in

the model. Number of blocked segments due to neuraxial blockade is not included as covariate in the model.<sup>28</sup>

In conclusion, in the presence of lumbar epidural blockade 30% less propofol is needed to reach and maintain adequate sedation, in our study conditions performed before surgery. This is unrelated to enhanced propofol sensitivity. The number of blocked segments after ropivacaine lumbar epidural injection aggravates the hemodynamic depressant effects of propofol directly, but also indirectly by reducing propofol elimination clearance leading to higher blood propofol concentration. Pharmacodynamic effects of combined lumbar ropivacaine and propofol TCI, measured by BIS monitoring, is unrelated to enhanced propofol sensitivity but limited to a pharmacokinetic phenomenon.

**Acknowledgements:**

Assistance with the study: We would like to thank René Mooren (BSc, Department Anaesthesiology, Leiden University Medical Centre, Leiden, The Netherlands) for the analysis of the blood propofol samples.

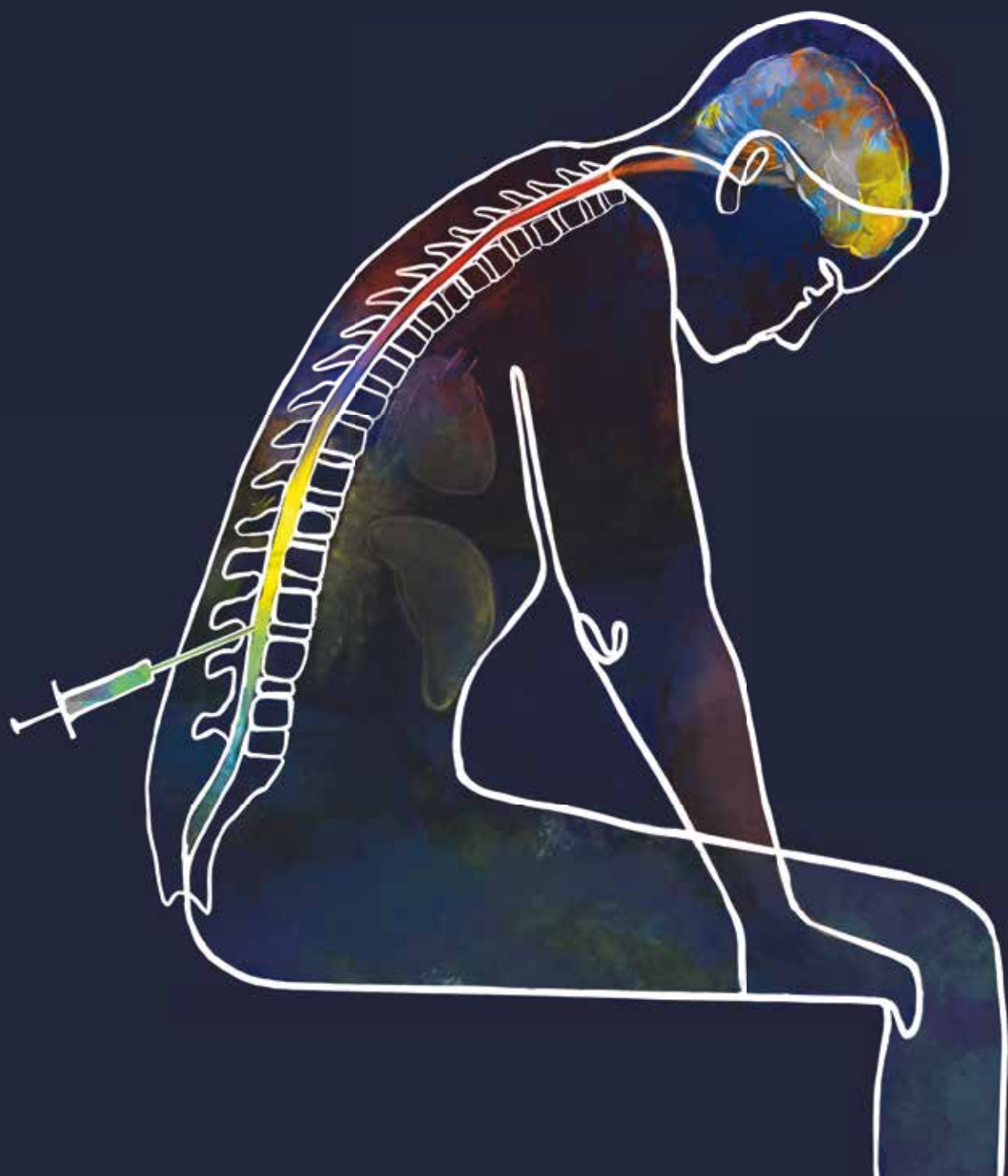
## References

1. Tverskoy M, Fleyshman G, Bachrak L, Ben-Shlomo I. Effect of bupivacaine-induced spinal block on the hypnotic requirement of propofol. *Anaesthesia* 1996; 51:652-653.
2. Tverskoy M, Shifrin V, Finger J, Fleyshman G, Kissin I. Effect of epidural bupivacaine block on midazolam hypnotic requirements. *Reg Anesth* 1996; 21:209-213.
3. Yang MK, Kim JA, Ahn HJ, Choi DH. Influence of the baricity of a local anaesthetic agent on sedation with propofol during spinal anaesthesia. *Br J Anaesth* 2007; 98:515-518.
4. Senturk M, Gucyetmez B, Ozkan-Seyhan T et al. Comparison of the effects of thoracic and lumbar epidural anaesthesia on induction and maintenance doses of propofol during total i.v. anaesthesia. *Br J Anaesth* 2008; 101:255-260.
5. Agarwal A, Pandey R, Dhiraaj S et al. The effect of epidural bupivacaine on induction and maintenance doses of propofol (evaluated by bispectral index) and maintenance doses of fentanyl and vecuronium. *Anesth Analg* 2004; 99:1684-1688, table of contents.
6. Dumans-Nizard V, Le Guen M, Sage E, Chazot T, Fischler M, Liu N. Thoracic Epidural Analgesia With Levobupivacaine Reduces Remifentanyl and Propofol Consumption Evaluated by Closed-Loop Titration Guided by the Bispectral Index: A Double-Blind Placebo-Controlled Study. *Anesth Analg* 2017; 125:635-642.
7. Xiang Y, Chen CQ, Chen HJ, Li M, Bao FP, Zhu SM. The effect of epidural lidocaine administration on sedation of propofol general anesthesia: a randomized trial. *J Clin Anesth* 2014; 26:523-529.
8. Ozkan-Seyhan T, Sungur MO, Senturk E et al. BIS guided sedation with propofol during spinal anaesthesia: influence of anaesthetic level on sedation requirement. *Br J Anaesth* 2006; 96:645-649.
9. Valverde A, Doherty TJ, Hernandez J, Davies W. Effect of lidocaine on the minimum alveolar concentration of isoflurane in dogs. *Vet Anaesth Analg* 2004; 31:264-271.
10. Foffani G, Humanes-Valera D, Calderon-Munoz F, Oliviero A, Aguilar J. Spinal cord injury immediately decreases anesthetic requirements in rats. *Spinal Cord* 2011; 49:822-826.
11. Pollock JE, Neal JM, Liu SS, Burkhead D, Polissar N. Sedation during spinal anesthesia. *Anesthesiology* 2000; 93:728-734.
12. Antognini JF, Jinks SL, Atherley R, Clayton C, Carstens E. Spinal anaesthesia indirectly depresses cortical activity associated with electrical stimulation of the reticular formation. *Br J Anaesth* 2003; 91:233-238.
13. Doufas AG, Wadhwa A, Shah YM, Lin CM, Haugh GS, Sessler DI. Block-dependent sedation during epidural anaesthesia is associated with delayed brainstem conduction. *Br J Anaesth* 2004; 93:228-234.
14. Lanier WL, Iazzo PA, Milde JH, Sharbrough FW. The cerebral and systemic effects of movement in response to a noxious stimulus in lightly anesthetized dogs. Possible modulation of cerebral function by muscle afferents. *Anesthesiology* 1994; 80:392-401.
15. Sitsen E, Olofsen E, Lesman A, Dahan A, Vuyk J. Epidural Blockade Affects the Pharmacokinetics of Propofol in Surgical Patients. *Anesth Analg* 2016; 122:1341-1349.

16. Marsh B, White M, Morton N, Kenny GN. Pharmacokinetic model driven infusion of propofol in children. *Br J Anaesth* 1991; 67:41-48.
17. Ishiyama T, Kashimoto S, Oguchi T, Yamaguchi T, Okuyama K, Kumazawa T. Epidural ropivacaine anesthesia decreases the bispectral index during the awake phase and sevoflurane general anesthesia. *Anesth Analg* 2005; 100:728-732, table of contents.
18. Hodgson PS, Liu SS. Epidural lidocaine decreases sevoflurane requirement for adequate depth of anesthesia as measured by the Bispectral Index monitor. *Anesthesiology* 2001; 94:799-803.
19. Zhang J, Zhang W, Li B. The effect of epidural anesthesia with different concentrations of ropivacaine on sevoflurane requirements. *Anesth Analg* 2007; 104:984-986.
20. Aguilar J, Humanes-Valera D, Alonso-Calvino E et al. Spinal cord injury immediately changes the state of the brain. *J Neurosci* 2010; 30:7528-7537.
21. Niesters M, Sitsen E, Oudejans L et al. Effect of deafferentation from spinal anesthesia on pain sensitivity and resting-state functional brain connectivity in healthy male volunteers. *Brain Connect* 2014; 4:404-416.
22. Bjorkman A, Rosen B, van Westen D, Larsson EM, Lundborg G. Acute improvement of contralateral hand function after deafferentation. *Neuroreport* 2004; 15:1861-1865.
23. Bjorkman A, Rosen B, Lundborg G. Acute improvement of hand sensibility after selective ipsilateral cutaneous forearm anaesthesia. *Eur J Neurosci* 2004; 20:2733-2736.
24. Flor H, Nikolajsen L, Staehelin Jensen T. Phantom limb pain: a case of maladaptive CNS plasticity? *Nat Rev Neurosci* 2006; 7:873-881.
25. Kazama T, Ikeda K, Morita K et al. Comparison of the effect-site  $k(eO)s$  of propofol for blood pressure and EEG bispectral index in elderly and younger patients. *Anesthesiology* 1999; 90:1517-1527.
26. Masui K, Kira M, Kazama T, Hagihira S, Mortier EP, Struys MM. Early phase pharmacokinetics but not pharmacodynamics are influenced by propofol infusion rate. *Anesthesiology* 2009; 111:805-817.
27. Masui K, Upton RN, Doufas AG et al. The performance of compartmental and physiologically based recirculatory pharmacokinetic models for propofol: a comparison using bolus, continuous, and target-controlled infusion data. *Anesth Analg* 2010; 111:368-379.
28. Eleveld DJ, Colin P, Absalom AR, Struys M. Pharmacokinetic-pharmacodynamic model for propofol for broad application in anaesthesia and sedation. *Br J Anaesth* 2018; 120:942-959.







Part 2

**Spinal anesthesia, pain  
perception and functional  
magnetic resonance  
imaging (fMRI) of the brain**



# Chapter 5

## Spinal anesthesia-induced deafferentation; resting-state functional brain connectivity and pain perception

E. Sitsen, M. de Rover, A. Dahan, M. Niesters  
Department of Anesthesiology, Leiden University Medical Center, The Netherlands

Adapted from

*Marieke Niesters, Elske Sitsen, Linda Oudejans, Jaap Vuyk, Leon P.H.J. Aarts, Serge A.R.B. Rombouts, Mischa de Rover, Najmeh Khalili-Mahani, and Albert Dahan. Effect of Deafferentation from Spinal Anesthesia on Pain Sensitivity and Resting-State Functional Brain Connectivity in Healthy Male Volunteers. Brain Connectivity 2014; Vol 4, 6.*

## Introduction

Deafferentation is the disruption of afferent and efferent signals between the central and peripheral nervous system.<sup>1</sup> Several experimental human and animal studies show that when peripheral sensory and motor input is removed (for example by application of ischemia or local anesthetic-induced nerve blocks, cutaneous anesthesia or peripheral nerve damage) detectable functional changes in the cortex occur.<sup>1,7</sup> One form of deafferentation that is performed yearly in millions of patients world-wide is spinal anesthesia where the sensory information from the lower part of the body is temporary removed to allow surgical intervention without the perception of pain.

The loss of sensory and motor input from the hand by peripheral nerve blockade is associated with supraspinal excitatory changes possibly mediated by disinhibition of unmasked (interhemispheric) cortical neuronal connections, and explains the enhanced functionality of the contralateral hand.<sup>3,6</sup> These cortical changes coincide often with perceptual changes. Also subcortical areas show changes upon deafferentation.<sup>1,8,9</sup> These changes are best described as reorganization of neuronal interactions due to a rebalancing of excitatory and inhibitory factors that mediate adaptation and neuronal plasticity.<sup>2,10</sup>

The use of central neuraxial blockade is associated with sedation, so could spinal anesthesia alone result in sedation.<sup>11</sup> The combination of epidural or spinal anesthesia with sedatives results in reduced dosing to achieve a certain level of sedation.<sup>12</sup> Even acute spinal cord injury leads to decreased dose requirements to achieve a certain level of sedation.<sup>13</sup> Research exploring the role of this sedative effect on the brain of decreased sensory and motor input and the influence of hemodynamic changes on brain function is not yet resolved. The plasticity of the brain and changes in functional outcome due to deafferentation could also play a role in the sedative effect. Some studies conclude the loss of neural input to the brain as potential driver of sedation, a downregulation of brainstem neural activity induced by deafferentation to be the driving cause of sedation.<sup>14-16</sup> One study of our hand, a pharmacokinetic study exploring the interaction of epidural blockade and propofol doses, showed a pure kinetic cause of the reduced dosing of propofol in the presence of an epidural block.<sup>17</sup>

It is well known that spinal anesthesia may coincide with sensory distortions. For example, some patients report body image distortions (such as swelling of the legs, illusionary limb position and changes of the length of the limbs) during regional (including spinal) anesthesia.<sup>18-20</sup> Additionally the affected limbs are often perceived as warm upon the administration of the local anesthetic while some patients perceive paradoxical heat sensation above the level of the anesthetic block (ie. a cold stimulus is perceived as warm) during the assessment of the spread of the spinal anesthetic.<sup>19,21</sup> These observations are typically made during the initial rapid rise of the anesthetic level and are suggestive of changes in central sensory modulation,

possibly related to the deafferentation from the spinal block. There is further the observation that epidural anesthesia (another form of deafferentation) can lead to occurrence of painful sensations in the deafferented area in an otherwise healthy individual.<sup>22</sup> Another observation was reactivation of phantom limb pain upon peripheral nerve block<sup>19, 23, 24</sup> Existing evidence presented above suggests that deafferentation from spinal anesthesia would lead to a change in functional organization of cortical and subcortical networks involved in sensory motor perception and pain.

A well-known paradigm to evaluate the efficacy of the endogenous pain modulatory system is “conditioned pain modulation” or CPM.<sup>25,26</sup> The CPM paradigm assumes that adding afferent nociceptive input at a remote area of the body inhibits the intensity of primary focal pain stimulus (“pain inhibits pain”) through activation of supra spinal centers including the anterior cingulate cortex (ACC), the insula and the prefrontal cortex. Therefore, it would be plausible that blockade of afferent input would have the reverse effect on pain perception. This means that if afferent input becomes “disconnected”, then pain perception would become more intense. However, there are no human studies assessing the effect of pain perception on areas remote from deafferentation sites (such as pain perception on the arm during spinal anesthesia). We aim to use this model of acute deafferentation by spinal anesthesia in healthy participants to further understand the mechanisms involved in endogenous modulation of pain.

Our placebo (sham-spinal anesthesia), crossover, randomized study investigates (1) whether we can detect a change in resting-state functional connectivity of brain networks involved in attention and/or awareness in healthy humans, and (2) whether pain perception above the level of the anesthetic is altered by spinal deafferentation. In the current study we obtained repeated resting-state functional magnetic resonance images (RS-fMRI) in two sessions (spinal and sham spinal peripheral anesthesia). It has been shown that this technique can be reliably used to evaluate alterations in intrinsic brain connectivity following pharmacological interventions in humans,<sup>27-30</sup> and deafferentation in rats.<sup>1</sup>

## Materials and Methods

### Subjects

Twelve right-handed, healthy, male volunteers (age 23,7 (3,4) year (mean (SD)); body mass index: 21,3 (2,4) kg/m<sup>2</sup>) were enrolled in the study after approval by the local institutional review board of the Leiden University Medical Center in Leiden, the Netherlands. All participants gave oral and written informed consent. The study was performed according to GCP guidelines and the ethical principles for medical research involving human subjects of the international Association of the Study of Pain ([www.iasp-pain.org/Education/Content.aspx?ItemNumber=1213](http://www.iasp-pain.org/Education/Content.aspx?ItemNumber=1213)) and according to the Declaration of Helsinki, ([www.wma.net/en/30publications/10policies/b3/](http://www.wma.net/en/30publications/10policies/b3/); amended in 2013). Before participation, all subjects were

screened to exclude the presence or history of any disease or their inability to maintain a regular diurnal rhythm, the presence or history of alcohol or drug abuse, the presence of metal implants (e.g., pacemaker, hip or knee prosthesis, cochlear implants, vessel clips) and claustrophobia. Additional exclusion included: < 18 or > 45 years of age, and a body mass index > 30 kg/m<sup>2</sup>. The study was registered in the Netherlands' Trial Register (NTR at [www.trialregister.nl](http://www.trialregister.nl)) under number NTR3491.

### **Study design**

The study was performed using a randomized crossover design. Upon arrival, an intravenous line was placed in the right hand or arm to allow fast administration of emergency medication when necessary. Next, baseline anatomical MRI (T1-weighted) and baseline resting-state functional MRI (RS-fMRI) scans were obtained followed by baseline heat pain measurements. After baseline measurements were complete, subjects received an intrathecal injection with a local anesthetic on one occasion and a sham procedure on the other as described below (time of injection is  $t = 0$ ). Responses to heat pain and the height of the sensory block (measured by the response to a cold 4 cm<sup>2</sup> surface applied to the skin in the left and right mid-axillary line) were measured at 15-min intervals. Additional RS-fMRI scans were obtained 1 and 2 hours after the spinal injection or the sham procedure. At the end of the study, subjects were monitored until fully recovered from the spinal anesthetic, as defined by return of motor functions and diuresis, and then allowed to go home.

### **Intrathecal injection and sham procedure**

The intrathecal injection was performed at the interspace between vertebrae L3 and L4 with 3 mL bupivacaine 5 mg/mL (AstraZeneca, Zoetermeer, the Netherlands) after the skin was locally infiltrated with 1-2 mL lidocaine 10 mg/mL (AstraZeneca, Zoetermeer, the Netherlands). For the spinal puncture a 27 Gauge Whitacre needle (Vygon, Valkenswaard, the Netherlands) was used to minimize the risk of post-spinal headache. The sham procedure was performed by insertion of a spinal needle at the interspace between vertebrae L3 and L4 through the skin, after the skin was locally infiltrated with 1-2 mL lidocaine 10 mg/mL. The dura mater was not punctured and no bupivacaine was injected. An independent anesthesiologist, who was not involved in conducting or analyzing other measurements made during the study, performed the injections. The instructions to the subject were similar on both occasions so that the subject and the investigators did not know which treatment was given at the moment of injection.

### **Pain assessment**

Heat pain was induced on the lower part of the left (ie. non-dominant) arm with a 3 x 3 cm thermal probe of the Pathway Neurosensory Analyzer (Medoc Ltd., Ramat Yishai, Israel). Baseline temperature was set at 32°C. During heat pain tests the temperature of the probe gradually increased (1.5°C/s) towards a pre-set destination temperature that was held constant for 30 seconds and then rapidly (6° C/s) returned to baseline temperature. To quantify



pain intensity of the heat pain stimulus, subjects rated the perceived pain stimulus using a computer-connected slider on an electrical potentiometer that ranged from 0 mm (no pain) to 100 mm (worst pain imaginable). This allowed for continuous electrical monitoring of the visual analogue scale during the noxious stimulation. The target temperature of the heat stimulus was determined at the start of each study day and was intended to evoke an electronic visual analogue scale (eVAS) of 40 mm. To evaluate pain responses after the intrathecal injection or sham procedures, pain tests were applied between imaging sessions at fixed time points:  $t = 15, 30, 45, 90, 105$  and 150 minutes.

### Resting-State functional Magnetic Resonance Imaging acquisition

A 3-Tesla Achieva Scanner (Philips Medical System, Best, The Netherlands) was used to acquire functional data at fixed time points (baseline,  $t = 60$  and  $t = 120$  min). The neuroimaging protocol included a high-resolution T1-weighted scan (repetition/echo time = 9.7/4.6 ms, flip angle = 8 degrees, 1 mm isotropic, 4 min) and 3 RS-fMRI series (each 220 T2\*-weighted whole-brain volumes, obtained with a gradient echo planar with repetition/echo time = 2180/30 ms, flip angle 80 degrees, 3.44 mm isotropic, duration 8 min; subjects were instructed to keep their eyes open and relax). A high resolution T2\*-weighted scan (~ 30 seconds) was acquired at the end of each repeated RS-fMRI in order to facilitate registering the functional data to the anatomical image.

### RS-fMRI analysis

Data analysis was performed with Functional Magnetic Resonance Imaging of the Brain Software Library (FSL 6.0.4, Oxford, United Kingdom, [www.fmrib.ox.ac.uk/fsl](http://www.fmrib.ox.ac.uk/fsl))<sup>31</sup>. Anatomical locations were determined using the Harvard-Oxford cortical and subcortical structures atlas integrated in FSL.

Preprocessing of fMRI images was carried out using FEAT (FMRI Expert Analysis Tool) Version 6.00, part of FSL. The following processing steps were applied: motion correction with affine image registration<sup>32</sup>, brain extraction<sup>33</sup>, spatial smoothing using a Gaussian kernel with a full width at a half maximum of 5 mm, and grand-mean intensity normalization of the entire 4D dataset by a single multiplicative factor. Non-smoothed fMRI data were used to estimate the registration parameters to transform fMRI scans into MNI152 standard space (T1 standard brain averaged over 152 participants; Montreal Neurological Institute, Montreal, QC, Canada;<sup>32, 34</sup> Images were coregistered with T1-weighted images using the Boundary-Based-Registration method,<sup>33, 35</sup> which in turn were non-linearly registered to MNI-152 standard space. Motion related artifacts were detected and removed using Automatic Removal of Motion Artifacts based on Independent Component Analysis (ICA-AROMA v0.3 beta). ICA-AROMA uses a data-driven approach to identify and remove independent components that represent motion related artifacts, while retaining the autocorrelation structure of the data.<sup>36, 37</sup> Next, the resulting denoised fMRI data were high-pass filtered using a 100 sec temporal filter and

registered to MNI-152 standard space using the registration parameters as derived from the non-smoothed data (in line with Pruim et al.<sup>36,37</sup>). Time series statistical analysis was carried out with local autocorrelation correction.<sup>38</sup>

Functional connectivity was assessed to evaluate the general effects of deafferentation from spinal anesthesia on functional brain connectivity, we used a model-free analysis of ten predefined networks of interest (NOIs) as previously described by Smith et al.<sup>39</sup> These networks are described based on their general function as the medial visual, occipital pole and lateral visual network, the default mode network, the cerebellum, the sensorimotor network, the auditory network, the executive control network, left and right frontoparietal network.<sup>39</sup> As we have previously shown for morphine, alcohol,  $\delta(9)$ -tetrahydrocannabinol and ketamine, RS-fMRI data analysis using resting state networks reveals localized and drug-specific changes in functional brain connectivity.<sup>27,28,29,30</sup>

The set of NOIs was used to generate subject-specific versions of the spatial maps, and associated timeseries, using dual regression.<sup>40</sup> First, for each subject, the NOIs are regressed (as spatial regressors in a multiple regression) into the subject's 4D space-time dataset. This results in a set of subject-specific timeseries, one per group-level spatial map. Next, those timeseries are regressed (as temporal regressors, again in a multiple regression) into the same 4D dataset, resulting in a set of subject-specific spatial maps, one per group-level spatial map. We then tested for [group differences, etc.] using FSL's randomise permutation-testing tool. Nuisance variables corresponding to fluctuations in the deep white matter (measured from the center of the corpus callosum) and cerebrospinal fluid (measured from the center of lateral ventricles) were included in the dual regression analysis to account for non-specific and physiological variations.<sup>41</sup> This resulted in statistical maps of z-scores, where each voxel of the brain represents the functional connectivity between that voxel and each of the NOIs. These statistical maps were later used for voxel-wise inference testing of the spinal anesthesia on each network.

### **Data, power and statistical analyses**

To determine the effect of deafferentation from spinal anesthesia on resting-state functional connectivity a mixed-effects analysis was applied with subject as random and time and drug as fixed within-subject variables. Voxel-wise statistical analysis on the z-score connectivity maps was performed using a permutation-based statistical inference with 5000 permutations. Statistical significance was set at  $p$ -value  $< 0.05$  after family wise error cluster-based correction (with cluster forming voxelwise thresholds set at  $p < 0.01$ ).<sup>42</sup> To further control for spurious effects, we report clusters that included a minimum of 10 adjacent voxels,  $80 \text{ mm}^3$ . In all stages of MRI analyses the FMRIB Software Library was used (FSL 6.0.4, Oxford, United Kingdom).<sup>31</sup>

To quantify pain intensity, the area-under-the-curve (AUC) of each eVAS response was calculated and presented relative to the baseline measurement.<sup>43</sup> The study was powered to detect a 50% treatment difference in the eVAS AUC at peak spinal level (estimated SD 35%,  $\alpha = 0.05$ ,  $1 - \beta = 0.9$ ).

The effect of spinal anesthesia on pain perception was tested by a repeated measures analysis of variance with post-hoc Bonferroni correction on the AUC values relative to baseline. The statistical analysis was performed in SigmaPlot version 12.0 (Systat Software Inc., Chicago, IL) and p-values < 0.05 were considered significant. Data are presented as mean (SEM) unless otherwise stated.

## Results

### Spinal anesthesia

All subjects completed the study without the occurrence of major side effects. Peak sensory blockade was achieved after 45 minutes with 17.5 (1.0) blocked segments corresponding to a sensory block level from dermatomes S5 to Th5. This sensory block persisted throughout the whole study period. The mean time of spinal anesthesia to full recovery of diuresis and motor function was 369 (11) minutes. No sensory blockade was observed after the sham procedure in any of the subjects. The spinal anesthetic and sham procedure did not result in significant cardiorespiratory changes. Blood pressure remained within 5% of control values. Due to the absence of spinal block following the sham procedure, blinding of the study was rapidly lost to both investigators and volunteers.

### Effect of spinal anesthesia on predefined general resting-state networks

Spinal anesthesia induced significant changes in functional connectivity in relation to one of the ten NOIs: the sensorimotor network. Regions that demonstrate functional connectivity changes in relation to this networks are given in Table 1 and Fig 3 and include primary motor cortex, superior frontal gyrus, supramarginal gyrus and frontal pole. Details regarding cluster size, z-score and location of the areas that show functional connectivity changes are provided in Table 1. Adding treatment order (sham first vs. spinal first) as a covariate to the statistical model did not affect the number, extent and location of these regions.

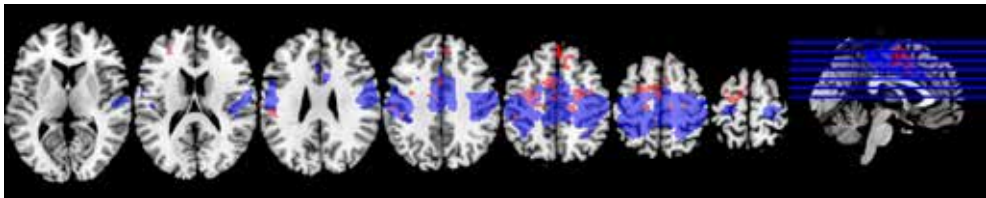


Figure 1: In blue the sensorimotor network of Smith et al. In red the voxels with significant increase in connectivity with the sensorimotor network due to spinal anesthesia.  $p < 0.05$  cluster corrected. Images are binarized Z-statistics thresholded at 2.3, masked for grey matter at 80%, and overlaid on the MNI-152 standard brain. Slices are displayed in radiological convention (left = right). All significant clusters are described in detail in Table 1.

Table 1. Effect of spinal anesthesia on functional connectivity in relation to the predefined general resting-state networks (cluster p-value < 0.05).

PNOI	Location	Cluster size (2 mm <sup>3</sup> voxels)	Peak Z-value	MNI coordinates (mm)		
				x	y	z
sensorimotor network. Includes: supplementary motor area (SMA), sensorimotor cortex, sec, sensory cortex	L primary motor cortex	1750	4.63	-18	-22	54
	*cluster also includes					
	<i>L Precentral gyrus</i>		4.41	-3	-6	44
	<i>L juxta positional lobule cortex</i>		4.35	-4	2	52
	<i>L sup frontal gyrus</i>		4.29	8	38	40
	R superior frontal gyrus	398	4.37	22	-4	50
	*cluster also includes					
	<i>R precentral gyrus</i>		4.17	24	-6	46
L supramarginal gyrus	204	3.99	-54	-26	30	
*cluster also includes						
L postcentral gyrus		3.55	-58	-22	36	
L frontal pole	25	4.12	-30	40	22	

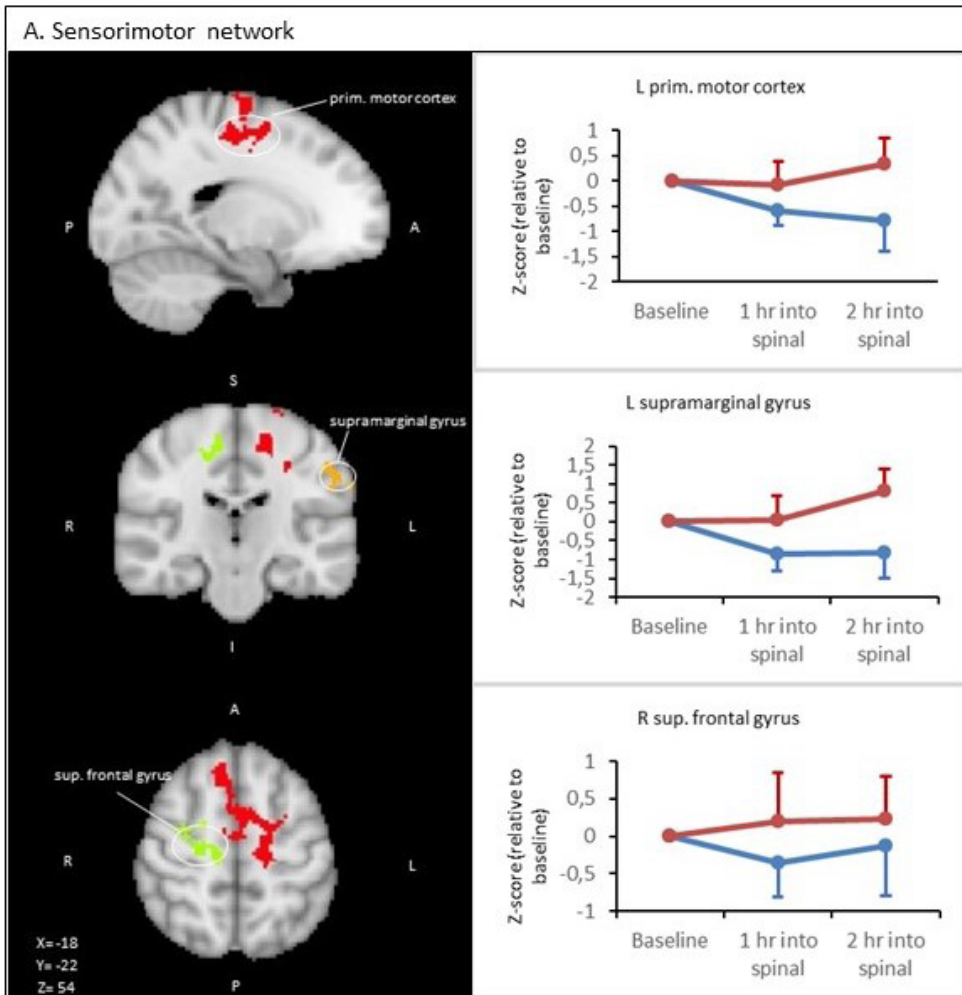


Fig 2. (A) Statistical connectivity map ( $p < 0.05$ ; cluster corrected) of the spinal anesthesia induced increase in resting-state network connectivity in relation to the sensorimotor network. (B) The effect of spinal anesthesia on connectivity over time is shown for the primary motor cortex, (C) the supramarginal gyrus, and (D) the superior frontal gyrus. Line: blue is placebo, red is spinal.

### Pain responses

The mean eVAS responses prior to treatment and at peak spinal anesthetic level and sham experiments are given in Figs. 3A and B. Spinal anesthesia significantly increased pain sensitivity on the skin of the lower forearm. Mean AUC values at baseline were 844.7 (63.2) mm/s on the study day with spinal injection and 898.6 (122.6) mm s on the day of the sham procedure ( $p = 0.644$ ). Mean AUC values at peak spinal level were 1165.0 (71.0) mm s after spinal injection and 877.1 (105.8) mm s after the sham procedure ( $p = 0.005$ ). Mean AUC values over time are shown in Fig. 3C showing that the hyperalgesic responses lasted for at least 3 hours (end of the study). There was no effect of study order on the pain AUC values (Fig. 3D).

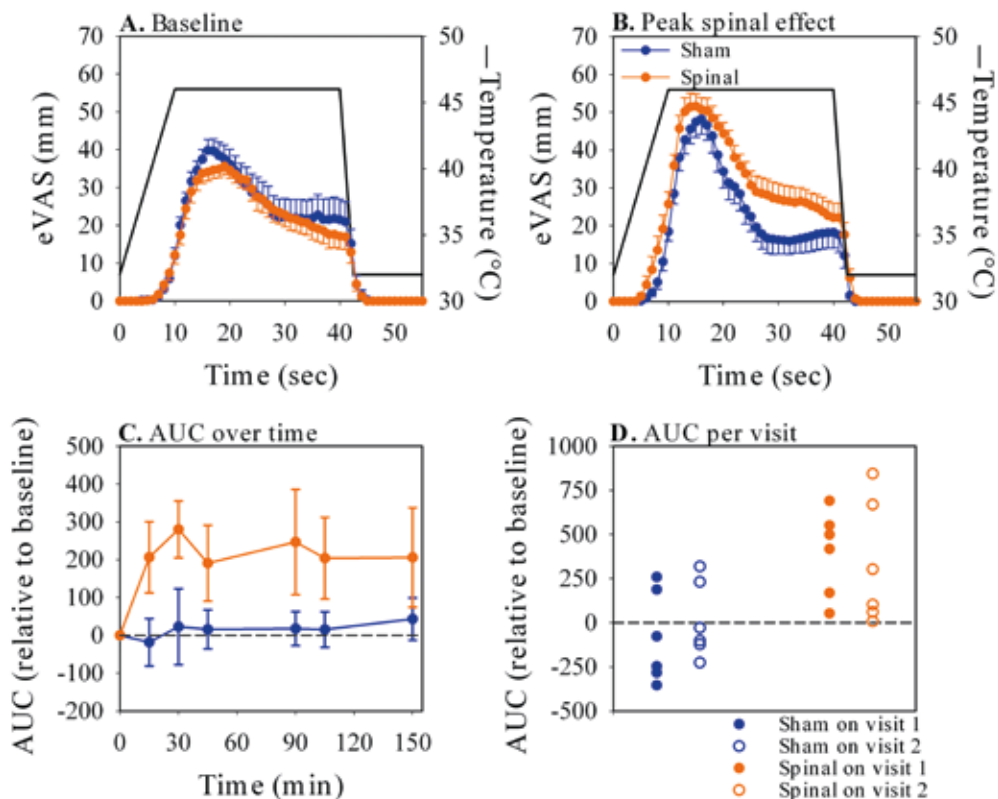


Figure 3. (A) Pain responses upon thermal stimulation (broken lines) on the skin of the lower arm at baseline and (B) at peak deafferentation effect (45 minutes). (C) Pain presented as area-under-the-curve (AUC) relative to baseline over the whole study period. The closed circles represent the pain sensitivity during spinal anesthesia; the open circles represent the pain perception after the sham procedure. Spinal anesthesia induced a significant increase in pain sensitivity ( $P < 0.001$ ). (D) Pain responses in subjects receiving sham (placebo) spinal treatment on visit 1 and spinal treatment on visit 2 (closed symbols), and in subjects in which the order of treatment was the reverse (open symbols). No order effect was observed. eVAS: electronic visual analogue scale.

## Discussion

Our hypothesis that spinal deafferentation would affect resting state networks involved in attention and or awareness was not confirmed. We only observed spinal deafferentation-induced connectivity changes in the sensorimotor network which is involved in the action-execution and perception-somesthesia paradigms (eg. supplementary motor area, sensorimotor cortex and secondary somatosensory cortex).<sup>39</sup>

Our second hypothesis that spinal deafferentation would enhance pain sensitivity was confirmed by our finding that nociceptive stimuli applied to dermatomes above the level of spinal deafferentation were perceived as hyperalgesic. This observation is suggestive of transient central cortical and subcortical changes in neuronal organization. These changes are associated with

warm and referred sensations, perceptual illusions, neuropathic pain and enhanced sensorimotor function of non-deafferented areas.<sup>5, 21, 22 4, 6, 19, 44</sup>

### **Effect of spinal deafferentation on resting state networks**

In the current study, the RS-fMRI technique was successfully used to evaluate deafferentation-induced changes in brain connectivity in awake humans. The changes in RSN connectivity induced by the symmetric spinal deafferentation included areas involved in the sensory discriminative components and motor areas.(see Table 1).

Our findings are in agreement with earlier animal and human studies showing that deafferentation of limbs is associated with changes in neuronal organization in the sensorimotor cortex.<sup>1, 7, 45</sup>

In our previous analysis published in 2014<sup>46</sup> we used the canonical networks of Beckmann et al.<sup>47</sup> These are described based on their general function as the medial and lateral visual network, the auditory and somatosensory network, the sensorimotor network, the default mode network, the executive salience network, the visual-spatial network, and the working memory network. The networks used in this re-analysis are an ICA based analysis of a database of nearly 30.000 subjects, resulting in 10 NOIs. The networks differ in number and brain regions involved which contributed to the difference in outcome of the analyses. Additionally, the method of preprocessing has improved over the years which may also have contributed to the differences in outcome in this relatively small group of subjects.

In two previous studies in an anesthetized rat model the effects of traumatic peripheral nerve- or spinal cord injury-related deafferentation were studied using RS-fMRI.<sup>1, 48</sup> Both studies show changes in connectivity between the thalamus and cortical and subcortical areas of the brain (eg. the primary somatosensory cortex). The authors argue that these changes are related to the loss of inhibitory influences within these brain neuronal networks. There is general agreement in the literature that deafferentation causes a rebalancing of excitatory and inhibitory neuronal activity towards disinhibition exposing formerly masked excitatory connections.<sup>3-6, 8, 48</sup> Krupa et al. further show that also feedback from cortex to thalamus plays an important role in plastic changes due to deafferentation.<sup>2, 9</sup> These deafferentation-related changes may be due to alterations in neuronal activity, such as due to reduced GABAergic inhibitory activity and/or enhanced glutamatergic excitatory activity, or due to changes in microcirculation, where reduced afferent input changes the neurovascular coupling.<sup>1, 10, 49</sup> Synaptic sprouting and development of structural changes between brain areas take more time to develop and seem to play a role in chronic deafferentation (in spinal cord injury (SCI), peripheral nerve injury or amputation).<sup>1, 50, 51</sup> Given the fact that we are unable to determine from the RS-fMRI analyses whether changes in connectivity coincide with increases or decreases in neuronal activity, attribution of the observed changes in RS-fMRI connectivity during spinal anesthesia to a shift from inhibitory towards excitatory nociceptive pathways is currently at best speculative.

We observed changes in connectivity of the primary motor cortex, superior frontal gyrus, supramarginal gyrus and frontal pole relative to the sensorimotor network. The reason for the selective association of spinal deafferentation with connectivity changes relative to these specific network cannot be deduced from our study. Possibly this networks is most sensitive to loss of peripheral afferent input. Irrespective of the mechanism, we argue that the observed change may cause specific behaviors like sedation, associated with neuraxial blockade. For example, epidural anesthesia is associated with block-height dependent sedation and reduced brainstem auditory evoked potentials.<sup>14, 52</sup> Further, several studies show that neuraxial blockade coincides with sedation and consequently reduced (volatile and intravenous) anesthetic requirements.<sup>12, 52</sup> These effects may be related to connectivity changes relative to the default mode network or attentional networks like the frontoparietal areas.<sup>53, 54</sup> Particularly the default mode network seems important in altered states of consciousness (anesthesia, coma, vegetative state, epileptic loss of consciousness and somnambulism).<sup>53-56</sup> The role of the sensorimotor network in sedation has scarcely been investigated, two studies showed increased functional connectivity during light sedation.<sup>56, 57</sup> We could not confirm with our study population the role of the sensorimotor network in sedative effects of deafferentation. Due to this limitation we cannot conclude whether in our population a change in arousal state occurred. Changes observed relative to the somatosensory network may be associated with nociceptive sensations (warm sensation/paradoxal heat sensation, and as observed here: hyperalgesia) and illusions of abnormal bodily position and recognition.<sup>19, 20</sup>

### **Blinding**

The inability of blinding the anesthetic treatment in both subjects and investigators in our study is inevitable with the procedure and paradigm in question. Anticipation is a critical aspect of subjective pain perception and it is plausible that awareness of subjects of the nature of the effect of the spinal injection could have affected the study outcome. We controlled for possible experimental order effects and debinding by including the order effect in our statistical model. In our small sample, we did not observe any order effect on the subjective scoring of pain intensity (Fig. 2D), nor did we find an effect on the RS-fMRI results. This, however, is not generalizable and some effect due to differences in the attention to the thermal pain in spinal vs. sham sessions cannot be excluded.<sup>58, 59</sup>

### **Conclusions**

Deafferentation from spinal anesthesia is associated with connectivity changes in the brain to the sensorimotor network. No influence was found on the default mode network and attentional networks. Furthermore, spinal anesthesia enhanced pain sensitivity. Changes observed relative to the somatosensory network may be associated with enhanced pain sensitivity.



## References

1. Pawela, C. P.; Biswal, B. B.; Hudetz, A. G.; Li, R.; Jones, S. R.; Cho, Y. R.; Matloub, H. S.; Hyde, J. S., Interhemispheric neuroplasticity following limb deafferentation detected by resting-state functional connectivity magnetic resonance imaging (fcMRI) and functional magnetic resonance imaging (fMRI). *Neuroimage* 2010, 49 (3), 2467-78.
2. Kaas, J. H., Is most of neural plasticity in the thalamus cortical? *Proc Natl Acad Sci U S A* 1999, 96 (14), 7622-3.
3. Weiss, T.; Miltner, W. H.; Liepert, J.; Meissner, W.; Taub, E., Rapid functional plasticity in the primary somatomotor cortex and perceptual changes after nerve block. *Eur J Neurosci* 2004, 20 (12), 3413-23.
4. Werhahn, K. J.; Mortensen, J.; Van Boven, R. W.; Zeuner, K. E.; Cohen, L. G., Enhanced tactile spatial acuity and cortical processing during acute hand deafferentation. *Nat Neurosci* 2002, 5 (10), 936-8.
5. Bjorkman, A.; Rosen, B.; Lundborg, G., Enhanced function in nerve-injured hands after contralateral deafferentation. *Neuroreport* 2005, 16 (5), 517-9.
6. Waberski, T. D.; Dieckhofer, A.; Remington, U.; Buchner, H.; Gobbele, R., Short-term cortical reorganization by deafferentation of the contralateral sensory cortex. *Neuroreport* 2007, 18 (11), 1199-203.
7. Melton, M. S.; Browndyke, J. N.; Harshbarger, T. B.; Madden, D. J.; Nielsen, K. C.; Klein, S. M., Changes in Brain Resting-state Functional Connectivity Associated with Peripheral Nerve Block: A Pilot Study. *Anesthesiology* 2016, 125 (2), 368-77.
8. Faggin, B. M.; Nguyen, K. T.; Nicolelis, M. A., Immediate and simultaneous sensory reorganization at cortical and subcortical levels of the somatosensory system. *Proc Natl Acad Sci U S A* 1997, 94 (17), 9428-33.
9. Krupa, D. J.; Ghazanfar, A. A.; Nicolelis, M. A., Immediate thalamic sensory plasticity depends on corticothalamic feedback. *Proc Natl Acad Sci U S A* 1999, 96 (14), 8200-5.
10. Levy, L. M.; Ziemann, U.; Chen, R.; Cohen, L. G., Rapid modulation of GABA in sensorimotor cortex induced by acute deafferentation. *Ann Neurol* 2002, 52 (6), 755-61.
11. Pollock, J. E.; Neal, J. M.; Liu, S. S.; Burkhead, D.; Polissar, N., Sedation during spinal anesthesia. *Anesthesiology* 2000, 93 (3), 728-34.
12. Hodgson, P. S.; Liu, S. S., Epidural lidocaine decreases sevoflurane requirement for adequate depth of anesthesia as measured by the Bispectral Index monitor. *Anesthesiology* 2001, 94 (5), 799-803.
13. Foffani, G.; Humanes-Valera, D.; Calderon-Munoz, F.; Oliviero, A.; Aguilar, J., Spinal cord injury immediately decreases anesthetic requirements in rats. *Spinal Cord* 2011, 49 (7), 822-6.
14. Doufas, A. G.; Wadhwa, A.; Shah, Y. M.; Lin, C. M.; Haugh, G. S.; Sessler, D. I., Block-dependent sedation during epidural anaesthesia is associated with delayed brainstem conduction. *Br J Anaesth* 2004, 93 (2), 228-34.

15. Jinks, S. L.; Dominguez, C. L.; Antognini, J. F., Drastic decrease in isoflurane minimum alveolar concentration and limb movement forces after thoracic spinal cooling and chronic spinal transection in rats. *Anesthesiology* 2005, 102 (3), 624-32.
16. Antognini, J. F.; Atherley, R.; Carstens, E., Isoflurane action in spinal cord indirectly depresses cortical activity associated with electrical stimulation of the reticular formation. *Anesth Analg* 2003, 96 (4), 999-1003, table of contents.
17. Sitsen, E.; Olofsen, E.; Lesman, A.; Dahan, A.; Vuyk, J., Epidural Blockade Affects the Pharmacokinetics of Propofol in Surgical Patients. *Anesth Analg* 2016, 122 (5), 1341-9.
18. Gandevia, S. C.; Phegan, C. M., Perceptual distortions of the human body image produced by local anaesthesia, pain and cutaneous stimulation. *J Physiol* 1999, 514 ( Pt 2), 609-16.
19. Paqueron, X.; Leguen, M.; Rosenthal, D.; Coriat, P.; Willer, J. C.; Danziger, N., The phenomenology of body image distortions induced by regional anaesthesia. *Brain* 2003, 126 (Pt 3), 702-12.
20. Silva, S.; Loubinoux, I.; Olivier, M.; Bataille, B.; Fourcade, O.; Samii, K.; Jeannerod, M.; Demonet, J. F., Impaired visual hand recognition in preoperative patients during brachial plexus anesthesia: importance of peripheral neural input for mental representation of the hand. *Anesthesiology* 2011, 114 (1), 126-34.
21. Kanai, A.; Niki, Y.; Hayashi, N.; Maeda, S.; Horie, K.; Okamoto, H., The Initial Subjective Sensory Change in the Dermatome During Intrathecal Injection of Plain Bupivacaine Predicts the Spread of Sensory Blockade: A Prospective Multi-Level Modeling Study. *Anesth Pain Med* 2019, 9 (5), e91216.
22. Mihic, D. N., Phantom limb pain during peridural anaesthesia. *Pain* 1981, 11 (2), 269-272.
23. Lee, E.; Donovan, K., Reactivation of phantom limb pain after combined interscalene brachial plexus block and general anesthesia: successful treatment with intravenous lidocaine. *Anesthesiology* 1995, 82 (1), 295-8.
24. Elkoundi, A.; Samali, M.; Meskine, A.; Bakkali, H.; Balkhi, H.; Bensghir, M., Transient phantom limb pain following high thoracic erector spinae plane block in an amputee. *Can J Anaesth* 2020, 67 (10), 1489-1490.
25. Dahan, A.; Niesters, M.; Sarton, E., Endogenous modulation of pain is visible in the brain. *Clin Neurophysiol* 2012, 123 (4), 642-3.
26. Ossipov, M. H.; Dussor, G. O.; Porreca, F., Central modulation of pain. *J Clin Invest* 2010, 120 (11), 3779-87.
27. Cole, D. M.; Beckmann, C. F.; Oei, N. Y.; Both, S.; van Gerven, J. M.; Rombouts, S. A., Differential and distributed effects of dopamine neuromodulations on resting-state network connectivity. *Neuroimage* 2013, 78, 59-67.
28. Khalili-Mahani, N.; Zoethout, R. M.; Beckmann, C. F.; Baerends, E.; de Kam, M. L.; Soeter, R. P.; Dahan, A.; van Buchem, M. A.; van Gerven, J. M.; Rombouts, S. A., Effects of morphine and alcohol on functional brain connectivity during "resting state": a placebo-controlled crossover study in healthy young men. *Hum Brain Mapp* 2012, 33 (5), 1003-18.

29. Klumpers, L. E.; Cole, D. M.; Khalili-Mahani, N.; Soeter, R. P.; Te Beek, E. T.; Rombouts, S. A.; van Gerven, J. M., Manipulating brain connectivity with delta(9)-tetrahydrocannabinol: a pharmacological resting state fMRI study. *Neuroimage* 2012, 63 (3), 1701-11.
30. Niesters, M.; Khalili-Mahani, N.; Martini, C.; Aarts, L.; van Gerven, J.; van Buchem, M. A.; Dahan, A.; Rombouts, S., Effect of subanesthetic ketamine on intrinsic functional brain connectivity: a placebo-controlled functional magnetic resonance imaging study in healthy male volunteers. *Anesthesiology* 2012, 117 (4), 868-77.
31. Smith, S. M.; Jenkinson, M.; Woolrich, M. W.; Beckmann, C. F.; Behrens, T. E. J.; Johansen-Berg, H.; Bannister, P. R.; De Luca, M.; Drobnjak, I.; Flitney, D. E.; Niazy, R. K.; Saunders, J.; Vickers, J.; Zhang, Y.; De Stefano, N.; Brady, J. M.; Matthews, P. M., Advances in functional and structural MR image analysis and implementation as FSL. *NeuroImage* 2004, 23 Suppl 1, S208-19.
32. Jenkinson, M.; Bannister, P.; Brady, M.; Smith, S., Improved optimization for the robust and accurate linear registration and motion correction of brain images. *Neuroimage* 2002, 17(2), 825-41.
33. Smith, S. M., Fast robust automated brain extraction. *Hum Brain Mapp* 2002, 17 (3), 143-55.
34. Jenkinson, M.; Smith, S., A global optimisation method for robust affine registration of brain images. *Med Image Anal* 2001, 5 (2), 143-56.
35. Greve, D. N.; Fischl, B., Accurate and robust brain image alignment using boundary-based registration. *NeuroImage* 2009, 48 (1), 63-72.
36. Pruim, R. H. R.; Mennes, M.; Buitelaar, J. K.; Beckmann, C. F., Evaluation of ICA-AROMA and alternative strategies for motion artifact removal in resting state fMRI. *Neuroimage* 2015, 112, 278-287.
37. Pruim, R. H. R.; Mennes, M.; van Rooij, D.; Llera, A.; Buitelaar, J. K.; Beckmann, C. F., ICA-AROMA: A robust ICA-based strategy for removing motion artifacts from fMRI data. *Neuroimage* 2015, 112, 267-277.
38. Woolrich, M. W.; Ripley, B. D.; Brady, M.; Smith, S. M., Temporal autocorrelation in univariate linear modeling of fMRI data. *Neuroimage* 2001, 14 (6), 1370-86.
39. Smith, S. M.; Fox, P. T.; Miller, K. L.; Glahn, D. C.; Fox, P. M.; Mackay, C. E.; Filippini, N.; Watkins, K. E.; Toro, R.; Laird, A. R.; Beckmann, C. F., Correspondence of the brain's functional architecture during activation and rest. *Proc Natl Acad Sci U S A* 2009, 106 (31), 13040-5.
40. Beckmann, C. F., Group comparison of resting-state fMRI data using multi-subject ICA and dual regression. *Neuroimage* 2009, 47(1), 148-156.
41. Birn, R. M., The role of physiological noise in resting-state functional connectivity. *Neuroimage* 2012, 62 (2), 864-70.
42. Forman, S. D.; Cohen, J. D.; Fitzgerald, M.; Eddy, W. F.; Mintun, M. A.; Noll, D. C., Improved assessment of significant activation in functional magnetic resonance imaging (fMRI): use of a cluster-size threshold. *Magn Reson Med* 1995, 33 (5), 636-47.

43. Niesters, M.; Dahan, A.; Swartjes, M.; Noppers, I.; Fillingim, R. B.; Aarts, L.; Sarton, E. Y., Effect of ketamine on endogenous pain modulation in healthy volunteers. *Pain* 2011, 152 (3), 656-663.
44. Rinaldi, P. C.; Young, R. F.; Albe-Fessard, D.; Chodakiewitz, J., Spontaneous neuronal hyperactivity in the medial and intralaminar thalamic nuclei of patients with deafferentation pain. *J Neurosurg* 1991, 74 (3), 415-21.
45. Metzler, J.; Marks, P. S., Functional changes in cat somatic sensory-motor cortex during short-term reversible epidural blocks. *Brain Res* 1979, 177 (2), 379-83.
46. Niesters, M.; Sitsen, E.; Oudejans, L.; Vuyk, J.; Aarts, L. P.; Rombouts, S. A.; de Rover, M.; Khalili-Mahani, N.; Dahan, A., Effect of deafferentation from spinal anesthesia on pain sensitivity and resting-state functional brain connectivity in healthy male volunteers. *Brain Connect* 2014, 4 (6), 404-16.
47. Beckmann, C. F.; DeLuca, M.; Devlin, J. T.; Smith, S. M., Investigations into resting-state connectivity using independent component analysis. *Philos Trans R Soc Lond B Biol Sci* 2005, 360 (1457), 1001-13.
48. Seminowicz, D. A.; Jiang, L.; Ji, Y.; Xu, S.; Gullapalli, R. P.; Masri, R., Thalamocortical asynchrony in conditions of spinal cord injury pain in rats. *J Neurosci* 2012, 32 (45), 15843-8.
49. Jacobs, K. M.; Donoghue, J. P., Reshaping the cortical motor map by unmasking latent intracortical connections. *Science* 1991, 251 (4996), 944-7.
50. Lundborg, G., Brain plasticity and hand surgery: an overview. *J Hand Surg Br* 2000, 25 (3), 242-52.
51. Navarro, X.; Vivo, M.; Valero-Cabre, A., Neural plasticity after peripheral nerve injury and regeneration. *Prog Neurobiol* 2007, 82 (4), 163-201.
52. Lu, C. H.; Chen, J. L.; Wu, C. T.; Liaw, W. J.; Yeh, C. C.; Cherng, C. H.; Wong, C. S., Effect of epidural neuraxial blockade-dependent sedation on the Ramsay Sedation Scale and the composite auditory evoked potentials index in surgical intensive care patients. *J Formos Med Assoc* 2010, 109 (8), 589-95.
53. Heine, L.; Soddu, A.; Gomez, F.; Vanhaudenhuyse, A.; Tshibanda, L.; Thonnard, M.; Charland-Verville, V.; Kirsch, M.; Laureys, S.; Demertzi, A., Resting state networks and consciousness: alterations of multiple resting state network connectivity in physiological, pharmacological, and pathological consciousness States. *Front Psychol* 2012, 3, 295.
54. Boveroux, P.; Vanhaudenhuyse, A.; Bruno, M. A.; Noirhomme, Q.; Lauwick, S.; Luxen, A.; Degueldre, C.; Plenevaux, A.; Schnakers, C.; Phillips, C.; Brichant, J. F.; Bonhomme, V.; Maquet, P.; Greicius, M. D.; Laureys, S.; Boly, M., Breakdown of within- and between-network resting state functional magnetic resonance imaging connectivity during propofol-induced loss of consciousness. *Anesthesiology* 2010, 113 (5), 1038-53.
55. Boly, M.; Phillips, C.; Balteau, E.; Schnakers, C.; Degueldre, C.; Moonen, G.; Luxen, A.; Peigneux, P.; Faymonville, M. E.; Maquet, P.; Laureys, S., Consciousness and cerebral baseline activity fluctuations. *Hum Brain Mapp* 2008, 29 (7), 868-74.

56. Martuzzi, R.; Ramani, R.; Qiu, M.; Rajeevan, N.; Constable, R. T., Functional connectivity and alterations in baseline brain state in humans. *Neuroimage* 2010, 49 (1), 823-34.
57. Greicius, M. D.; Kiviniemi, V.; Tervonen, O.; Vainionpaa, V.; Alahuhta, S.; Reiss, A. L.; Menon, V., Persistent default-mode network connectivity during light sedation. *Hum Brain Mapp* 2008, 29 (7), 839-47.
58. Miron, D.; Duncan, G. H.; Bushnell, C. M., Effects of attention on the intensity and unpleasantness of thermal pain. *Pain* 1989, 39 (3), 345-352.
59. Wiech, K.; Farias, M.; Kahane, G.; Shackel, N.; Tiede, W.; Tracey, I., An fMRI study measuring analgesia enhanced by religion as a belief system. *Pain* 2008, 139 (2), 467-476.



# Chapter 6

## Hyperalgesia and reduced offset analgesia during spinal anesthesia

Elske Sitsen, Monique van Velzen, Mischa de Rover, Albert Dahan, Marieke Niesters

*J Pain Res* 2020 Aug 24; 13:2143-2149.

## Introduction

Deafferentation or the traumatic or anesthetic disruption of afferent input from the peripheral to the central nervous system results in cortical, subcortical or brainstem reorganization and alters neuronal connectivity.<sup>1,7</sup> Using resting-state functional magnetic resonance imaging (fMRI), we previously showed that short-term spinal anesthesia-induced deafferentation is associated with functional connectivity changes in the thalamus in relation to the thalamo-cortical network and in the anterior cingulate cortex and insula in relation to the thalamo-parietal network.<sup>5</sup> In general, deafferentation causes adaptive plasticity, such as cortical expansion of brain areas adjacent to deafferentated areas, due to a rebalancing of excitatory and inhibitory neuronal modulators involved in plasticity.<sup>6</sup> Deafferentation may be associated with behavioral changes. While some studies show improved acuity of motor or sensory function related to cortical plasticity,<sup>3,8</sup> it is well known that deafferentation may additionally have negative behavioral effects related to maladaptive plasticity, as may occur in traumatic deafferentation, including phantom limb pain or pain after spinal cord injury.<sup>1,2,6</sup>

Spinal and epidural anesthesia are forms of short-term deafferentation. There is evidence that both types of neuraxial blockade are associated with sensory distortions or pain.<sup>4,9,10</sup> In patients that require a subarachnoid or epidural block for surgery, illusionary limb position, pain in the deafferented limbs, or paradoxical heat perception upon application of a cold stimulus on the transition from normal to deafferentated skin are often observed.<sup>4,9,10</sup> Additionally, in healthy volunteers we showed that spinal deafferentation is associated with hyperalgesic responses above the level of deafferentation.<sup>5</sup>

The current study was performed to first determine whether we could replicate the observation of hyperalgesic responses above the level of spinal anesthesia-induced deafferentation. Next, we studied the effect of spinal deafferentation on offset analgesia (OA), a manifestation of endogenous pain modulation. OA is characterized by profound analgesia after a slight decrease in noxious stimulation and is considered an expression of temporal filtering of nociception related to post-stimulus inhibition.<sup>11-13</sup> Both peripheral and central mechanisms are suggested to regulate OA.<sup>11,14-23</sup> We tested the effect of the spinal anesthesia deafferentation paradigm on OA, and hypothesized that OA responses would be decreased during spinal deafferentation, possibly due to plastic changes in areas of the brain involved pain modulation.

## Materials and methods

### Subjects and Ethics

Twenty-two volunteers were recruited after approval of the protocol by the local institutional review board (Commissie Medische Ethiek, Leiden University Medical Center). None of the subjects had participated in earlier studies. Participants were enrolled in the study and they gave oral and written informed consent. All subjects were right-handed healthy males, aged 18



years or older. Exclusion criteria included: body mass index > 30 kg/m<sup>2</sup>, (history of) any medical or psychiatric disease, use of any medication in the last 3 months that could interfere with pain perception, (history of) illicit drug use in the last 3 months, consumption of more than 3 alcohol units/day, or any condition that could interfere with the placement of a spinal needle. This study is part of a large project on the influence of spinal deafferentation on central pain processing as measured by fMRI in healthy male volunteers. We here report on the influence of spinal deafferentation on offset analgesia. The study was registered at the trial register of the Dutch Cochrane Center ([www.trialregister.nl](http://www.trialregister.nl)) under identifier NL3874. All procedures were performed in compliance with the latest version of the Declaration of Helsinki and Good Clinical Practice guidelines. The study was performed from June 2013 to February 2014. All subjects received a small monetary compensation for their participation.

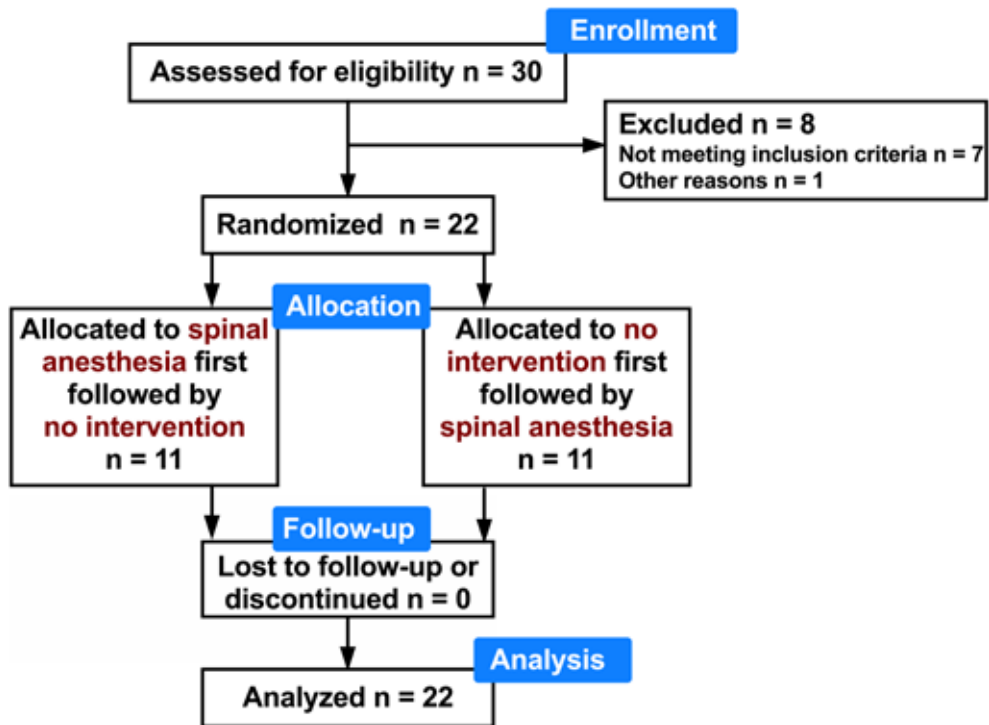


Figure 1. Consort flow diagram

### Study Design

The study had a randomized, placebo-controlled, single-blind, crossover design. Randomization relates to the fact that the occasions were randomized, the single-blind design relates to the fact that an independent pain researcher (LO, not further involved in the trial) performed the static and offset analgesia pain tests in a fully blinded fashion; the subjects could not be blinded. Additionally, the data analysis was performed on a blinded data set. Participants were

randomized to receive an intrathecal injection with a local anesthetic on occasion A and “no intervention” on occasion B, with one week in between the two occasions. Randomization was performed using a computer-generated randomization list. All subjects were requested not to eat or drink during the 8-hours prior to their visit to the research unit and none received any prehydration prior to administration of spinal anesthesia or no intervention.

Prior to the spinal injection, the skin was infiltrated with 1 mL lidocaine (10 mg/mL; AstraZeneca, Zoetermeer, The Netherlands) to induce local anesthesia after which a pencil point 27G spinal needle (Vygon, Valkenswaard, The Netherlands) was inserted in the skin at the interspace between vertebrae L3 and L4 and advanced towards the intrathecal space. After the needle point had reached the spinal space, 3 mL bupivacaine (5 mg/mL; AstraZeneca) was slowly injected. In control experiments subjects were positioned in the lateral position but the skin was not punctured and no medication was injected. Dermatome evaluation was by cold sensation. All procedures were performed by a single anesthetist (ES) with ample experience in the placement of spinal anesthesia under strict sterile conditions. Emergency medication, ephedrine 5 mg or 0.5 mg atropine could be administered intravenously if deemed necessary.

### **Static Pain and Offset Analgesia Tests**

Heat pain was applied on the left volar forearm (dermatome C8-Th1) using a 3 cm<sup>2</sup> thermal probe of the Pathway Neurosensory Analyzer (Medoc Ltd., Ramat Yishai, Israel). The temperature of the thermode was computer-controlled and could be set at any desired value between 120°C and 500°C. To quantify the pain intensity during the static pain tests, the subjects rated their pain on a 100-mm paper visual analogue scale (VAS) ranging from 0 (no pain) to 100 mm (most intense pain imaginable). To quantify the pain intensity in the offset analgesia tests, the subjects rated their pain scores on a slider of an electric 100-mm long potentiometer that was connected to the computer; the slider ranged from 0 (no pain) to 100 mm (most intense pain imaginable). This enabled the continuous monitoring of the electronic visual analogue scale (eVAS) during noxious stimulation.

The target temperature of the pain tests was determined prior to the spinal injection by administering a series of heat stimuli, ranging from 420°C to 500°C in steps of 10°C for 10 s, with 5-10 min interval between stimuli. The lowest temperature evoking an eVAS of 50 mm was used during the remainder of the study. To overcome adaptation the thermode was moved in-between three non-overlapping skin areas between stimuli.<sup>12</sup> After this “calibration” process, a first static pain test was obtained at the target temperature applied for 10 s. Thereafter the study started with induction of spinal anesthesia or the “no intervention”, as described above. Ninety min after the spinal injection or 90 min into the control condition, the static pain test was repeated and 5-10 min later the offset analgesia test was performed on a different part of the skin of the lower arm. Offset analgesia was studied using a three-temperature paradigm (T1-T2-T3). The temperature of the thermode was increased from 32°C to the target

temperature at 1.5°C/s and kept constant for 5 s (T<sub>1</sub>), after which it was increased by 1°C for 5 s (T<sub>2</sub>), then decreased by 1°C and kept constant for 2 s (T<sub>3</sub>), after which it returned to baseline values (32°C) at 6°C/s.

### Data and Statistical Analysis

The study was powered to determine a significant effect of spinal deafferentation on BOLD-signals in brain regions activated by the pain tests (difference between spinal anesthesia and the control condition = 0.25, SD = 0.20,  $\alpha = 0.05$ ,  $1 - \beta = 0.90$ ). A number of 16 subjects were deemed necessary. To consider any margin of uncertainty in the effect size and SD the group size was enlarged to 22. Previously we tested the effect of spinal deafferentation on static pain perception and observed a significant increase in pain intensity of  $6.3 \pm 3.8$  mm (mean  $\pm$  SD) in a group of 12 volunteers during spinal anesthesia, while the effect in the control condition treatment was negligible. We therefore argue that our current sample size is sufficient to address the primary end-points of the study.

The eVAS data were averaged over 1-s periods. To quantify OA, the decrease in eVAS from peak eVAS value to the eVAS nadir after the 10°C decrease of the test stimulus was measured ( $\Delta$ eVAS), corrected for the value of the peak eVAS,  $\Delta$ eVAS<sub>c</sub> = ( $\Delta$ eVAS/[peak eVAS])  $\times$  100 (i.e., correction for the variation in the peak response among participants).<sup>12,25</sup> To compare static pain VAS scores and  $\Delta$ eVAS<sub>c</sub> between control and spinal anesthesia, a paired two-tailed t-test was performed with p-values < 0.05 considered significant (GraphPad Prism 8.3.0 for Mac OS X, GraphPad Software, San Diego, CA). All data are presented as mean  $\pm$  SD, unless otherwise stated.

### Results

Twenty-two males were randomized with median age (interquartile range) 22 years (21-23 years) and body mass index  $22.2 \pm 1.9$  kg.m<sup>-2</sup> (Figure 1). All volunteers completed the study without adverse effects. No hemodynamic effects occurred and none of the subjects complained of post-spinal headache. The number of blocked dermatomes was  $16 \pm 3$  at the time of pain testing, corresponding to an average upper block level at thoracic dermatome 6. At baseline (prior to spinal or “no intervention”) the lowest temperature that caused a pain VAS of at least 50 mm on the skin of the lower forearm was  $48.0 \pm 1.6^\circ\text{C}$  (control) and  $48.1 \pm 1.2^\circ\text{C}$  (spinal; mean difference  $+0.07^\circ\text{C}$ , 95% confidence interval  $-0.35$  to  $0.49^\circ\text{C}$ ,  $p = 0.74$ ). The static pain test was performed at the individualized temperatures. Under control conditions, the average pain score at baseline was  $52.3 \pm 18.0$  mm and 90 min later  $51.7 \pm 19.7$  mm (mean difference  $-0.60$  mm, 95% confidence interval  $-0.64$  to  $0.52$  mm,  $p = 0.84$ ). On the active treatment visit, the average pain score was at baseline  $51.0 \pm 15.4$  mm and 90 min after the spinal injection  $59.1 \pm 15.0$  mm (mean difference  $+8.0$  mm, 95% confidence interval  $1.2$  to  $14.9$  mm,  $p = 0.02$ ). Pain scores on the arm during spinal anesthesia were higher than 90 min into the control conditions (mean difference  $7.4$  mm, 95% confidence interval  $0.7$ - $14.0$ ,  $p = 0.03$ ;

Figure 2). No correlation was observed between the number of blocked dermatomes and increase in static eVAS scores.

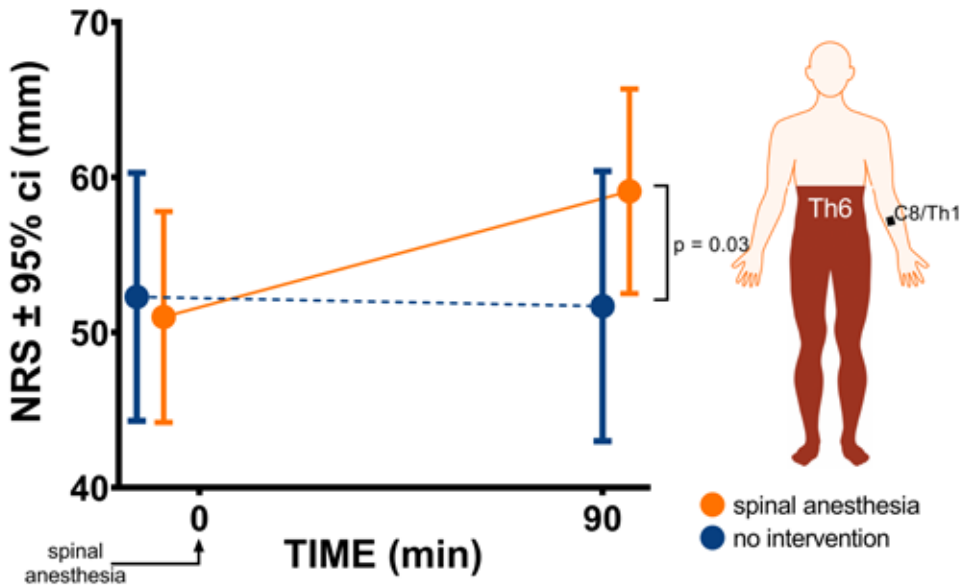


Figure 2. Effect of spinal anesthesia to dermatome level Th6 on pain perception at a remote area above the level of anesthesia (dermatome C8/Th1). Ninety minutes after placement of the anesthetic, a similar noxious heat stimulus caused more pain during spinal anesthesia (orange symbols) compared to the control condition (blue symbols).

Offset analgesia was also tested on dermatome level C8-Th1 but on a skin area adjacent to the area at which the static pain test was performed. Examples of offset analgesia responses of two subjects are given in Fig. 3A and B. In both examples the offset analgesia response is less during spinal anesthesia (orange symbols) than in the control condition (blue symbols). In subject A (Fig. 3A) the  $\Delta eVAS_c$  values were 79% and 57% under the control condition and during spinal anesthesia, respectively, while corresponding values in subject B (Fig. 3B) were 100% and 75%. The average  $\Delta eVAS_c$  values were  $90 \pm 17\%$  (control) and  $79 \pm 27\%$  (spinal anesthesia; mean difference -11% with 95% confidence interval -20 to -2%,  $p = 0.016$ ; Fig. 3C). Individual  $\Delta eVAS_c$  values in the two treatment conditions are given in Fig. 3D. No correlation was observed between number of blocked dermatomes and changes in OA responses.

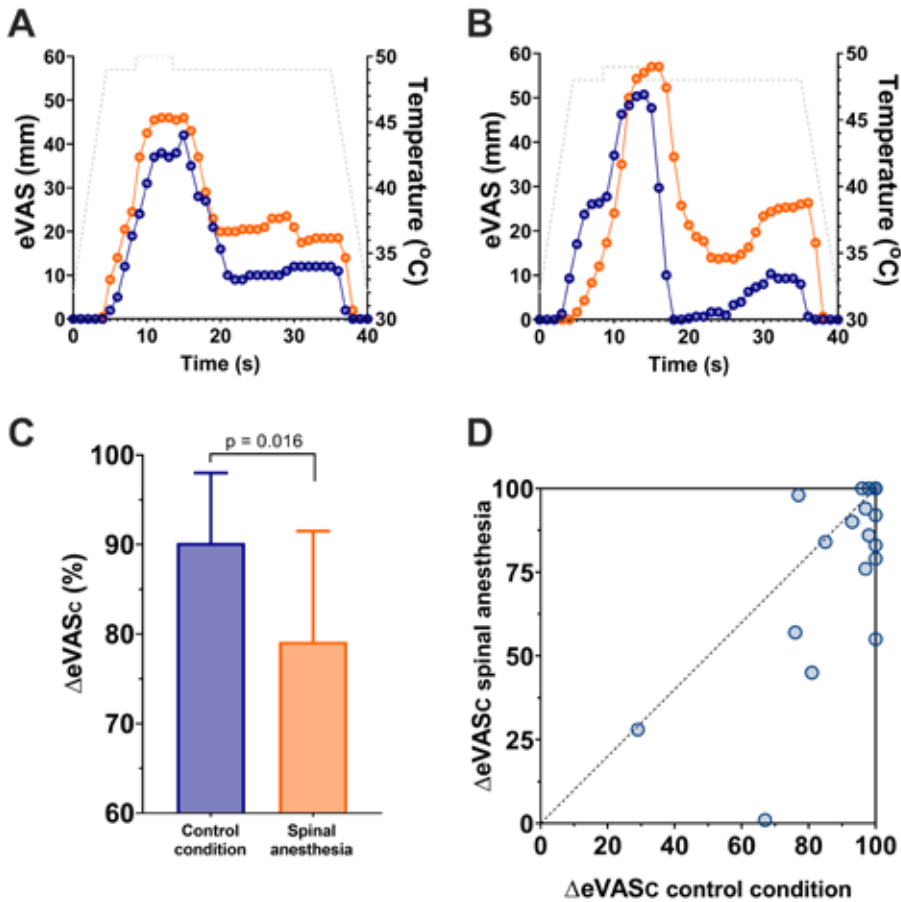


Figure 3. A and B. Examples of offset analgesia responses in two subjects under control conditions (blue symbols) and during spinal anesthesia (orange symbols). The temperature profiles (T1-T2-T3) were 49-50-49°C and 48-49-48°C in panels A and B, respectively. C.  $\Delta eVASC_c$  values under control conditions and during spinal anesthesia; values mean  $\pm$  95% confidence interval. D. Individual  $\Delta eVASC_c$  values under control (no intervention) conditions and during spinal anesthesia.

## Discussion

There is ample evidence that even short-term peripheral deafferentation is associated with behavioral effects, such as referred sensations, pain, bodily illusions or enhanced sensorimotor acuity of non-deafferented areas.<sup>4, 8-10</sup> In the current study we confirm our previous finding that noxious thermal stimuli applied during spinal anesthesia (maximum block level Th6 or 16 blocked dermatomes) are perceived as more painful than similar stimuli applied in the control condition.<sup>5</sup> Hyperalgesia, in magnitude a 14% increase in pain intensity, was consistently observed among participants, and in magnitude in close agreement with our previous study. In that study, using resting-state fMRI, we showed that hyperalgesia was correlated to changes in brain networks involved in the sensory discriminative and the affective dimensions of pain perception. Several of the brain areas within these networks are considered essential elements

of the pain modulatory system.<sup>5</sup> The changes in network connectivity that we observed made us speculate that spinal deafferentation causes a shift of the endogenous pain system from pain inhibition towards pain facilitation. The hyperalgesic response to a static thermal noxious stimulus is then the consequence of such a shift. To test this hypothesis, we assessed whether spinal deafferentation would change offset analgesia, an expression of endogenous pain modulation.

Offset analgesia is defined by the reduction in pain intensity perception observed during noxious thermal stimulation towards hypoalgesia after a small decrease (10C) in noxious thermal stimulation.<sup>11-13</sup> OA is considered the altered spatiotemporal processing of noxious stimuli aimed at amplifying reductions in noxious stimulation. Loss of proper OA engagement has been observed in neuropathic pain patients and in patients with fibromyalgia.<sup>11, 14, 24</sup> We earlier showed that in fibromyalgia patients, reduced OA responses were associated with earlier onset of pain (reduced pain threshold) and increased sensory sensitivity (hyperalgesia) to heat stimuli,<sup>24</sup> both phenomena may be involved in the persistence or chronification of pain symptoms. The mechanism of OA is not yet fully understood. The literature indicates various possible offset analgesia mechanisms such as a central mechanism involving activation of descending inhibition from central sites,<sup>14-16</sup> spinal mechanisms,<sup>22, 23</sup> peripheral mechanisms involving the nerves innervating the skin,<sup>17, 18</sup> and combined central or spinal and peripheral mechanisms.<sup>22, 23</sup>

We observed the reduction of OA responses during spinal anesthesia, in agreement with our hypothesis of the rebalancing of the endogenous pain system during peripheral deafferentation. Although it seems attractive to associate these OA changes to connectivity changes in brain networks (*i.e.* a central mechanism), alternative mechanisms cannot be excluded. We previously tested OA responses in a large group of healthy subjects (without pain) and a group of chronic neuropathic pain patients and calculated a  $\Delta eVAS_c$  cutoff of 88% (with sensitivity 90% and specificity 91%) to distinguish abnormal OA from healthy responses.<sup>11</sup> Extrapolation of this analysis to our current data set suggests that OA responses are similarly abnormal in chronic pain patients and in individuals without pain during spinal anesthesia. Still, whether the resemblance in responses has a similar mechanistic origin is difficult to determine from our current protocol.

An important limitation of our study was the lack of blinding of the subjects. The nature of the study precludes blinding. Since all subjects were properly instructed prior to participation in the study, all were aware that an anesthetic was present or not. In our previous trial we performed a sham injection after insertion of a spinal needle into the skin at the interspace of L<sub>3</sub> and L<sub>4</sub>.<sup>5</sup> For the current study, the ethics committee decided against such a procedure as the committee reasoned that it would not enhance the blinding of the study. Hence, we cannot exclude some bias of the lack of blinding of the subjects. Pain responses could have

been differently affected in the two anesthetic states (real/control) because of more intense unpleasantness, fear or distraction during spinal anesthesia.<sup>25</sup> How this affected our study outcome remains unknown. Still we detected no order effect in either static pain rating or OA response, which suggests that these symptoms were not overwhelmingly influential.

We tested our hypothesis in a group of male volunteers. We did so to have standardized conditions for measurement of the effect spinal anesthesia on the brain connectivity by using resting-state fMRI.<sup>5</sup> We previously tested OA responses in 110 men and women over a large age range (6-80 years) and observed no differences in OA responses in healthy volunteers and patients with neuropathic pain.<sup>11</sup> Hence, as we assume similar effects of spinal anesthesia on the spinal cord and brain in men and women, we argue that our results may be extrapolated to women but suggest to perform additional studies in a mixed population in future studies to confirm our results.

In conclusion, we observed that spinal deafferentation caused hyperalgesia and reduced offset analgesia responses in dermatomes remote from and above the level of anesthesia. Further studies should address the mechanism of the spinal anesthesia-related reduced offset analgesia responses.

## References

1. Bramati, I. E.; Rodrigues, E. C.; Simoes, E. L.; Melo, B.; Hofle, S.; Moll, J.; Lent, R.; Tovar-Moll, F., Lower limb amputees undergo long-distance plasticity in sensorimotor functional connectivity. *Sci Rep* 2019, 9 (1), 2518.
2. Kambi, N.; Halder, P.; Rajan, R.; Arora, V.; Chand, P.; Arora, M.; Jain, N., Large-scale reorganization of the somatosensory cortex following spinal cord injuries is due to brainstem plasticity. *Nat Commun* 2014, 5, 3602.
3. Kelly, M. K.; Carvell, G. E.; Kodger, J. M.; Simons, D. J., Sensory loss by selected whisker removal produces immediate disinhibition in the somatosensory cortex of behaving rats. *J Neurosci* 1999, 19 (20), 9117-25.
4. Melton, M. S.; Browndyke, J. N.; Harshbarger, T. B.; Madden, D. J.; Nielsen, K. C.; Klein, S. M., Changes in Brain Resting-state Functional Connectivity Associated with Peripheral Nerve Block: A Pilot Study. *Anesthesiology* 2016, 125 (2), 368-77.
5. Niesters, M.; Sitsen, E.; Oudejans, L.; Vuyk, J.; Aarts, L. P.; Rombouts, S. A.; de Rover, M.; Khalili-Mahani, N.; Dahan, A., Effect of deafferentation from spinal anesthesia on pain sensitivity and resting-state functional brain connectivity in healthy male volunteers. *Brain Connect* 2014, 4 (6), 404-16.
6. Pawela, C. P.; Biswal, B. B.; Hudetz, A. G.; Li, R.; Jones, S. R.; Cho, Y. R.; Matloub, H. S.; Hyde, J. S., Interhemispheric neuroplasticity following limb deafferentation detected by resting-state functional connectivity magnetic resonance imaging (fcMRI) and functional magnetic resonance imaging (fMRI). *Neuroimage* 2010, 49 (3), 2467-78.
7. Weiss, T.; Miltner, W. H.; Liepert, J.; Meissner, W.; Taub, E., Rapid functional plasticity in the primary somatomotor cortex and perceptual changes after nerve block. *Eur J Neurosci* 2004, 20 (12), 3413-23.
8. Petoe, M. A.; Jaque, F. A.; Byblow, W. D.; Stinear, C. M., Cutaneous anesthesia of the forearm enhances sensorimotor function of the hand. *J Neurophysiol* 2013, 109 (4), 1091-6.
9. Harrison, G., Phantom limb pain occurring during spinal analgesia. *Anaesthesia* 1951, 6 (2), 115-6; passim.
10. Kishikawa, H.; Wajima, Z.; Shitara, T.; Shimizu, T.; Adachi, H.; Sakamoto, A., Subarachnoid Block-Induced Deafferentation Pain Successfully Treated with Pentazocine. *J Nippon Med Sch* 2017, 84 (4), 183-185.
11. Niesters, M.; Hoitsma, E.; Sarton, E.; Aarts, L.; Dahan, A., Offset analgesia in neuropathic pain patients and effect of treatment with morphine and ketamine. *Anesthesiology* 2011, 115 (5), 1063-71.
12. Yelle, M. D.; Rogers, J. M.; Coghill, R. C., Offset analgesia: a temporal contrast mechanism for nociceptive information. *Pain* 2008, 134 (1-2), 174-86.
13. Yelle, M. D.; Oshiro, Y.; Kraft, R. A.; Coghill, R. C., Temporal filtering of nociceptive information by dynamic activation of endogenous pain modulatory systems. *J Neurosci* 2009, 29 (33), 10264-71.



14. Zhang, S.; Li, T.; Kobinata, H.; Ikeda, E.; Ota, T.; Kurata, J., Attenuation of offset analgesia is associated with suppression of descending pain modulatory and reward systems in patients with chronic pain. *Mol Pain* 2018, 14, 1744806918767512.
15. Derbyshire, S. W.; Osborn, J., Offset analgesia is mediated by activation in the region of the periaqueductal grey and rostral ventromedial medulla. *Neuroimage* 2009, 47 (3), 1002-6.
16. Nahman-Averbuch, H.; Martucci, K. T.; Granovsky, Y.; Weissman-Fogel, I.; Yarnitsky, D.; Coghill, R. C., Distinct brain mechanisms support spatial vs temporal filtering of nociceptive information. *Pain* 2014, 155 (12), 2491-2501.
17. Darian-Smith, I.; Johnson, K. O.; LaMotte, C.; Shigenaga, Y.; Kenins, P.; Champness, P., Warm fibers innervating palmar and digital skin of the monkey: responses to thermal stimuli. *J Neurophysiol* 1979, 42 (5), 1297-315.
18. Naugle, K. M.; Cruz-Almeida, Y.; Fillingim, R. B.; Riley, J. L., 3rd, Offset analgesia is reduced in older adults. *Pain* 2013, 154 (11), 2381-2387.
19. Martucci, K. T.; Eisenach, J. C.; Tong, C.; Coghill, R. C., Opioid-independent mechanisms supporting offset analgesia and temporal sharpening of nociceptive information. *Pain* 2012, 153 (6), 1232-1243.
20. Niesters, M.; Proto, P. L.; Aarts, L.; Sarton, E. Y.; Drewes, A. M.; Dahan, A., Tapentadol potentiates descending pain inhibition in chronic pain patients with diabetic polyneuropathy. *Br J Anaesth* 2014, 113 (1), 148-56.
21. Olesen, A. E.; Nissen, T. D.; Nilsson, M.; Lelic, D.; Brock, C.; Christrup, L. L.; Drewes, A. M., Offset Analgesia and The Impact of Treatment with Oxycodone and Venlafaxine: A Placebo-Controlled, Randomized Trial in Healthy Volunteers. *Basic Clin Pharmacol Toxicol* 2018, 123 (6), 727-731.
22. Sprenger, C.; Stenmans, P.; Tinnermann, A.; Buchel, C., Evidence for a spinal involvement in temporal pain contrast enhancement. *Neuroimage* 2018, 183, 788-799.
23. Ligato, D.; Petersen, K. K.; Morch, C. D.; Arendt-Nielsen, L., Offset analgesia: The role of peripheral and central mechanisms. *Eur J Pain* 2018, 22 (1), 142-149.
24. Oudejans, L. C. J.; Smit, J. M.; van Velzen, M.; Dahan, A.; Niesters, M., The influence of offset analgesia on the onset and offset of pain in patients with fibromyalgia. *Pain* 2015, 156 (12), 2521-2527.
25. Hird, E. J.; Charalambous, C.; El-Deredy, W.; Jones, A. K. P.; Talmi, D., Boundary effects of expectation in human pain perception. *Sci Rep* 2019, 9 (1), 9443.



# Chapter 7

## Effect of spinal anesthesia-induced deafferentation on pain processing in healthy male volunteers: A task-related fMRI study

Elske Sitsen MD, Najmeh Khalili-Mahani PhD, Mischa de Rover PhD,  
Albert Dahan MD PhD, Marieke Niesters MD PhD

*Accepted for publication November 2022 Frontiers in Pain Research.*

## Introduction

Spinal anesthesia is induced by injection of a controlled dose of local anesthetics in the cauda equina, resulting in temporary and localized loss of sensation in the lower part of the body. Spinal anesthesia causes a transient pharmacological deafferentation of the peripheral nervous system by blocking the sodium channels of the nerves, thus inhibiting the afferent and efferent signaling between the peripheral and central nervous system that process sensory-motor and pain inputs.

Spinal anesthesia provides a plausible experimental model for studying pain associated with peripheral nerve damage. For example, phantom limb pain is believed to be related to alterations in the somatotopic map in the primary sensory and motor cortex resulting from loss of peripheral signaling from nerves of the affected limb to the central nervous system.<sup>1</sup> We have used this experimental model in a previous resting state fMRI study (RS-fMRI), to show that indeed a pharmacological spinal deafferentation was associated with increased pain scores (hyperalgesia) at the non-deafferented skin areas. Moreover, we observed changes in connectivity between specific brain areas and several canonical resting state networks.<sup>2</sup> Namely, increased pain sensation was correlated with changes in functional connectivity of the thalamus to the thalamo-prefrontal network, and changes in functional connectivity of the anterior cingulate cortex and insula to the thalamo-parietal network.<sup>2</sup>

A limitation of the previous RS-fMRI study was that the noxious stimuli were administered before or after the scan, as such we could not make inferences about the impact of spinal anesthesia on CNS processing of pain stimuli. Furthermore, our previous RS-fMRI results were contingent on spontaneous fluctuations within specific canonical networks of interest. The aim of the current study was to overcome those limitations by investigating differences caused by spinal anesthesia to brain activation (BOLD response to a calibrated, timed, pain task).

In a randomized cross-over task-based fMRI study we examined whether spinal anesthesia modulated pain perception in the non-deafferented skin areas and whether spinal anesthesia change the brains response to pain stimuli and if those changes were associated with variation in pain perception due to spinal anesthesia.

## Materials and Methods

### Study design

The study had a randomized crossover design and involved two visits (spinal anesthesia session or control session), at least one week apart. Randomization of the order of the two visits was performed using a computer-generated randomization list. Because the spinal anesthesia causes a strong reaction (temporary paralysis of the legs), the study was unable to be conducted blindly. Because the Ethics committee did not give permission to administer

a sham injection, we performed two fMRI scans in each session: one fMRI scan (under pain condition) at the beginning (pre) and at the end (post). In both sessions, whether the participants received spinal anesthesia or not (control condition) in between the two scans, the interval between the two scans was around one hour. To have acquired data at two time points allowed us to examine the reliability of brain response to the pain task across different conditions, and also to control for possible ordering effects in the absence of intervention, the spinal anesthesia. At the end of the study, participants were monitored until they were fully recovered from the spinal anesthetic, with a full return of motor functions and diuresis, and were then allowed to go home.

### **Participants**

Twenty-two right handed healthy male volunteers (aged 21-23 years) participated in the study after written informed consent was obtained and after approval of the protocol was given by the human ethics committee of the Leiden University Medical Center. The study was registered in the trial register of the Dutch Cochrane Center under identification number 3874. The study was performed according to Good Clinical Practice guidelines and the ethical principles of the Declaration of Helsinki (amended in 2013). All subjects were screened before participation in the study. Exclusion criteria included: body mass index  $> 30 \text{ kg/m}^2$ ; significant history or presence of any medical disorder, including bleeding disorders, or any medical issue that might interfere with optimal participation or pose any risk from spinal anesthesia; history of chronic alcohol or illicit drug use; the presence of metal devices; claustrophobia; allergy to study medications; and inability to maintain a regular diurnal rhythm.

### **Procedures**

Figure 1 depicts the timeline of the study procedures. After arrival in the MRI suite, a video demonstration of the spinal procedure was presented to the participant after which an intravenous access-line was placed in the left arm to allow administration of emergency medication if deemed necessary. After a short relaxation period, we calibrated pain stimulus to individual tolerance levels. Baseline thermal stimuli were applied on the right forearm to determine the temperature evoking a pain score of 60-70 mm out of 100 mm on a visual analog scale (VAS) for later use in the MRI experiment (see 'pain task in the MRI scanner' below). This procedure was repeated during the second visit. The temperature used in the experiment could differ between the two visits, evoking the same heat pain score.

During the spinal anesthesia session, participants received an intrathecal injection with 15 mg bupivacaine (3 mL; AstraZeneca, Zoetermeer, the Netherlands) between vertebrae L3 and L4 (spinal condition). During the control session no injection was made.

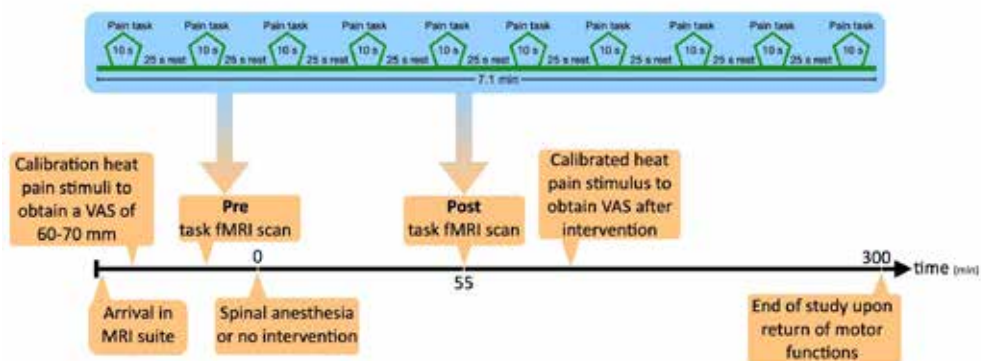


Figure 1. The timeline of the experiment.

### Noxious Stimulus and Interventions

Each session consisted of two task-based fMRI acquisitions (pre-scan and post-scan), one hour apart--duration necessary for administering and stabilization of the spinal anesthesia. During the wait interlude, ambulatory variables (blood pressure, heart rate and oxygen saturation) were monitored.

The noxious thermal stimuli (whose intensity was calibrated prior to the scan) were applied on the lower part of the right forearm with an MRI compatible 3 x 3 cm thermal probe attached to a Pathway Neurosensory Analyzer (Medoc Ltd., Ramat Yishai, Israel). During calibration and during the scans (pre and post) the temperature of the probe started at 32°C (baseline temperature) and rapidly increased (5°C/s) towards a preset destination temperature that was held constant for 10 seconds and then returned (5°C/s) to baseline temperature. The heat pain stimulus was alternated with a 25 seconds lag time (block design). In total 10 pain stimuli were given, with a total task duration of 7.1 min (Figure 1).

The second MRI-scan (post) was conducted under the same stimulus intensity conditions as in in the first MRI-scan (pre). At the end of the post-scan, the noxious stimuli were applied once more on the right forearm to measure VAS scores at the end of the scanning session. This procedure was necessary because we did not want to rate the pain during scanning to avoid confounds associated with cognitive processing of pain scores.

### Data Acquisition

#### Scanning

Imaging data were acquired on a Philips 3 Tesla Achieva TX MRI scanner using a 32-channel SENSE head coil (Philips Medical Systems, Best, The Netherlands). Whole-brain fMRI data sets were acquired using T2\*-weighted gradient-echo echo-planar imaging with the following scan parameters: 190 volumes; 38 axial slices scanned in ascending order; repetition time (TR) = 2.2 sec; echo time (TE) = 30 millisecond(ms); flip angle = 80°; FOV = 220 x 220 mm; 2.75

mm isotropic voxels with a 0.275 mm slice gap. For registration purposes, a high-resolution anatomical image (T1-weighted ultra-fast gradient-echo acquisition; TR=9.76 ms; TE= 4.59 ms; flip angle= 8°; 140 axial slices; FOV= 224 x 177.33 mm; in plane voxel resolution = 0.875 mm x 0.875 mm; slice thickness= 1.2 mm) was acquired for each participant. In order to control for confounding effects of experiment induced variations in physiological signals, participants were fit with a respiration belt and pulse oximeter, and for each fMRI dataset, ambulatory signals were measured at 500 Hz frequency.

### **fMRI data preprocessing**

All fMRI scans were visually inspected to ensure that no gross artefacts were present. We excluded 4 datasets due to the presence of movement artefacts in the raw data, which could not be reliably removed or corrected (n = 18). Data preparation for fMRI included standard fMRI preprocessing, as well as additional cautionary physiological noise screening. For the standard fMRI preprocessing, FEAT (fMRI Expert Analysis Tool) Version 6.00, part of FSL (FMRIB's Software Library, [www.fmrib.ox.ac.uk/fsl](http://www.fmrib.ox.ac.uk/fsl)) was used with standard motion correction using MCFLIRT;<sup>3</sup> skull removal using BET;<sup>4</sup> and spatial smoothing (Gaussian kernel, 5mm FWHM), as well as high pass temporal filtering (Gaussian-weighted least-squares straight line fitting, with  $\sigma=21.0s$ ), and grand-mean intensity normalization of the entire 4D dataset by a single multiplicative factor.

Physiological noise monitoring was carried out according to.<sup>5</sup> Briefly, this involved estimating the average heart rate (HR) (beats/min) and respiration variation (per min) obtained by taking the difference between respiration minimum and maximum values (peaks) divided by the time between the peaks and smoothed with a 6-s moving average filter. In addition, we performed RETROICOR<sup>6</sup> and RVHRCOR<sup>7</sup> to the raw data (Using PhysIO<sup>8</sup> on CBRAIN.<sup>9</sup> We subjected all physiological-corrected images to first-level statistics, to ensure that the activation patterns were not altered by noise.

### **First-level analysis of task-induced BOLD response**

First level fMRI analysis was performed using FEAT (fMRI Expert Analysis Tool) Version 6.00. Time-series statistical analysis was carried out using FILM with local autocorrelation correction,<sup>10</sup> including standard, and extended motion parameters in the subject level design matrix (block design, square shaped, including the temporal derivatives and temporal filtering). A standard double-Gamma hemodynamic response function was convolved with the box-car regressors in the model. We computed the Z-scores of the model fitting to the BOLD response in pain (on) versus no pain (off). In the first level analysis, positive BOLD responses ( $Z > 2.3$ ) are reported as activation; and negative BOLD responses as deactivation.

### **Group analyses of the effects of interventions**

Prior to group level analysis, we performed a multi-level image registration, by first registering each fMRI-dataset to a brain-extracted high-resolution T2\*W image of the participant; then

registering this data to the T1W image of each subject, and finally performing a registration to MNI152 (12 parameters).

Group Level Analysis was carried out using the high-level analysis feature in FEAT. Given the contextual specificity of the pharmacological intervention we used a fixed effects model, by forcing the random effects variance to zero in FLAME (FMRIB's Local Analysis of Mixed Effects).<sup>11-13</sup> Different GLMs were constructed to test the effects of Time (post vs pre), Interventions (Spinal<sub>(post-pre)</sub> versus Control<sub>(post-pre)</sub>), and stimulus intensity (temperature), and pain perception (VAS). In all models, the within-subject variations were modeled as an independent column per participant. In addition, because the trial was not blinded, we explored the effect of order on brain activation. To improve readability, we explained the details of the models in the results section. All maps were thresholded at voxel-wise  $Z=3.1$ , and cluster-corrected at  $p<0.05$ .

## Statistical Analysis

For studying the effects of stimulus intensity (temperature) and pain, we used SPSS 22, IBM. In order to investigate the impact of experimental conditions (condition, time and order of administering spinal anesthesia in the randomized design) on pain scores, we used generalized estimating equations (a specific form of generalized linear modeling that controls for within-subject variations in repeated measures studies such as ours.) Details are explained adjacent to the results.

## Results

### Effects of spinal anesthesia on pain intensity scores

The mean ( $\pm$  SEM) age of participants (18/22) was  $21 \pm 0,4$  years, weight  $73 \pm 1,3$  kg and height  $183 \pm 1,6$  cm. The mean dermatome level of anesthesia during the first 50 min after spinal injection was at Th6  $\pm 3,5$  (i.e. at level of the xiphoid). The pain temperature, which induced a VAS of 60-70 mm, ranged from 44.5 to 50°C (mean  $48.3 \pm 1.3^\circ\text{C}$ ).

We expected that VAS scores and Temperature to be correlated. Indeed, performing partial correlation (controlling for Time and Session) we found a significant inverse correlation between VAS scores and temperature applied during the scan ( $r = -0.553$ ,  $df = 68$ ,  $p < 0.001$ ), in other words, more than 30% of the variation in pain scores could be explained by the calibration temperature (Figure 2). The inverse correlation, surprising to us, might suggest that subjects who tolerated higher probe temperatures during the calibration session, had a lower pain sensitivity.



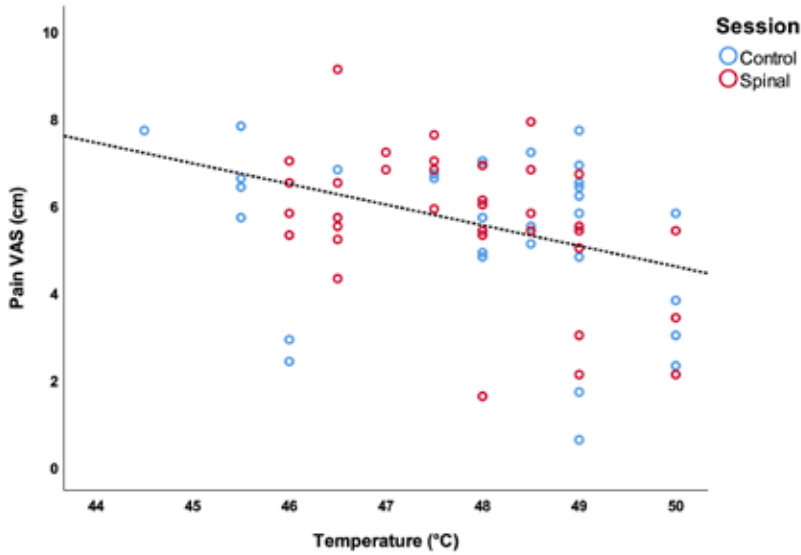


Figure 2. Scatterplot of the VAS scores and temperature of the control session and spinal anesthesia session.

As will be discussed later, the order of visits and receiving spinal anesthesia did impact the neural correlates of pain perception, however this correlation was significantly present in all conditions except in the control condition of participants who received spinal anesthesia in their first visit (See Supplementary Materials).

Table 1 summarizes the average pain scores at different time points in the study. A GEE model including Time, Session, Time by Session and Temperature, revealed significant time by session interaction effect on pain score (Wald  $\chi^2(df=1) = 7.73, P = 0.005$ ), and this effect was mainly driven by higher pain scores after Spinal session (post - pre) compared to Control (post-pre) (95% CI= 0.233 to 1.345). It should be noted that the effect of session on temperature was not significant (Wald  $\chi^2(df=1) = 0.54, P 0.46$ ).

Table 1. Summary pain scores. Max VAS = 10 cm.

	Control session	Spinal session
	Mean $\pm$ SD	Mean $\pm$ SD
Mean temperature(°C)	47.86 $\pm$ 1.6	47.86 $\pm$ 1,27
Pre Pain VAS (cm)	5.61 $\pm$ 1.75	5.22 $\pm$ 1.77
Post Pain VAS (cm)	5.57 $\pm$ 1.98	5.97 $\pm$ 1.58

## BOLD response to noxious thermal stimuli

In order to investigate the replicability of the brain response to pain stimulation with respect to existing evidence from the Meta-analysis by Xu et al,<sup>14</sup> and also to explore gross differences in the average response to spinal anesthesia compared to the control (non-anesthesia) condition, we tested the average effects of pain stimulation at each time point separately.

Figure 3 shows average BOLD response to the noxious thermal stimulus for each MRI session. Table 2 summarizes the overlaps between brain activations and deactivations in our study and the regions reported by Meta-analysis of Xu et al<sup>14</sup> to be sensitive to sensation of pain.

Table 2. Brain region activation and deactivation per session and time (pre, post). Deactivation were not part of the meta-analysis of Xu et al,<sup>14</sup>

Brain activation upon thermal pain (Positive BOLD response)					
Location	Xu et al (2020)	pre Control	post Control	pre Spinal	post Spinal
Harvard-Oxford cortical structural atlas					
Central opercular cortex	-	✓	✓	✓	✓
Frontal opercular cortex	-	✓	✓	✓	✓
Frontal pole	-	✓(R)	✓	-	✓
Middle frontal gyrus	✓(R)	-	-	-	✓(R)
Insula	✓	✓	✓	✓	✓
Thalamus	✓	✓	✓(L)	✓(L)	✓
Anterior/ midcingulate gyrus	✓	✓	✓	-	✓
juxta positional cortex	-	✓(R)	✓	-	✓
Brainstem	✓	✓	-	-	✓
Temporal pole	-	✓(R)	✓	✓	✓
Cerebellum	✓(L)	✓	✓	-	✓
Putamen	✓	✓	✓	✓	✓
Caudate	✓	✓	✓(L)	✓	✓
Amygdala	✓	-	-	-	✓(R)
Supramarginal gyrus	✓	-	-	-	✓(R)
Precentral gyrus	✓(R)	-	✓	-	✓(R)
Brain deactivation upon thermal pain (Negative BOLD response)					
Harvard-Oxford cortical structural atlas					
Precentral gyrus		✓	✓	✓	✓
Postcentral gyrus		✓	✓	✓	✓
Frontal pole		✓	✓	✓	-
Frontal medial cortex		✓	✓	✓	-
Precuneus cortex		✓	-	-	✓
Cingulate gyrus, post. div.		✓	-	-	✓
Angular gyrus		✓	-	-	-
Lat. occipital cortex		✓	-	-	✓
Temporal fusiform cortex		✓	-	-	✓
Hippocampus		✓	-	-	-
Parahippocampal gyrus		✓	-	-	✓

Among the four conditions, we found generally comparable patterns of brain activation consistent with the literature. The noxious thermal stimuli caused consistent activations in the bilateral central opercular cortex, secondary somatosensory cortex, insula and thalamus. Consistent deactivations were present in all four scans in the precentral gyrus and postcentral gyrus.

However, the patterns of brain activation (red) and deactivation (blue) in the medial prefrontal and anterior cingulate regions appeared to be different in the case of spinal anesthesia (Figure 3D). Specifically, qualitative and quantitative inconsistencies were observed in activations in the anterior cingulate cortex, the brainstem, juxta positional lobule cortex, cerebellum, frontal operculum cortex, inferior frontal cortex and putamen, across the four scans. Similarly, deactivations across the four scans were inconsistent in the precuneus cortex, paracingulate gyrus, frontal medial cortex, middle/ inferior temporal gyrus, lateral occipital cortex, hippocampus and angular gyrus. The frontal pole and medial frontal cortex were deactivated in all sessions, except in the post-scan during spinal anesthesia. See Figure 3, and Tables 3a, 3b, 4a and 4b in the Appendix for the complete lists.

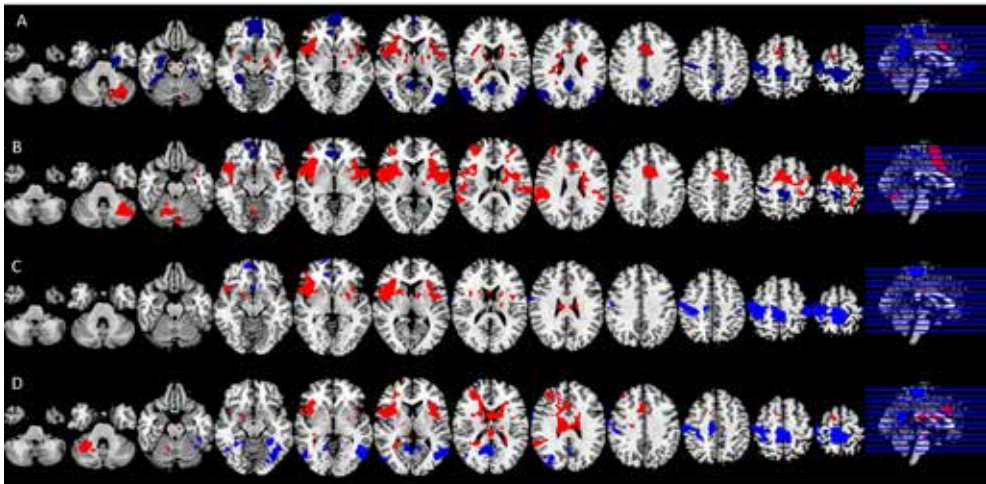


Figure 3. Significant neural responses to thermal noxious stimuli, resulting from a whole-brain analysis of (A) the control condition first scan (pre) and (B) the control condition second scan (post) (C) the spinal session first scan (pre) and (D) spinal session second scan (post). Significantly activated voxels are shown in red, significantly deactivated voxels in blue,  $p < 0.05$  cluster corrected. Images are Z-statistics thresholded at  $(-2.3)$ , overlaid on the MNI-152 standard brain. Slices are displayed in radiological convention (left = right). All significant clusters are described in detail in Tables 3a, 3b, 4a and 4b (Appendix).

### Effect of spinal anesthesia versus control

In order to formally test the differences in brain activity during Spinal anesthesia, we tested a general linear model (GLM) with all 72 data points, while modeling the random effect of subject, and fixed effects of time and intervention. In other words, the effect of time (Post-Pre), and the effect of condition (Spinal - Control) were treated as within subject variables. This model revealed significant differences in the BOLD response between the spinal anesthesia and

control condition in the bilateral angular gyrus (IPL) (more positive) and the bilateral post- and precentral gyri (more negative) (Figure 4, Table 5).

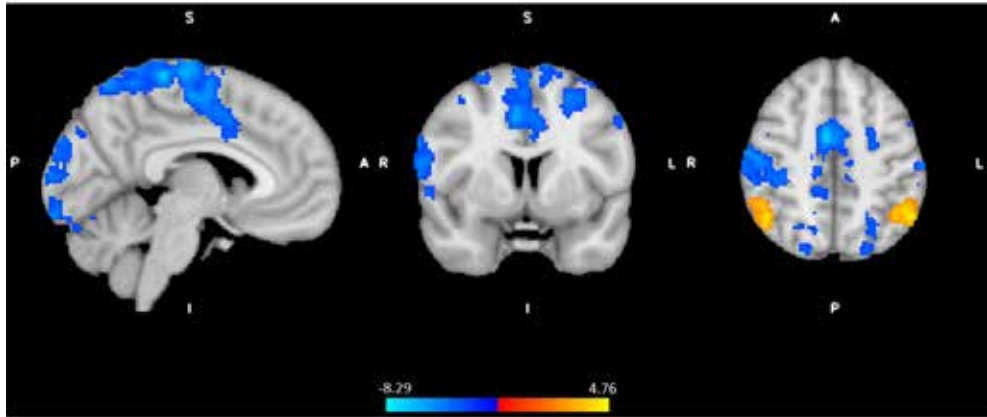


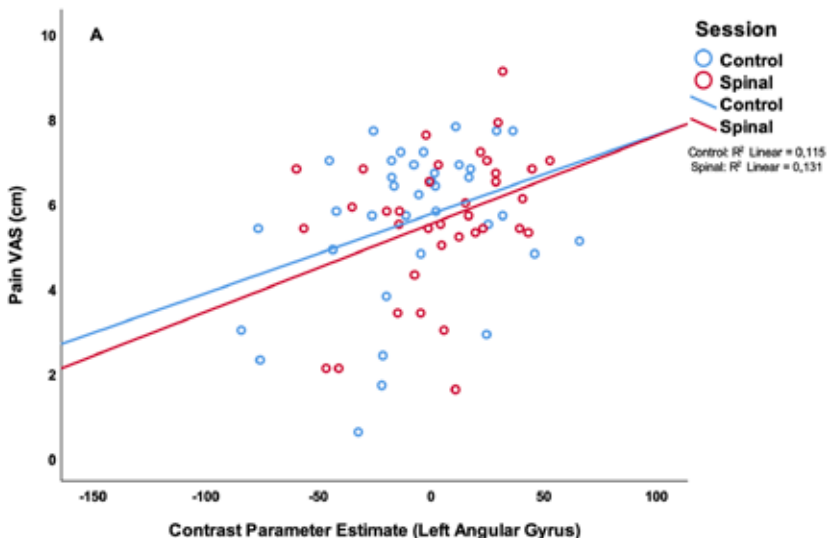
Figure 4. Significant neural responses to thermal noxious stimuli, resulting from a whole-brain analysis of the spinal session versus the control session ( $Spin_{(post-pre)} - Control_{(post-pre)}$ ), main effect of intervention. Red-yellow clusters correspond to higher BOLD response during spinal anesthesia compared to control, blue clusters correspond to a lower BOLD response during spinal anesthesia,  $p < 0.05$  cluster corrected. Images are Z-statistics thresholded at  $(-)2.3$ , overlaid on the MNI-152 standard brain. A=Anterior, I=Inferior, L=Left, P=posterior, S=Superior, R=Right. The significant clusters are described in detail in Table 5.

Table 5. Spinal Anesthesia effect on heat pain stimulus.

Location	Spinal $_{(post-pre)} > Control_{(post-pre)}$				
	Cluster size (1 mm <sup>3</sup> voxels)	Peak Z- value	MNI coordinates (mm)		
			x	y	z
L angular gyrus	769	4.81	-52	-58	48
*This cluster also includes:					
L supramarginal gyrus		4.34	-54	-50	-40
R lateral occipital cortex	696	4.25	48	-60	52
*This cluster also includes:					
R angular gyrus		4.2	45	-56	52
Location	Spinal $_{(post-pre)} < Control_{(post-pre)}$				
	Cluster size (1 mm <sup>3</sup> voxels)	Peak Z- value	MNI coordinates (mm)		
			x	y	z
R postcentral gyrus	19742*	8.20	10	-46	76
*This cluster also includes:					
L precentral gyrus		7.97	-2	-34	68
L postcentral gyrus		7.15	-20	-40	72
R precentral gyrus		7.01	8	-18	78
L postcentral gyrus	642*	4.6	-60	-22	46
*This cluster also includes:					
L precentral gyrus		3.33	-54	6	42
L postcentral gyrus		3.3	-56	-10	32
L cerebral white matter		3.26	-38	-28	28

Significant clusters of brain response to spinal anesthesia (compared to control), significant at  $p < 0.05$  cluster corrected. A Z-threshold of 2.3 was used; L = Left; R = Right.

In order to avoid circularity, we did not include effects of pain or temperature in the model described above. Instead, we asked whether brain regions activated by the task would be associated with pain perception. We extracted the contrast parameter estimates at the highest peak within the significant clusters where effects of spinal anesthesia (compared to control) was detected and performed a GEE by including Session x time x Pain score as predictive variables. This model revealed a significant interaction effect (Wald  $\chi^2(df=4) = 11.23$ ,  $P=0.024$ ) on the peak activity in the inferior parietal lobule (IPL,  $X=-52$ ,  $Y=-58$ ,  $Z=48$ ). In all condition, except in the post scan during the control session, higher pain scores were significantly correlated with increased BOLD response in this region. A similar effect was also observed in the right side of the IPL ( $X=60$ ,  $Y=-48$ ,  $Z=30$ ), (Wald  $\chi^2(df=4) = 13.39$ ,  $P=0.01$ ), however correlations between pain score and BOLD activity were only significant in the post condition of the spinal session. Interestingly, we found no correlations between pain scores and peaks in the postcentral regions which seemed to be less activated during the spinal compared to control. However, testing a GEE with Temperature x Session by Time as a predictive variable showed a significant interaction effect (Wald  $\chi^2(df=4) = 9.73$ ,  $P=0.045$ ) in the left postcentral region ( $X=60$ ,  $Y=-22$ ,  $Z=46$ ), but no significant correlation across the four scans ( $P$ 's  $> 0.08$ ). Figure 5 illustrates the distribution of pain-scores and the contrast of parameter estimate (COPE) at some peaks. We used COPE instead of BOLD response percentage, because our stimulus was relatively long (~10 seconds), and we did not have an existing estimate of the scale factor for a gamma-fit necessary to compute the percentage of the response.



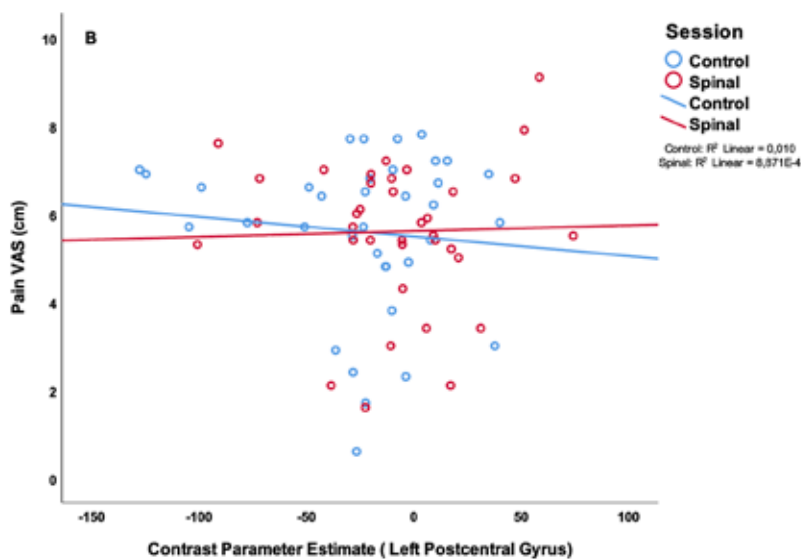


Figure 5. Scatterplot of the painscore (VAS in cm) and temperature parameter estimates of the (A):peak voxel of the left angular gyrus, part of the IPL (X=-52, Y=-58, Z=48 (B): the peak voxel of the left postcentral gyrus (X=-60, Y=-22, Z=46). In blue the scores of the control session in red the scores of the spinal session.

### Effect of treatment order

Because the order of conditions was randomized, and the study could not be blinded, we examined whether the order of the two visits (spinal anesthesia first visit or second visit) had any impact on pain perception. We repeated the GEE model by including order in the model (Pain VAS = Time x Session x Order + Time x Session + Time x Order + Session x Order + Time + Session + Order). This model revealed significant three-way interactions (Wald  $\chi^2$ (df =1) = 7.58, P =0.006), as well as two-way interaction between Time x Session (Wald  $\chi^2$ (df =1) = 10.98, P =0.001), thus confirming previous results; and two-way interaction between order x Session (Wald  $\chi^2$ (df =1) = 7.01, P =0.008). Compared to those who received the spinal session in the first visit, pain scores were lower in those who received the spinal anesthesia in the second visit (95% CI = -3.59 to -9.94). In those who received the spinal anesthesia in the second visit, the range of increase in pain perception was even more pronounced than what we found without accounting for the order effect (95% CI = 0.38 to 2.24). However, the fact that this effect was missing in those who received the spinal anesthesia first might suggest that differences in anticipation of the intervention interacted with pain scoring. In the absence of more fine grained qualitative data, we will not be able to make inferences about this observation.

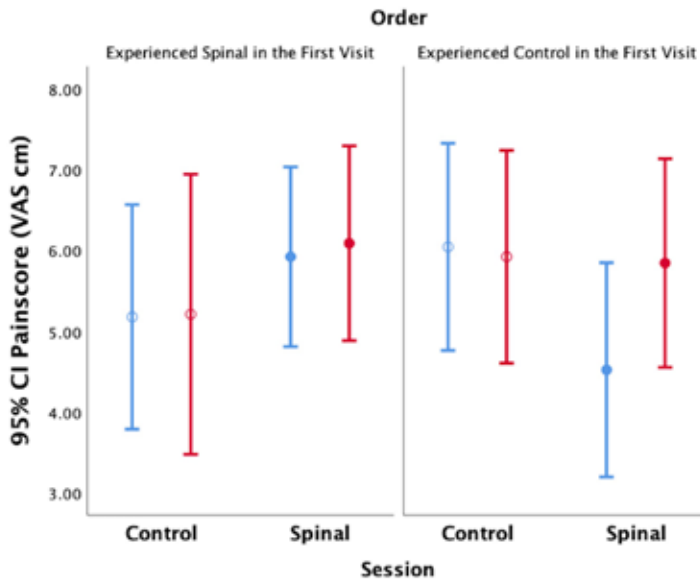


Figure 6. Average pain scores are shown without accounting for with-subject parameter estimation across time and session. In blue the pre-sessions, red post-sessions.

Figure 7 shows the results of the effect of order in the spinal condition visit on the BOLD response to noxious thermal stimuli. Those who experienced the spinal condition in the second visit, had significantly higher BOLD responses in several regions including the prefrontal and posterior areas where between-conditions inconsistencies were also present namely, the bilateral precentral gyrus, right postcentral gyrus, left supramarginal gyrus, right lateral occipital cortex including precuneus cortex, right middle frontal gyrus including superior frontal gyrus (Figure 7, Table 6). The BOLD response in the angular regions (where significant spinal (versus control) effects were observed) were not affected by the order ( $P$ 's > 0.4). Recall that although we had found an effect of spinal anesthesia in the postcentral regions, they were not significantly associated with pain.

However, we observed a significant association between activity in the middle frontal gyrus ( $X = 46, Y = 4, Z = 56$ ) and pain scores (GEE model variables: Pain score x Session x Time by order; Wald  $\chi^2$ (df = 8) = 16.45,  $P = 0.036$ ), with the effect being driven by positive correlation between BOLD response and pain in the control, and the spinal conditions of those who received the Spinal anesthesia in the second visit. Figure 8 illustrates these correlations.

It is noteworthy that while a consistent positive correlation is observed between pain scores and neural activity in three cases, this correlation was absent in the control condition of those who received spinal anesthesia on their first visit. This effect is similar to the observation of a discordant pain/temperature correlation during this condition, suggesting that other cognitive processes may have contributed to pain scoring during this presumably more “relaxed” condition (See Supplementary Materials).

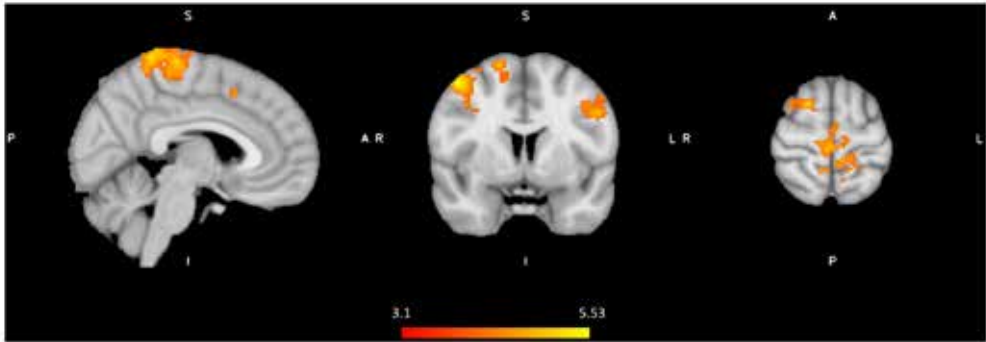


Figure 7. Significant neural responses to thermal noxious stimuli, resulting from a whole-brain analysis of the spinal condition visit first versus the spinal condition visit secondly (Spinal second<sub>(post-pre)</sub> - Spinal first<sub>(post-pre)</sub>). Red clusters correspond to higher BOLD response during spinal anesthesia second visit compared to spinal anesthesia first visit,  $p < 0.05$  cluster corrected. Images are Z-statistics thresholded at  $(-)3.1$ , overlaid on the MNI-152 standard brain. A=Anterior, I=Inferior, L=Left, P=posterior, S=Superior, R=Right. The significant clusters are described in detail in Table 6.

Table 6. Treatment order effect of spinal anaesthesia, spinal condition Second versus spinal condition First.

Spinal Second <sub>(post-pre)</sub> > Spinal First <sub>(post-pre)</sub>					
Location	Cluster size (1 mm <sup>3</sup> voxels)	Peak Z- value	MNI coordinates (mm)		
			x	y	z
R postcentral gyrus	1597*	5.28	8	-42	74
*This cluster also includes:					
R precentral gyrus		5.17	2	-26	70
L precentral gyrus		4.51	-8	-38	64
L supramarginal gyrus	1048*	4.26	-36	-50	32
*This cluster also includes:					
L angular gyrus		4.12	-46	-54	36
L lateral occipital cortex		3.94	-32	-68	38
R lateral occipital cortex	637*	3.95	28	-58	40
*This cluster also includes:					
R precuneus cortex		3.71	20	-64	38
R middle frontal gyrus	624*	5.48	46	4	56
*This cluster also includes:					
R superior frontal gyrus		4.49	20	8	64
R paracingulate gyrus		3.32	6	14	48
L precentral gyrus	441	4.19	-50	0	34

Significant clusters of brain response to spinal anaesthesia ( Second versus First) significant at  $p < 0.05$  cluster corrected. A Z-threshold of 3.1 was used; L = Left; R = Right.



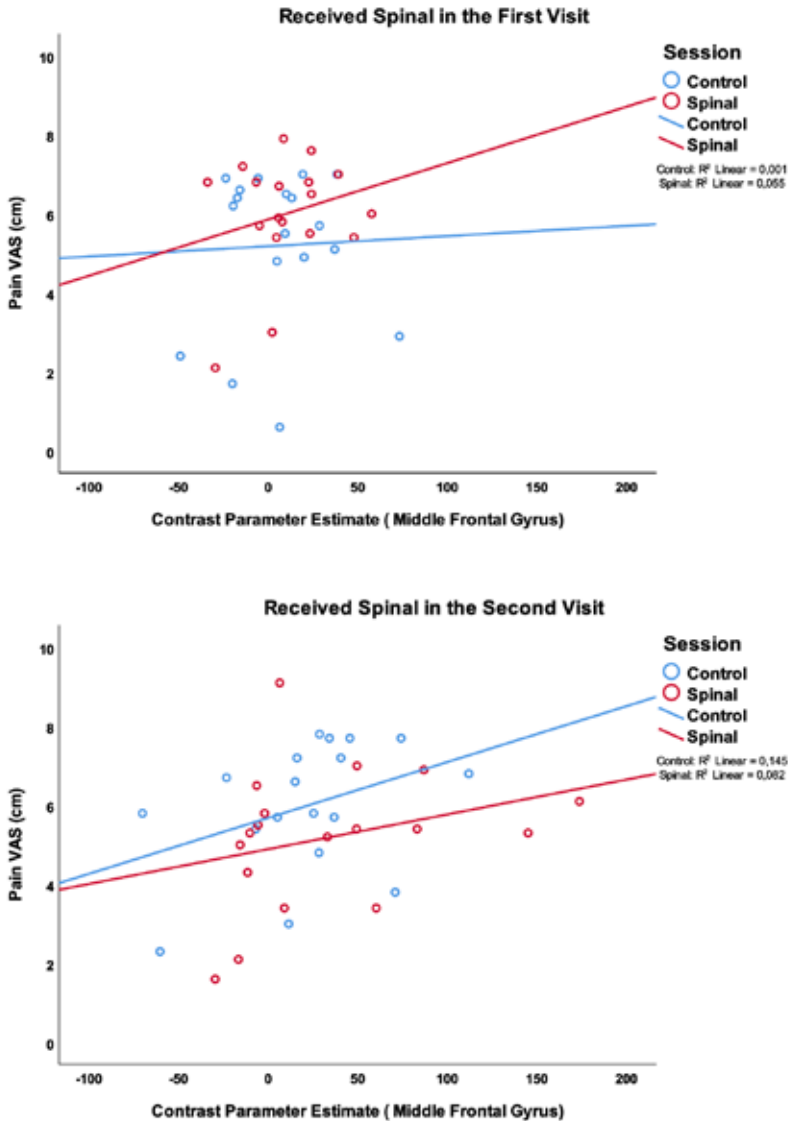


Figure 8. Association between pain scores and the medial prefrontal region which was significantly more activated in the group who received the spinal anesthesia in the second visit.

## Discussion

We postulated that spinal anesthesia provides a plausible experimental model for studying pain associated with peripheral nerve damage. We tested this experimental model to replicate observations from our previous study, and to examine the effect of pharmacological spinal deafferentation on brain activation in response to a calibrated thermal pain stimulus. Indeed, we found a significant effect on pain sensitivity during deafferentation at the skin above

the anesthetized dermatomes. The temporary deafferentation resulted in increased BOLD response to noxious thermal stimuli in the bilateral angular gyrus (IPL) and reduction of BOLD response in the pre and postcentral gyrus. Effects observed in the angular regions were associated with pain scores and were independent from order effect. We discuss the strength of our findings in the context of the existing body of knowledge and explain methodological challenges in mechanistic evaluations of the neurobiology pain processing.

### **Effect of noxious task on BOLD response**

One of the strengths of our study is we have acquired repeated task-based fMRI data under a common block-designed using thermal pain stimulation. This allowed us to examine the replicability of our results against the existing body of literature. Namely, as we have shown in Table 2, brain response to our fMRI task was to a large extent concordant with the findings of a recent meta-analysis of 222 fMRI studies of experimentally induced pain in healthy volunteers.<sup>14</sup> In that study, Xu and colleagues found a core set of brain regions, including the thalamus, secondary somatosensory cortex (SII), insula and mid-cingulate cortex (MCC), to be activated irrespective of stimulus location or modality.<sup>14</sup> For thermal noxious stimuli specifically, Xu and colleagues reported a subset of brain areas including the Rolandic operculum, MCC, middle frontal cortex, precentral gyrus and cerebellum to be activated. Our results also correspond to two other meta-analyses, except that they also emphasized the involvement of the anterior cingulate cortex (ACC) in response to pain.<sup>15, 16</sup> Indeed, as can be seen in Figure 1, the ACC was involved in pain processing in all conditions, except pre-scan of the spinal session. As we will describe later, the absence of this effect may be due to anticipatory factors that resulted from random ordering of a condition that could not be blinded.

Our findings corroborate that a broad network is deactivated during exposure to noxious stimuli. The deactivated regions in our study are in line with deactivations reported by others<sup>17-19</sup> For example, Kong et al. have reported decreased activity in key regions of the default mode network (DMN), such as bilateral medial prefrontal cortex (MPFC), posterior cingulate cortex/precuneus, parahippocampus, hippocampus and lateral temporal cortex. They have also observed deactivation in brain regions involved in sensory motor analysis, such as lateral occipital gyri, premotor area, superior frontal gyrus, and ipsilateral primary S1/M1.<sup>17</sup> Often, reduced BOLD response in the first level analysis is assumed to represent a decrease in neuronal activity.<sup>20</sup> We exercise caution in such interpretation, acknowledging the fact that the assumptions of a canonical hemodynamic response to a 10-second pain stimulus may not be valid.

Notwithstanding hemodynamic modeling limitations, the consistent deactivation in the ipsilateral sensorimotor cortex across the four conditions in our study is in line with the literature that attributes it to functional interhemispheric inhibition in order to optimize the differentiation of tactile information.<sup>21, 22</sup> Transient suppression of the ipsilateral sensorimotor cortex during tactile finger stimulation using balloon diaphragms driven by compressed air has

been described by Hlushchuk and colleagues.<sup>21</sup> Both painful and sensory stimulation had the same transient suppression in ipsilateral sensory cortex, according to Taylor and colleagues.<sup>23</sup>

The deactivation in the MPFC, known for its role in direction of internal conscious activity,<sup>24</sup> in all but the post-scan in the spinal anesthesia visit, might suggest a disruption of the normal internally directed cognitive activity as a result of spinal anesthesia. This is not necessarily or directly related to pain processing. The experience of loss of sensation in the legs caused by the acute deafferentation could explain these differences, and be interpreted as a outcome of increased attention to a new experience, diverting attention from processing the pain stimulus. This interpretation is further supported by our observation of the proportionate reduction of brain activity in response to noxious stimuli, in the posterior part of the DMN (Figure 4).

### **Effect of spinal anesthesia on brain activity**

Spinal anesthesia causes a temporary paralysis of the lower part of the body and as such it is a powerful model for disruption of afferent neural signaling from the limbs. Expectedly, pharmacological deafferentation is associated with changes in the network topography of brain regions involved in descending control and affective and sensory pain processing.<sup>2, 25, 26</sup> In our previous resting-state fMRI study we showed that spinal deafferentation was associated with increased pain sensitivity (hyperalgesia);<sup>2</sup> as well as a reduction in endogenous pain modulation expressed by reduced offset analgesia.<sup>27</sup> A limitation of the previous study was that the noxious stimulus was administered outside the scanner. Therefore, performing a task-based fMRI under spinal anesthesia aimed to help us gain a more precise view into whether the previously observed changes were related to instantaneous pain processing.

In this current study, we observed that spinal anesthesia was associated with a moderate hyperalgesia, as well as BOLD response in the bilateral angular gyrus (IPL) that were significantly more activated during spinal anesthesia (compared to control). Desmurget and colleagues stimulated awake patients using a bipolar electrode during awake surgery at the inferior parietal regions, which resulted in intention to move with no actual movement. They concluded that the intention of motor movement emerges from the IPL bilaterally.<sup>28</sup> Given that the angular gyrus is part of the IPL which is important for mediation of movement intention and execution of motor tasks,<sup>28-31</sup> we postulate that the observed effect reflects changes related to attentive pain processing. The right-sided IPL is known to play a role in attention, encoding salient events and conflict tasks.<sup>32</sup> The IPL is also part of multiple canonical resting state networks, such as the default mode network, the frontoparietal control network and the cingulo-opercular networks<sup>33, 34</sup> that also constitute the affective pain network.<sup>35, 36</sup> Given our study design, the highly localized difference observed in this region (during spinal anesthesia) corroborates interpretations by a previous study by Kong et al, that suggested IPL played a role in introspection and environmental monitoring.<sup>17</sup> Budell and colleagues used healthy volunteers in a

task-fMRI study with two tasks, one evaluating the amount of pain expressed (pain task) and the second discriminating movements (movement task) by watching one-second video clips displaying facial expressions of various levels of pain. They concluded that the bilateral IPL is predominantly involved in motor mirroring.<sup>31</sup> Buckner and colleagues have suggested that the IPL serves as a communication hub where numerous networks converge and interact.<sup>37</sup> Spinal anesthesia creates a strong somatosensory and interoceptive response as a result of losing sensation and the ability to move legs. We postulate that the effect observed by contrasting spinal versus control condition, irrespective of the order, was related to feeling the strong effect of this intervention.

Spinal anesthesia was also associated with reduced BOLD signal in the bilateral precentral and postcentral gyri. The postcentral gyrus receives somesthetic information of the body,<sup>38</sup> partly blocked by the spinal anesthesia. Interestingly effects in this region were not significantly correlated with pain scores, but an association with the temperature of the noxious stimuli was observed. Recall that we noted an inverse correlation between the thermal intensity and the pain score, suggesting that 30% of variations in pain perception were explained by pain tolerance. Moulton and colleagues differentiated heat sensation and pain sensation motivated by the fundamental concept that physical stimuli elicit distinguishable sensations such as heat besides pain. They concluded that the primary somatosensory cortex, positioned in the postcentral gyrus, better reflect magnitude of heat sensation than pain intensity in experimental heat pain studies.<sup>39</sup> Therefore, our results add to existing evidence for the involvement of these brain structures in conscious processing of sensorimotor-related activity, which were disrupted by a very strong somatosensory intervention.

### **The effect of order of experiencing spinal anesthesia or control**

One of the challenges in pharmacological neuroimaging is blinding. Randomization is a standard clinical practice that aims to remove the perceptual variations and reveal the mechanistic variations targeted by drugs. In the case of a complex sensation like pain, and a relatively complex and plausible stressful intervention, it is practically impossible to control for or remove all confounding effects. Although the increase in pain sensitivity caused by the spinal anesthesia (post - pre) seemed to be robust, we did observe a significant Session by Order interaction effect on pain scores (Figure 6), suggesting that anticipation may have played a role in pain scoring. The effect of ordering on main results observed in angular regions was not significant ( $P$ 's  $>0.4$ ). However, comparing the effect of spinal anesthesia (versus control) in those who received the spinal intervention in the first visit versus those who received it in the second visit, revealed significant differences within the same regions where inconsistencies between the four conditions were observed.

We postulate that those who received the spinal anesthesia in the first visit were potentially more 'relaxed' about what to expect in the second visit (no spinal anesthesia). By contrast, those who received the spinal anesthesia in the second visit were likely more hypervigilant about what to expect even during control. This interpretation is partially supported by the observation that the correlation between pain and temperature (See Appendix 1), and pain and brain activation (Figure 8) were similar in all but those who experiences the control session in the second visit. Anticipation of upcoming events and experiences has been shown to impact the brain network that was activated by the noxious stimulation in our experiment.<sup>40</sup> Indeed, we found that the BOLD response to the noxious heat stimuli in the task in those who received the spinal anesthesia in the second visit was higher in the right middle frontal gyrus and in the left superior frontal gyrus. As one of our reviewers suggested, the observed order effect could be due to the drug effects on pain reporting during the visit and not necessarily anticipation of pain itself (e.g. cognitive influences of pain processing). It is plausible to speculate that emotional and attentional differences caused by ordering might have contributed to the increase in pain scores.<sup>41-43</sup> Activity in prefrontal and precentral regions are also reported to be associated with placebo-analgesia.<sup>44</sup> We observed increased pain scores to be associated with the increased activity in the lateral prefrontal brain regions, during spinal anesthesia. The prefrontal cortex is known for its role in cognitive control of painful experiences.<sup>45-47</sup> Because the examiners placed the heat probe on participant's arm, this lack of control may have contributed to stress as well. The prefrontal cortex is often reported to play an important role in cognitive stress modulation.<sup>48-50</sup> Geva and colleagues examined the impact of an experimental psychosocial stress that modulates the prefrontal activity<sup>50</sup> on different dimensions of pain and showed that acute stress did not appear to impair pain sensitivity, but it did modulate the perception of pain magnitude, albeit with considerable interindividual differences.<sup>51</sup> However, both increased and decreased pain sensitivity has been reported in presence of experimentally induced stress,<sup>52-54</sup> which is plausibly related to interaction between different pain processing networks,<sup>55, 56</sup> and the dynamics of their response to different sensory or affective factors.<sup>57</sup> These issues need to be examined in a follow-up study with a more granular recording of perceptual and contextual experiences of study participants.

### Study limitations

Besides limitations in data collection to help us resolve the unexpected ordering effects, studies such as this are limited in blinding. Spinal anesthesia results in acute loss of motor and sensorimotor function, and the participants must be fully briefed about the procedure and expected effects prior to joining the study. Given the loss of motor and sensory control in lower limbs, those who received the intervention in the first session would be aware of what to not expect in the second session. Having observed the order effects, it is important to capture data that helps decipher the impact of acute unpleasantness, anxiety, or diversion during spinal anesthesia in the two sessions (spinal anesthesia and control).

Our study did not include any female participants. To include only male participants in pharmacological experiments is customary, as sex hormones influence pain sensitivity, especially during different phases of women's cycle.<sup>58</sup> While this design reflects a pragmatic necessity (because otherwise, a larger sample is needed to control for hormonal cycles), interpretations from such designs remain very limited. Besides biological factors, gender differences in pain reporting might have psychosocial underpinnings.<sup>59</sup> These differences may also manifest in cognitive and emotional processing of the noxious stimuli which will modulate neuronal activation.<sup>60, 61</sup> To repeat this experiment in a sample including women is necessary.

We used standard first-level analysis using canonical hemodynamic response functions available in the FEAT (FSL V6.0). Some infrared spectroscopy imaging studies have shown that pain stimuli invoke a specific hemodynamic response.<sup>62, 63</sup> In addition, the duration of the pain block (~10 seconds) and differences in pain intensity (which was calibrated) might lead to hemodynamic response functions that are not fully captured with our canonical models.<sup>64, 65</sup> We have explored some of these issues by introducing variations to the HRF model used for the first level analysis (e.g., by using different canonical functions, modeling the effect of temperature and time of stimulus onset, as well as removal of respiratory and cardiac pulses, in the first level analysis, however we did not observe differences in the topography of first order effects. Future studies need to explore the impact of block duration, as well as event-related pain stimulus tasks on results.

*In conclusion*, the loss of sensory and motor activity caused by spinal anesthesia has a significant impact on brain regions involved in the sensorimotor and cognitive processing of noxious thermal stimuli. Alterations in pain sensitivity were seen in non-deafferentated skin regions, *i.e.* at dermatomes above the level of the spinal anesthetic in a subset of participants. Treatment order significantly influenced pain sensitivity and activation of brain regions involved in heat sensation and cognitive processing of pain. This important and unexpected observation warrant attention in design of future randomized controlled trials that cannot be blinded. In these cases, additional psychometric, and phenomenological data can improve interpretations.

## Appendix

Table 3a: Brain activation and deactivation pre scan control condition

Brain activation upon thermal pain					
Location	Cluster size (1 mm <sup>3</sup> voxels)	Peak Z- value	MNI coordinates (mm)		
			x	y	z
R temporal pole	7398*	4.21	56	10	-2
*This cluster also includes:					
R Anterior cingulate gyrus		4.21	0	12	40
R Central opercular cortex		4.2	52	6	0
R juxta positional cortex		4.14	12	4	54
brainstem		4.04	10	-18	-20
L anterior cingulate gyrus		3.89	-10	6	34
B cerebellum	927	3.95	-32	-60	-30
Brain deactivation upon thermal pain					
R precentral gyrus	4075*	4.03	4	-28	60
*This cluster also includes:					
R postcentral gyrus		3.68	48	-24	60
B frontal pole	2498*	3.78	0	70	12
*This cluster also includes:					
R frontal medial cortex		3.59	12	40	-12
R precuneus cortex	2283*	3.79	6	-54	10
*This cluster also includes:					
R cingulate gyrus, post. div.		3.66	2	-52	30
L angular gyrus	1762*	3.99	-52	-60	24
*This cluster also includes:					
L lat. occipital cortex		3.63	-40	-72	10
R lat. occipital cortex	1420	3.77	52	-68	26
R temporal fusiform cortex	1408*	3.86	24	-36	-22
*This cluster also includes:					
R hippocampus		3.73	30	-10	-22
R parahippocampal gyrus		3.58	24	0	-22
L parahippocampal gyrus	700	3.71	-30	-26	-24

Brain activation in response to thermal pain, significant at  $p < 0.05$  cluster corrected. A Z threshold of 2.3 was used. B=Bilateral; L = Left; R = Right.

Table 3b: Brain activation and deactivation post scan control condition

Brain activation upon thermal pain					
Location	Cluster size (1 mm <sup>3</sup> voxels)	Peak Z- value	MNI coordinates (mm)		
			x	y	z
L central opercular cortex	9500*	5.47	-50	2	6
*This cluster also includes:					
L insular cortex		5.39	-36	4	8
Juxta positional lobule cortex		4.9	2	-4	68
R insular cortex	5990*	5.37	46	6	-2
*This cluster also includes:					
R Central opercular cortex		5.32	50	2	8
R temporal pole		5.32	52	8	-4
Cerebellum	1840	4.5	-40	-64	-30
Brain deactivation upon thermal pain					
R postcentral gyrus	1340*	4.4	16	-30	76
*This cluster also includes:					
R precentral gyrus		3.56	30	-26	56
L precentral gyrus		3.37	-2	-34	62
R cingulate gyrus, anterior div.	1256*	3.78	12	42	0
*This cluster also includes:					
R paracingulate cortex		3.74	4	42	-4
R frontal pole		3.23	16	58	-10
L subcallosal cortex		3.06	-6	28	-8

Brain activation and deactivation in response to thermal pain, significant at  $p < 0.05$  cluster corrected. A Z-threshold of 2.3 was used. B=Bilateral; L = Left; R = Right.



Table 4a. Brain activation and deactivation pre scan spinal condition

Brain activation upon thermal pain					
Location	Cluster size (1 mm <sup>3</sup> voxels)	Peak Z- value	MNI coordinates (mm)		
			x	y	z
R central opercular cortex	3009*	4.48	50	0	8
*This cluster also includes:					
R frontal operculum cortex		4.27	38	16	6
R insular cortex		4.16	40	18	0
R inferior frontal gyrus		3.91	48	14	12
L central opercular cortex	1791*	4.13	-38	2	12
*This cluster also includes:					
L frontal opercular cortex		4.02	-36	16	6
L WM sup. occipito-frontal fascicle		3.87	-20	4	22
L putamen		3.64	-28	0	-6
Brain deactivation upon thermal pain					
R postcentral gyrus	5240*	4.67	56	-12	54
*This cluster also includes:					
R precentral gyrus		4.05	30	-22	66
L paracingulate gyrus	835*	3.74	-10	38	-8
*This cluster also includes:					
R frontal medial cortex		3.35	4	46	-10
R paracingulate gyrus		3.35	4	40	-6
Subcallosal cortex		3.27	-2	14	-14
L postcentral gyrus	635	3.46	-54	-22	60

Brain activation and deactivation in response to thermal pain, significant at  $p < 0.05$  cluster corrected. A Z threshold of 2.3 was used. B=Bilateral; L = Left; R = Right.

Table 4b. Brain activation and deactivation post scan spinal condition

Brain activation upon thermal pain					
Location	Cluster size (1 mm <sup>3</sup> voxels)	Peak Z- value	MNI coordinates (mm)		
			x	y	z
R paracingulate gyrus	9265*	4.36	2	24	34
*This cluster also includes:					
L central opercular cortex		4.24	-38	8	8
L WM		4.21	-8	-4	24
R central opercular cortex		4.15	40	10	4
L insular cortex		4.11	-38	14	2
R cerebellum	619	3.71	38	-56	-30
Brain deactivation upon thermal pain					
R postcentral gyrus	4875	4.67	2	-38	66
L lat. Occipital cortex	2075*	4.13	-58	-64	6
*This cluster also includes:					
L temporal occipital fusiform cortex		3.65	-38	-58	-14
L middle temporal gyrus		3.39	-56	-54	0
R lingual gyrus	1449*	3.46	18	-42	-16
*This cluster also includes:					
R precuneus cortex		3.43	14	-50	10
R lateral occipital cortex	848*	3.28	32	-72	24
*This cluster also includes:					
R inferior temporal gyrus		3.16	48	-56	-12

Brain activation and deactivation in response to thermal pain, significant at  $p < 0.05$  cluster corrected. A Z threshold of 2.3 was used. B=Bilateral; L = Left; R = Right.

## References:

1. Andoh, J.; Milde, C.; Tsao, J. W.; Flor, H., Cortical plasticity as a basis of phantom limb pain: Fact or fiction? *Neuroscience* 2018, 387, 85-91.
2. Niesters, M.; Sitsen, E.; Oudejans, L.; Vuyk, J.; Aarts, L. P.; Rombouts, S. A.; de Rover, M.; Khalili-Mahani, N.; Dahan, A., Effect of deafferentation from spinal anesthesia on pain sensitivity and resting-state functional brain connectivity in healthy male volunteers. *Brain Connect* 2014, 4 (6), 404-16.
3. Jenkinson, M.; Bannister, P.; Brady, M.; Smith, S., Improved optimization for the robust and accurate linear registration and motion correction of brain images. *Neuroimage* 2002, 17 (2), 825-41.
4. Smith, S. M.; Zhang, Y.; Jenkinson, M.; Chen, J.; Matthews, P. M.; Federico, A.; De Stefano, N., Accurate, robust, and automated longitudinal and cross-sectional brain change analysis. *Neuroimage* 2002, 17 (1), 479-89.
5. Khalili-Mahani, N.; Chang, C.; van Osch, M. J.; Veer, I. M.; van Buchem, M. A.; Dahan, A.; Beckmann, C. F.; van Gerven, J. M.; Rombouts, S. A., The impact of “physiological correction” on functional connectivity analysis of pharmacological resting state fMRI. *Neuroimage* 2013, 65, 499-510.
6. Glover, G. H.; Li, T. Q.; Ress, D., Image-based method for retrospective correction of physiological motion effects in fMRI: RETROICOR. *Magn Reson Med* 2000, 44 (1), 162-7.
7. Chang, C.; Glover, G. H., Effects of model-based physiological noise correction on default mode network anti-correlations and correlations. *Neuroimage* 2009, 47 (4), 1448-59.
8. Kasper, L.; Bollmann, S.; Diaconescu, A. O.; Hutton, C.; Heinzle, J.; Iglesias, S.; Hauser, T. U.; Sebold, M.; Manjaly, Z. M.; Pruessmann, K. P.; Stephan, K. E., The PhysIO Toolbox for Modeling Physiological Noise in fMRI Data. *J Neurosci Methods* 2017, 276, 56-72.
9. Sherif, T.; Rioux, P.; Rousseau, M. E.; Kassis, N.; Beck, N.; Adalat, R.; Das, S.; Glatard, T.; Evans, A. C., CBRAIN: a web-based, distributed computing platform for collaborative neuroimaging research. *Front Neuroinform* 2014, 8, 54.
10. Woolrich, M. W.; Ripley, B. D.; Brady, M.; Smith, S. M., Temporal autocorrelation in univariate linear modeling of FMRI data. *Neuroimage* 2001, 14 (6), 1370-86.
11. Beckmann, C. F.; Jenkinson, M.; Smith, S. M., General multilevel linear modeling for group analysis in FMRI. *Neuroimage* 2003, 20 (2), 1052-63.
12. Woolrich, M. W.; Behrens, T. E.; Beckmann, C. F.; Jenkinson, M.; Smith, S. M., Multilevel linear modelling for FMRI group analysis using Bayesian inference. *Neuroimage* 2004, 21 (4), 1732-47.
13. Woolrich, M., Robust group analysis using outlier inference. *Neuroimage* 2008, 41 (2), 286-301.
14. Xu, A.; Larsen, B.; Baller, E. B.; Scott, J. C.; Sharma, V.; Adebimpe, A.; Basbaum, A. I.; Dworkin, R. H.; Edwards, R. R.; Woolf, C. J.; Eickhoff, S. B.; Eickhoff, C. R.; Satterthwaite, T. D., Convergent neural representations of experimentally-induced acute pain in healthy volunteers: A large-scale fMRI meta-analysis. *Neurosci Biobehav Rev* 2020, 112, 300-323.

15. Jensen, K. B.; Regenbogen, C.; Ohse, M. C.; Frasnelli, J.; Freiherr, J.; Lundstrom, J. N., Brain activations during pain: a neuroimaging meta-analysis of patients with pain and healthy controls. *Pain* 2016, 157 (6), 1279-86.
16. Duerden, E. G.; Albanese, M. C., Localization of pain-related brain activation: a meta-analysis of neuroimaging data. *Hum Brain Mapp* 2013, 34 (1), 109-49.
17. Kong, J.; Loggia, M. L.; Zyloney, C.; Tu, P.; LaViolette, P.; Gollub, R. L., Exploring the brain in pain: activations, deactivations and their relation. *Pain* 2010, 148 (2), 257-267.
18. Atlas, L. Y.; Wager, T. D., A meta-analysis of brain mechanisms of placebo analgesia: consistent findings and unanswered questions. *Handb Exp Pharmacol* 2014, 225, 37-69.
19. Jones, S. A.; Cooke, H. E.; Wilson, A. C.; Nagel, B. J.; Holley, A. L., A Pilot Study Examining Neural Response to Pain in Adolescents With and Without Chronic Pain. *Front Neurol* 2019, 10, 1403.
20. Shmuel, A.; Augath, M.; Oeltermann, A.; Logothetis, N. K., Negative functional MRI response correlates with decreases in neuronal activity in monkey visual area V1. *Nat Neurosci* 2006, 9 (4), 569-77.
21. Hlushchuk, Y.; Hari, R., Transient suppression of ipsilateral primary somatosensory cortex during tactile finger stimulation. *J Neurosci* 2006, 26 (21), 5819-24.
22. Frahm, J.; Baudewig, J.; Kallenberg, K.; Kastrop, A.; Merboldt, K. D.; Dechent, P., The post-stimulation undershoot in BOLD fMRI of human brain is not caused by elevated cerebral blood volume. *Neuroimage* 2008, 40 (2), 473-481.
23. Taylor, K. S.; Davis, K. D., Stability of tactile- and pain-related fMRI brain activations: an examination of threshold-dependent and threshold-independent methods. *Hum Brain Mapp* 2009, 30 (7), 1947-62.
24. Gusnard, D. A.; Akbudak, E.; Shulman, G. L.; Raichle, M. E., Medial prefrontal cortex and self-referential mental activity: relation to a default mode of brain function. *Proc Natl Acad Sci U S A* 2001, 98 (7), 4259-64.
25. Waberski, T. D.; Dieckhofer, A.; Remington, U.; Buchner, H.; Gobbele, R., Short-term cortical reorganization by deafferentation of the contralateral sensory cortex. *Neuroreport* 2007, 18 (11), 1199-203.
26. Pawela, C. P.; Biswal, B. B.; Hudetz, A. G.; Li, R.; Jones, S. R.; Cho, Y. R.; Matloub, H. S.; Hyde, J. S., Interhemispheric neuroplasticity following limb deafferentation detected by resting-state functional connectivity magnetic resonance imaging (fcMRI) and functional magnetic resonance imaging (fMRI). *Neuroimage* 2010, 49 (3), 2467-78.
27. Sitsen, E.; van Velzen, M.; de Rover, M.; Dahan, A.; Niesters, M., Hyperalgesia and Reduced Offset Analgesia During Spinal Anesthesia. *J Pain Res* 2020, 13, 2143-2149.
28. Desmurget, M.; Sirigu, A., Conscious motor intention emerges in the inferior parietal lobule. *Curr Opin Neurobiol* 2012, 22 (6), 1004-11.
29. Fogassi, L.; Ferrari, P. F.; Gesierich, B.; Rozzi, S.; Chersi, F.; Rizzolatti, G., Parietal lobe: from action organization to intention understanding. *Science* 2005, 308 (5722), 662-7.

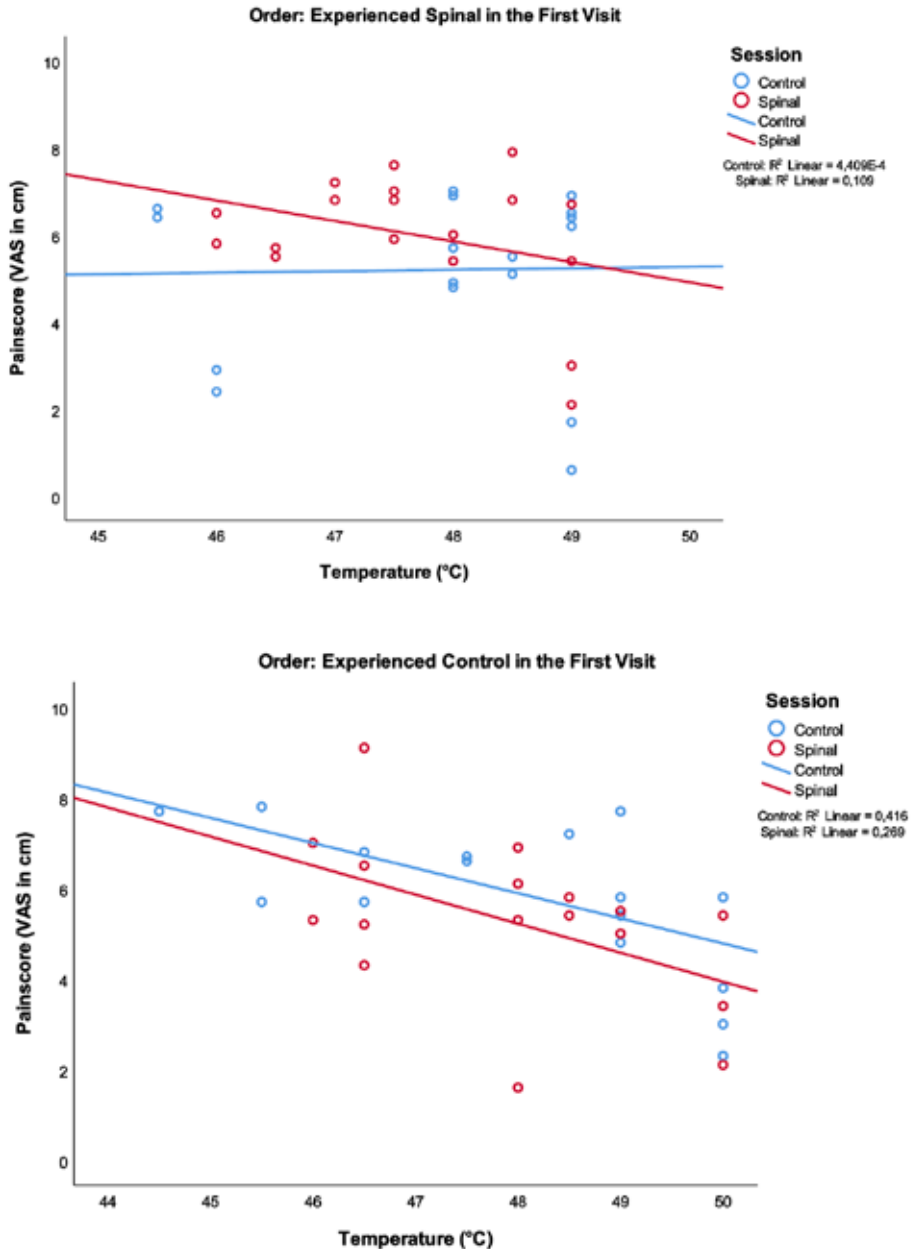
30. Rizzolatti, G.; Ferrari, P. F.; Rozzi, S.; Fogassi, L., The inferior parietal lobule: where action becomes perception. *Novartis Found Symp* 2006, 270, 129-40; discussion 140-5, 164-9.
31. Budell, L.; Jackson, P.; Rainville, P., Brain responses to facial expressions of pain: emotional or motor mirroring? *Neuroimage* 2010, 53 (1), 355-63.
32. Seghier, M. L., The angular gyrus: multiple functions and multiple subdivisions. *Neuroscientist* 2013, 19 (1), 43-61.
33. Smith, S. M.; Fox, P. T.; Miller, K. L.; Glahn, D. C.; Fox, P. M.; Mackay, C. E.; Filippini, N.; Watkins, K. E.; Toro, R.; Laird, A. R.; Beckmann, C. F., Correspondence of the brain's functional architecture during activation and rest. *Proc Natl Acad Sci U S A* 2009, 106 (31), 13040-5.
34. Igelstrom, K. M.; Graziano, M. S. A., The inferior parietal lobule and temporoparietal junction: A network perspective. *Neuropsychologia* 2017, 105, 70-83.
35. De Ridder, D.; Vanneste, S.; Smith, M.; Adhia, D., Pain and the Triple Network Model. *Front Neurol* 2022, 13, 757241.
36. Mano, H.; Seymour, B., Pain: a distributed brain information network? *PLoS Biol* 2015, 13 (1), e1002037.
37. Buckner, R. L.; Sepulcre, J.; Talukdar, T.; Krienen, F. M.; Liu, H.; Hedden, T.; Andrews-Hanna, J. R.; Sperling, R. A.; Johnson, K. A., Cortical hubs revealed by intrinsic functional connectivity: mapping, assessment of stability, and relation to Alzheimer's disease. *J Neurosci* 2009, 29 (6), 1860-73.
38. Burton, H., Cerebral Cortical Regions Devoted to the Somatosensory System: Results from Brain Imaging Studies in Humans. In *The somatosensory system*, 1st ed.; CRC Press: Boca Raton, 2001; p 424.
39. Moulton, E. A.; Pendse, G.; Becerra, L. R.; Borsook, D., BOLD responses in somatosensory cortices better reflect heat sensation than pain. *J Neurosci* 2012, 32 (17), 6024-31.
40. Amanzio, M.; Palermo, S., Pain Anticipation and Nocebo-Related Responses: A Descriptive Mini-Review of Functional Neuroimaging Studies in Normal Subjects and Precious Hints on Pain Processing in the Context of Neurodegenerative Disorders. *Front Pharmacol* 2019, 10, 969.
41. Hoegh, M.; Seminowicz, D. A.; Graven-Nielsen, T., Delayed effects of attention on pain sensitivity and conditioned pain modulation. *Eur J Pain* 2019, 23 (10), 1850-1862.
42. Roy, M.; Lebus, A.; Peretz, I.; Rainville, P., The modulation of pain by attention and emotion: a dissociation of perceptual and spinal nociceptive processes. *Eur J Pain* 2011, 15 (6), 641 e1-10.
43. Villemure, C.; Bushnell, M. C., Mood Influences Supraspinal Pain Processing Separately from Attention. *Journal of Neuroscience* 2009, 29 (3), 705-715.
44. Amanzio, M.; Benedetti, F.; Porro, C. A.; Palermo, S.; Cauda, F., Activation likelihood estimation meta-analysis of brain correlates of placebo analgesia in human experimental pain. *Hum Brain Mapp* 2013, 34 (3), 738-52.

45. Bräscher, A.-K.; Becker, S.; Hoeppli, M.-E.; Schweinhardt, P., Different Brain Circuitries Mediating Controllable and Uncontrollable Pain. *The Journal of Neuroscience* 2016, 36 (18), 5013-5025.
46. Brown, C. A.; Seymour, B.; El-Deredy, W.; Jones, A. K. P., Confidence in beliefs about pain predicts expectancy effects on pain perception and anticipatory processing in right anterior insula. *Pain* 2008, 139 (2), 324-332.
47. Mohr, C.; Leyendecker, S.; Helmchen, C., Dissociable neural activity to self- vs. externally administered thermal hyperalgesia: a parametric fMRI study. *European Journal of Neuroscience* 2008, 27 (3), 739-749.
48. Yuen, E. Y.; Liu, W.; Karatsoreos, I. N.; Feng, J.; McEwen, B. S.; Yan, Z., Acute stress enhances glutamatergic transmission in prefrontal cortex and facilitates working memory. *Proc Natl Acad Sci U S A* 2009, 106 (33), 14075-9.
49. Henze, G. I.; Konzok, J.; Kreuzpointner, L.; Bartl, C.; Peter, H.; Giglberger, M.; Streit, F.; Kudielka, B. M.; Kirsch, P.; Wust, S., Increasing Deactivation of Limbic Structures Over Psychosocial Stress Exposure Time. *Biol Psychiatry Cogn Neurosci Neuroimaging* 2020, 5 (7), 697-704.
50. Pruessner, J. C.; Dedovic, K.; Khalili-Mahani, N.; Engert, V.; Pruessner, M.; Buss, C.; Renwick, R.; Dagher, A.; Meaney, M. J.; Lupien, S., Deactivation of the limbic system during acute psychosocial stress: evidence from positron emission tomography and functional magnetic resonance imaging studies. *Biol Psychiatry* 2008, 63 (2), 234-40.
51. Geva, N.; Pruessner, J.; Defrin, R., Acute psychosocial stress reduces pain modulation capabilities in healthy men. *Pain* 2014, 155 (11), 2418-25.
52. Butler, R. K.; Finn, D. P., Stress-induced analgesia. *Prog Neurobiol* 2009, 88 (3), 184-202.
53. Cathcart, S.; Petkov, J.; Pritchard, D., Effects of induced stress on experimental pain sensitivity in chronic tension-type headache sufferers. *Eur J Neurol* 2008, 15 (6), 552-8.
54. Crettaz, B.; Marziniak, M.; Willeke, P.; Young, P.; Hellhammer, D.; Stumpf, A.; Burgmer, M., Stress-induced allodynia--evidence of increased pain sensitivity in healthy humans and patients with chronic pain after experimentally induced psychosocial stress. *PLoS One* 2013, 8 (8), e69460.
55. Roy, M.; Piché, M.; Chen, J.-I.; Peretz, I.; Rainville, P., Cerebral and spinal modulation of pain by emotions. *Proceedings of the National Academy of Sciences* 2009, 106 (49), 20900-20905.
56. Bingel, U.; Tracey, I., Imaging CNS Modulation of Pain in Humans. *Physiology* 2008, 23 (6), 371-380.
57. Bastuji, H.; Frot, M.; Perchet, C.; Magnin, M.; Garcia-Larrea, L., Pain networks from the inside: Spatiotemporal analysis of brain responses leading from nociception to conscious perception. *Hum Brain Mapp* 2016, 37 (12), 4301-4315.
58. Wiesenfeld-Hallin, Z., Sex differences in pain perception. *Gender Medicine* 2005, 2 (3), 137-145.
59. Dao, T. T.; LeResche, L., Gender differences in pain. *J Orofac Pain* 2000, 14 (3), 169-84; discussion 184-95.

60. Mischkowski, D.; Palacios-Barrios, E. E.; Banker, L.; Dildine, T. C.; Atlas, L. Y., Pain or nociception? Subjective experience mediates the effects of acute noxious heat on autonomic responses. *Pain* 2017, 159 (4), 699-711.
61. Malfliet, A.; De Pauw, R.; Kregel, J.; Coppieters, I.; Meeus, M.; Roussel, N.; Danneels, L.; Cagnie, B.; Nijs, J., Gender Differences in the Association of Brain Gray Matter and Pain-Related Psychosocial Characteristics. *Pain Physician* 2019, 22 (3), E191-E203.
62. Peng, K.; Yucel, M. A.; Aasted, C. M.; Steele, S. C.; Boas, D. A.; Borsook, D.; Becerra, L., Using prerecorded hemodynamic response functions in detecting prefrontal pain response: a functional near-infrared spectroscopy study. *Neurophotonics* 2018, 5 (1), 011018.
63. Yucel, M. A.; Aasted, C. M.; Petkov, M. P.; Borsook, D.; Boas, D. A.; Becerra, L., Specificity of hemodynamic brain responses to painful stimuli: a functional near-infrared spectroscopy study. *Sci Rep* 2015, 5, 9469.
64. Birn, R. M.; Bandettini, P. A., The effect of stimulus duty cycle and “off” duration on BOLD response linearity. *Neuroimage* 2005, 27 (1), 70-82.
65. Chen, J. E.; Glover, G. H.; Fultz, N. E.; Rosen, B. R.; Polimeni, J. R.; Lewis, L. D., Investigating mechanisms of fast BOLD responses: The effects of stimulus intensity and of spatial heterogeneity of hemodynamics. *Neuroimage* 2021, 245, 118658.

## Supplementary Materials

Correlation between pain scores and temperature are plotted by splitting the sample according to the order of the visit. This shows a consistent inverse correlation in both spinal and control condition of those who received Control in the first visit and Spinal in the second visit. However, this correlation was absent in cases where participants received the control session in their second visit.









Part 3

# Synthesis



# *Chapter 8*

## **Summary, conclusions and future perspectives**

Central neuraxial blockade (CNB) is a well-known and relative easy way to perform surgery without pain and it can be used to achieve good postoperative analgesia. The two most frequently used techniques, spinal and epidural anesthesia, are the main subject of this thesis. Both spinal and epidural anesthesia are worldwide applied in tens of thousands patients on a daily basis and consequently in millions each year. Still many effects of especially the deafferentation caused by neuraxial blockade is poorly studied and poorly understood. Neuraxial blockade results in disruption of ascending and descending input to the brain, *i.e.*, deafferentation, and has an impact on a range of factors such as the pharmacology of anesthetics (e.g., propofol) and the balance between the excitatory and inhibitory modulation of afferent stimuli. These effects will cause changes in pharmacokinetics and pharmacodynamics of general anesthetics, pain perception and connectivity in functional brain networks. This thesis describes a subset of topics related to temporary deafferentation in patients and healthy volunteers. All chapters describe studies that were aimed at understanding the effect of neuraxial blockade and the subsequent short-term deafferentation on the development of propofol anesthesia and pain perception.

In **Chapter 2** the effect of two different local anesthetics combined with an opioid during epidural analgesia was studied on efficacy in postoperative pain management. The two local anesthetics are stereo-isomers, enantiomers, they have identical atomic composition and chemical properties but different spatial arrangement of their atoms. Bupivacaine is the racemic mixture of these two enantiomers. The two local anesthetics studied, also called enantiomers, are ropivacaine and levobupivacaine. They have identical physicochemical properties but differ in pharmacokinetic and pharmacodynamic properties, caused by stereoselective interactions. Sixty-three patients were randomized to receive either ropivacaine 0.2% or 0.125% solution or levobupivacaine 0.125%, all combined with sufentanil 1 µg/mL. Patients underwent a total knee replacement, an operation with a high level of postoperative pain. There were no differences in postoperative pain scores, postoperative satisfaction, motor block, hourly sufentanil consumption, postoperative nausea/vomiting or pruritus. This study indicates that postoperative pain control from an epidural anesthetic/opioid combination was primarily determined by the opioid, sufentanil, without any pharmacodynamic difference between the two tested local anesthetics, ropivacaine and levobupivacaine. In contrast to earlier studies, we were unable to detect an enhancement of anesthetic potency with addition of an opioid.

Epidural anesthesia is used to induce pain relief during and after surgery and to minimize the need for systemic opioids. In **Chapter 3**, we studied the pharmacokinetic interaction of epidural anesthesia (with ropivacaine) with the general anesthetic propofol. In a randomized double blind study twenty-eight patients were included and assigned to receive an epidural injection of 0 (control condition), 50, 100 or 150 mg ropivacaine. After the epidural blockade was established, a standardized target controlled intravenous infusion of propofol was started. Patients were intensively monitored during the study period. A three-compartmental

model was fitted to the data using the non-linear mixed effects modelling statistical program NONMEM. To optimize the model, sex and weight were added to the model; adding the number of blocked segments as a covariate to the model further improved the data fits. With an increasing epidural blockade from 0 to 20 blocked segments, the metabolic clearance of propofol was reduced from  $2.64 \pm 0.12$  to  $1.87 \pm 0.08$  L/min, a 30% decrease. Simulations showed the effect of epidural blockade on blood propofol concentrations during a standard clinical propofol administration regimen. These findings agree with earlier studies on opioid and midazolam interaction with propofol. *i.e.*, an increase in blood propofol concentrations.<sup>1,2</sup> The mechanism of this pharmacokinetic interactive effect may be related to the hemodynamic changes of epidural anesthesia, *i.e.*, the reduction of systemic vascular resistance with consecutive reduced preload and mean arterial pressure. All of which causing a significant effect on anesthetic distribution within and clearance from the body.

To improve our understanding of the pharmacodynamic interactive effects of epidural anesthesia and propofol, we studied mean arterial pressure, cardiac output and bispectral index of the EEG (BIS) in **Chapter 4**. The influences of the dose and subsequent number of blocked segments after injection of the local anesthetic ropivacaine were explored. Main effects were tested on propofol pharmacodynamic model parameters: propofol potency ( $C_{50}$ ), baseline parameter values (BLN) and maximal effect ( $E_{MAX}$ ). Prior to propofol infusion, the epidural blockade caused a significant reduction in mean arterial pressure without affecting BIS or cardiac output. Adding covariates “number of blocked segments” or ropivacaine dose to the pharmacodynamic models did not affect the potency parameter of propofol for any of the studied endpoints. The absence of effect of epidural anesthesia on the BIS indicates that deafferentation has no influence on the level of arousal from propofol. This contrasts findings from earlier studies that, however, were unable to disentangle pharmacokinetic from pharmacodynamic effects of the epidural anesthetic. In our two studies (chapters 3 and 4), we showed that the interactive effects are pharmacokinetic in nature and that changes in sedation are related to an increase in plasma concentration rather than a central effect.

To examine the effect of deafferentation on brain networks, we performed a series of studies on the effect of spinal anesthesia on resting-state and task functional magnetic (fMRI) imaging. **Chapter 5** describes the effect of spinal anesthesia on resting-state functional connectivity in healthy volunteers and on pain perception at non-deafferented skin areas (*i.e.*, skin above the level of the anesthetic block). A total of 12 subjects received either an intrathecal injection with 15 mg bupivacaine or a sham injection. To determine the general effects of spinal deafferentation on functional connectivity, we used a model-free analysis of ten predefined networks of interest (NOIs). The acute spinal deafferentation resulted in rapid connectivity changes in the brain, most importantly in one of the ten NOIs, the sensorimotor network. This network is involved in action execution and perception somesthesia. Additionally, a significant increase in pain sensitivity during spinal anesthesia at non-deafferented skin area was

detected. We argue that the increase in pain sensitivity is best explained by the rebalancing in pain inhibitory and facilitatory pathways triggered by acute deafferentation.

To test the effect of spinal deafferentation on endogenous pain modulation, we tested spinal deafferentation on offset analgesia (OA), a relatively newly discovered, temporal rather than spatial discovered manifestation of endogenous pain modulation in **Chapter 6**. OA is defined by the reduction in pain intensity perception observed during noxious thermal stimulation towards hypoalgesia after a small decrease (1 °C) in noxious thermal stimulation. OA is caused by spatiotemporal processing of noxious stimuli aimed at amplifying reductions in noxious stimulation at spinal or central sites. In this randomized controlled crossover trial, static thermal pain responses and offset analgesia were obtained in 22 healthy male volunteers during spinal anesthesia and a control condition (absence of spinal anesthesia). The hyperalgesic response to heat pain on non-deafferented skin area during spinal anesthesia, as reported in Chapter 5, was confirmed. During deafferentation the OA response was less than in the control condition. Loss of proper OA engagement has been observed in neuropathic pain patients and in patients with fibromyalgia. Discussion regarding the mechanism of OA is still ongoing but our data supports the notion that we are witnessing that OA originates at brain sites involved in activation of descending pain modulatory pathways.

Next, we assessed the effect of spinal deafferentation on the brain by performing a task functional magnetic resonance study as described in Chapter 7. Twenty-two healthy subjects participated in this randomized cross-over study (spinal vs. control experiments performed on two occasions). On each occasion, subjects were scanned at two-time points: before and after spinal anesthesia/control (pre and post). Spinal anesthesia resulted in sensory loss up to dermatome Th6. Calibrated heat-pain stimuli were administered to the right forearm (C8-Th1) using a box-car design (blocks of 10 s on /25 s off) during MRI scanning. We tested different general linear models to examine: 1) Differences in BOLD response to pain stimulus under spinal anesthesia versus control and 2) Effects of spinal anesthesia on pain-related modulation of the cerebral activation. The results of the study are summarized by: the loss of sensory and motor activity caused by spinal anesthesia has a significant impact on brain regions involved in the sensorimotor and cognitive processing of noxious heat pain stimuli. Alterations in pain sensitivity were seen in non-deafferented skin regions, *i.e.* at dermatomes above the level of the spinal anesthetic in a subset of participants. Treatment order significantly influenced pain sensitivity and activation of brain regions involved in heat sensation and cognitive processing of pain.

### Future perspectives

Central neuraxial blockade (CNB), *i.e.*, spinal or epidural anesthesia, is a common technique in anesthesia to permit surgical interventions in the lower part of the body. For various surgeries, the use of neuraxial anesthesia is beneficial. For example, for spinal anesthesia,



the success rate is high with additionally high predictability, high patient satisfaction, low complication rate, better pain control than intravenous narcotics, earlier recovery of bowel function, less need for systemic opioids, less hypo- or hyperventilation due to better pain control, and improved recovery and early revalidation/rehabilitation. Central neuraxial blockade is frequently used in combination with sedatives to comfort the patient during surgery and reduce anxiety. In this thesis two main themes emerge: (1) CNB influences the cardiovascular system mainly by sympathetic blockade, thereby reducing systemic vascular resistance and mean arterial pressure. These hemodynamic changes affect the distribution and clearance of anesthetic medication and thus influence the pharmacology of systemic administered anesthetics; and (2) The abrupt blockade of afferent and efferent signals by CNB to the central nervous system leads to rebalancing of central brain networks and brain regions involved in pain regulation. These are important observations that deserve further evaluation and application. For example, the effect of the hemodynamic effects on anesthetic pharmacokinetics is not considered in target-controlled infusion models of, for example, propofol. Improved infusion algorithms may be developed that consider the hemodynamic effects of neuraxial blockade and consequently will reduce the occurrence and probability of side effects, such as overdosing causing deeper levels of anesthesia/sedation than required or hypotension.

Earlier studies concluded that the enhanced sedative effect of neuraxial blockade observed during sedation or anesthesia is related to deafferentation *per se*.<sup>3,5</sup> The results reported in this thesis do not agree with this conclusion, as we observed that not deafferentation but the number of blocked dermatomes and consequently changes in pharmacokinetics is responsible for higher blood concentrations of propofol, and therefore a seemingly deeper level of anesthesia/arousal. Further studies are needed to address whether other anesthetics or hypnotics, such as dexmedetomidine and remimazolam, are similarly affected by neuraxial blockade.

The above does not mean that deafferentation is without pharmacodynamic effects. Blockade of afferent and efferent input to the central nervous system did affect both resting-state and task fMRI output. There is ample evidence that upon deafferentation plastic changes in the brain evolve, for example after acute stroke or spinal cord injury. Here we show that pain perception is affected during neuraxial blockade due to plastic changes in several brain networks. Pain is a complex sensation with multiple factors influencing its perception. Factors such as genetics, neurodegeneration, cognition, context, sensitization, emotion, mood, resilience, sex/gender, prior experience are some of the factors involved in the personal pain perception. Self-reported pain intensity is considered the gold standard of pain measurement in clinical practice, however, the reliability of these subjective measures can be readily influenced by the patients' physiological and psychological condition, as well as by assessor's bias. As a result, there is an increasing need for a tool that could objectify the evaluated pain.

Previous fMRI studies were able to consistently detect those brain regions engaged in pain processing and quantify these effects as function of pain intensity.<sup>6</sup> Hence, we argue that fMRI studies lifted some of the aspects of the complexity of pain processing and perception. Still, other studies show that fMRI is unable to reveal divergent fMRI activity in patients with chronic pain. Possibly only subtle and spatially diffuse differences may exist within the pain network<sup>7</sup> or fMRI may be most sensitive to new experimental (acute) pain. Evidently, further studies are needed, possibly studies using deep learning of fMRI data, that enable detection of specific fMRI-related biomarkers for pain.<sup>8</sup>

## Conclusions

The following conclusions may be drawn from the data presented in this thesis:

1. Postoperative pain control from an epidural anesthetic/opioid combination is primarily determined by the opioid;
2. Epidural anesthesia significantly interacts with the pharmacokinetics of propofol, leading to a decrease in propofol clearance and accompanying increased propofol plasma concentration;
3. There is no pharmacodynamic interaction between epidural anesthesia and intravenously administered propofol;
4. Spinal anesthesia induced significant changes in resting-state functional connectivity in relation to one of the ten resting state networks, the sensorimotor network;
5. Spinal anesthesia reduced the offset analgesia response relative a sign that spinal deafferentation affects endogenous modulation of pain;
6. Spinal anesthesia leads to increased pain sensitivity in non-deafferented skin areas and changes activation in brain regions involved in the sensorimotor and cognitive processing of noxious heat pain stimuli.

## References

1. Mertens, M.J., et al., Mixed-effects modeling of the influence of alfentanil on propofol pharmacokinetics. *Anesthesiology*, 2004. 100(4): p. 795-805.
2. Vuyk, J., et al., Mixed-effects modeling of the influence of midazolam on propofol pharmacokinetics. *Anesth Analg*, 2009. 108(5): p. 1522-30.
3. Yang, M.K., et al., Influence of the baricity of a local anaesthetic agent on sedation with propofol during spinal anaesthesia. *Br J Anaesth*, 2007. 98(4): p. 515-8.
4. Pollock, J.E., et al., Sedation during spinal anesthesia. *Anesthesiology*, 2000. 93(3): p. 728-34.
5. Hodgson, P.S., S.S. Liu, and T.W. Gras, Does epidural anesthesia have general anesthetic effects? A prospective, randomized, double-blind, placebo-controlled trial. *Anesthesiology*, 1999. 91(6): p. 1687-92.
6. Xu, A., et al., Convergent neural representations of experimentally-induced acute pain in healthy volunteers: A large-scale fMRI meta-analysis. *Neurosci Biobehav Rev*, 2020. 112: p. 300-323.
7. Xu, A., et al., Brain Responses to Noxious Stimuli in Patients With Chronic Pain: A Systematic Review and Meta-analysis. *JAMA Netw Open*, 2021. 4(1): p. e2032236.
8. Santana, A.N., et al., Using Deep Learning and Resting-State fMRI to Classify Chronic Pain Conditions. *Front Neurosci*, 2019. 13: p. 1313.



# *Chapter 9*

## **Nederlandse samenvatting en conclusies**

De ruggenprik, ook wel centrale neuraxiale blokkade (CNB) genoemd, is een veelal bekende en relatief gemakkelijke manier om een verdoving te realiseren van de onderste helft van het lichaam en daarmee een operatie in dit gebied uit te voeren zonder de gewaarwording van pijn. Deze techniek kent 3 vormen, epidurale anesthesie, spinale anesthesie en gecombineerd spinale epidurale anesthesie. Deze technieken dragen ook bij aan een goede postoperatieve pijnstilling. De twee meest gebruikte technieken, spinale en epidurale anesthesie, vormen het hoofdonderwerp van dit proefschrift. Zowel spinale als epidurale anesthesie worden wereldwijd bij tienduizenden patiënten dagelijks toegepast en dus jaarlijks bij miljoenen patiënten. Veel effecten van deze technieken zijn nog steeds slecht onderzocht en worden slecht begrepen. CNB leidt tot verstoring van informatie uitwisseling verzonden via de zenuwbanen van en naar de hersenen, ook wel deafferentieatie genoemd, en heeft gevolgen voor 1) de farmacologie van via de bloedbaan (intraveneus) toegediende anesthetica (b.v. propofol), 2) pijnverwerking door het nieuwe evenwicht dat ontstaat tussen de stimulerende en remmende modulatie van aanvoerende pijnprikkels, en 3) de verandering van netwerken in de hersenen. Samenvattend, CNB veroorzaakt wijzigingen in de farmacokinetiek en farmacodynamiek van algemene verdovingsmiddelen, verandering in pijnperceptie en verbindingen/communicatie tussen hersennetwerken. Dit proefschrift beschrijft een aantal van deze onderwerpen bij zowel patiënten als gezonde vrijwilligers. Alle hoofdstukken beschrijven studies die gericht waren op het begrijpen van het effect van CNB en de daaropvolgende kortdurende deafferentieatie op de werking van gebruikte lokaal anesthetica, propofol anesthesie en pijnperceptie.

In **Hoofdstuk 2** wordt het effect van twee verschillende lokaalanesthetica (middelen die de zenuwgeleiding tijdelijk blokkeren) in combinatie met een opiaat, sufentanil, tijdens epidurale analgesie bestudeerd op de werkzaamheid van postoperatieve pijnbestrijding. De twee lokaalanesthetica zijn zogenaamde stereo-isomeren, ze hebben een identieke atomaire samenstelling en chemische eigenschappen, maar bezitten een verschillende ruimtelijke rangschikking van de atomen. Bijvoorbeeld, bupivacaïne is een mengsel van deze twee stereo-isomeren, het is een racemisch mengsel. De twee bestudeerde lokaalanesthetica, ook enantiomeren genoemd, die wij bestudeerden zijn ropivacaïne en levobupivacaïne. Zij hebben identieke fysisch-chemische eigenschappen, maar verschillen in farmacokinetische en farmacodynamische eigenschappen, veroorzaakt door stereoselectieve interacties. Drieënzestig patiënten werden gerandomiseerd om middels een epiduraal ropivacaïne 0.2% of 0.125% of levobupivacaïne 0,125% toegediend te krijgen, gecombineerd met 1 µg/mL sufentanil. De patiënten ondergingen een totale knie vervanging, een operatie die gepaard gaat met veel postoperatieve pijn. Er waren geen verschillen in postoperatieve pijnscores, postoperatieve patiënttevredenheid, motorisch blok, sufentanil verbruik per uur, postoperatieve misselijkheid/braken of jeuk (een bijwerking van opiaten). De groep die ropivacaïne 0,2% kreeg verbruikte significant meer lokaal anestheticum. Deze resultaten geven aan dat de postoperatieve pijnstilling veroorzaakt door deze epidurale toegediende lokaal anesthetica met het opiaat

sufentanil voornamelijk werd bepaald door sufentanil, zonder farmacodynamisch verschil tussen de twee geteste lokaal anesthetica, ropivacaïne en levobupivacaïne. In tegenstelling tot eerdere studies konden wij geen potentieverschil vaststellen tussen de lokaalanesthetica; dit werd waarschijnlijk veroorzaakt door de toevoeging van het opiaat.

Epidurale anesthesie wordt toegepast om pijnbestrijding tijdens en na de operatie te bewerkstelligen, en zodoende om de behoefte aan systemische opiaten postoperatief te minimaliseren. In **Hoofdstuk 3** bestudeerden wij de farmacokinetische interactie van epidurale anesthesie (met ropivacaïne) met het anestheticum (slaapmiddel) propofol. In een gerandomiseerde dubbelblinde studie werden achtentwintig patiënten geïncubeerd en toegewezen aan een epidurale injectie met 0 (controleconditie), 50, 100 of 150 mg ropivacaïne. Nadat de epiduraal toegediende medicatie was ingewerkt, werd een gestandaardiseerd toedieningsschema met intraveneus propofol gestart. De patiënten werden gedurende de studieperiode intensief gemonitord. De data werd geanalyseerd met drie-compartmenten-farmacokinetisch. Met een toename van de epidurale blokkade van 0 tot 20 geblokkeerde segmenten daalde de metabole klaring van propofol met ca. 30% van  $2.64 \pm 0.12$  tot  $1.87 \pm 0.08$  L/min. Simulaties toonden verder het effect van epidurale blokkade op de propofol concentraties in het bloed tijdens een standaard klinisch propofol toedieningsschema. Het mechanisme van de aangetoonde interactie kan gerelateerd zijn aan hemodynamische veranderingen veroorzaakt door de epidurale anesthesie, zoals bijvoorbeeld de vermindering van de weerstand in de bloedvaten met aansluitend een verminderde vulling (preload) van het hart en daardoor een lagere bloeddruk. Dit alles heeft een aanzienlijk effect op de verdeling van propofol in het lichaam en de klaring uit het lichaam.

Om meer inzicht te krijgen in de farmacodynamische interactie van epidurale anesthesie en propofol, hebben wij in **Hoofdstuk 4** de bloeddruk, het hartminuutvolume en de bispectrale index-(BIS)-van het electroencefalogram (EEG) bestudeerd. De BIS meet de anesthesiediepte, een maat die wordt aangegeven met een getal tussen de 0 (isoelectrische EEG) en 100 (volledig wakker). De invloed van de dosis en het aantal geblokkeerde segmenten na injectie van het lokaalanestheticum ropivacaïne werd onderzocht en gemodelleerd met een farmacodynamisch sigmoidaal  $E_{MAX}$  model met als parameters: propofol potentie ( $C_{50}$ ), basis parameterwaarden (BLN) en maximaal effect ( $E_{MAX}$ ). Voordat er propofol was toegediend veroorzaakte de epidurale blokkade een significante verlaging van de gemiddelde bloeddruk zonder invloed op de BIS of het hartminuutvolume. Toevoeging van de variabelen “aantal geblokkeerde segmenten” of ropivacaïnedosis aan de farmacodynamische modellen had geen invloed op de propofol  $C_{50}$ , voor geen van de bestudeerde eindpunten. De afwezigheid van een effect van epidurale anesthesie op de BIS wijst erop dat deafferentieatie geen invloed heeft op de diepte van sedatie door propofol. Dit staat in schril contrast met de bevindingen van eerdere gepubliceerde studies, deze studies konden echter geen onderscheid maken tussen farmacokinetische en farmacodynamische effecten van epidurale anesthesie. In onze twee

studies (**Hoofdstukken 3 en 4**) toonden wij aan dat de interactieve effecten van epiduraal toegediende ropivacaïne en het slaapmiddel propofol farmacokinetisch van aard zijn en dat veranderingen in sedatie eerder verband houden met een toename van de plasmaconcentratie dan met een centraal effect in de hersenen.

Om het effect van deafferentiatie op hersennetwerken te onderzoeken, hebben wij een reeks studies verricht naar het effect van spinale anesthesie in rusttoestand en door het uitvoeren van een taak met behulp van beeldvorming: functionele magnetische resonantie (fMRI). **Hoofdstuk 5** beschrijft het effect van spinale anesthesie op functionele verbindingen tussen delen in de hersenen in de rusttoestand bij gezonde vrijwilligers en op pijnperceptie in niet-verdoofde huidgebieden (d.w.z. huid boven het niveau van het verdovingsblok). In totaal kregen 12 proefpersonen een spinale anesthesie met 15 mg bupivacaïne of een “nep” injectie. Om de effecten van spinale deafferentiatie op de functionele verbindingen tussen hersengebieden te bepalen, gebruikten we een modelvrije analyse van tien bekende, vooraf gedefinieerde breinnetwerken. De acute spinale deafferentiatie resulteerde in snelle veranderingen in de hersennetwerken, vooral in één van de tien netwerken, het sensorisch-motorische netwerk. Dit netwerk is betrokken bij de uitvoering van bewegingen en de waarneming van sensaties, zoals pijn en warmte, in het lichaam. Bovendien werd een significante toename van de pijngevoeligheid tijdens spinale anesthesie op het niet-verdoofde huidgebied vastgesteld. Wij stellen dat de toename van de pijngevoeligheid het best verklaard kan worden door het ontstaan van een nieuwe balans in breinnetwerken door het ontbreken van aanvoerende sensore informatie naar het brein (veroorzaakt door de acute deafferentiatie).

Gezonde mensen kunnen pijnsignalen beïnvloeden door deze signalen te dempen. Dit mechanisme wordt endogene pijnstilling genoemd. Om het effect van spinale deafferentiatie op endogene pijnmodulatie te kwantificeren, testten wij het effect van spinale anesthesie op offset analgesia (OA), een relatief nieuw ontdekte uiting van endogene pijnmodulatie in **Hoofdstuk 6**. OA wordt gedefinieerd door de vermindering van de waarneming van de pijnintensiteit tijdens een pijnprikkel met behulp van hitte op de huid (thermische stimulatie) na een kleine afname (1 °C) van de temperatuur. OA wordt veroorzaakt doordat op spinaal of centraal niveau de systemen die zijn gericht op het versterken van de pijnvermindering gestimuleerd worden. In deze gerandomiseerde gecontroleerde cross-over studie bij 22 gezonde mannelijke vrijwilligers tijdens spinale anesthesie en een controle conditie (afwezigheid van spinale anesthesie) werden statische thermische pijnprikkelers toegediend en offset analgesie gemeten. De toegenomen pijnwaarneming op een niet-verdoofd huidgebied tijdens spinale anesthesie, zoals gerapporteerd in **Hoofdstuk 5**, werd bevestigd. Tijdens de deafferentiatie was de OA-respons minder dan in de controleconditie. Bij onderzoek in neuropathische pijnpatiënten en patiënten met fibromyalgie is al eerder een verlies van de OA-respons waargenomen. De discussie over het mechanisme van OA is nog gaande, maar onze gegevens ondersteunen het idee dat OA ontstaat op plaatsen in de hersenen die betrokken



zijn bij de activering van pijnmodulerende zenuwbanen. Dat wil zeggen dat er centraal in de hersenen zenuwsystemen geactiveerd worden die de pijnstilling bevorderen.

Vervolgens beoordeelden wij het effect van spinale deafferentiatie op de hersenen door een fMRI studie uit te voeren waarbij we tijdens het scannen van de proefpersonen een pijnprikkel toedienden, beschreven in **Hoofdstuk 7**. Tweeëntwintig gezonde proefpersonen namen deel aan deze gerandomiseerde cross-over studie (spinale versus controle-experimenten uitgevoerd op twee verschillende dagen). Op beide dagen werden de proefpersonen op twee tijdstippen gescand: voor en na de spinale anesthesie of voor en na de controleconditie (pre en post). Spinale anesthesie resulteerde in verlies van motoriek en gevoel tot de hoogte van het borstbeen. Gekalibreerde warmte/pijnstimuli werden toegediend in de MRI aan de rechter (niet-verdoofde) onderarm in een box-car design (blokken van 10 seconden aan en daarna 25 seconden uit). Wij waren vooral geïnteresseerd in de verschillen in BOLD-respons op de pijnprikkel onder spinale anesthesie versus controleconditie, de effecten van spinale anesthesie op pijn-gerelateerde verandering van hersenactiviteit. Samengevat zagen we dat het verlies van sensorische en motorische activiteit ten gevolge van spinale anesthesie een significante invloed had op hersengebieden die betrokken zijn bij de sensorisch-motorische en cognitieve verwerking van pijnprikkels door warmte. Veranderingen in de pijngevoeligheid werden gezien in niet-gedeafferentierde huidgebieden, dat wil zeggen, op dermatomen boven het niveau van de spinale verdoving, althans in een deel van de deelnemers. De volgorde van behandeling beïnvloedde significant de pijngevoeligheid en activering van hersengebieden die betrokken zijn bij warmtesensatie en cognitieve verwerking van pijn.

### Toekomstperspectief

Centrale neuraxiale blokkade (CNB), dat wil zeggen spinale of epidurale anesthesie, is een gangbare techniek in de anesthesie om chirurgische ingrepen in het onderste deel van het lichaam mogelijk te maken. Voor verschillende operaties is het gebruik van neuraxiale anesthesie nuttig. Voor spinale anesthesie bijvoorbeeld is het succespercentage zeer hoog met bovendien een hoge voorspelbaarheid, een hoge patiënten tevredenheid, een laag complicatiepercentage, een betere pijncontrole dan intraveneuze anesthesie, een vroeger herstel van de darmfunctie, minder behoefte aan systemische opioïden, minder hypo- of hyperventilatie door een betere pijncontrole, een beter herstel en een vroege revalidatie/revalidatie. Centrale neuraxiale blokkade wordt vaak gebruikt in combinatie met een slaapmiddel om de patiënt tijdens de operatie te laten slapen. In dit proefschrift komen twee hoofdthema's tot uiting: (1) CNB beïnvloedt het cardiovasculaire systeem hoofdzakelijk door sympathische blokkade, waardoor de systemische vaatweerstand en de bloeddruk worden verlaagd. Deze hemodynamische veranderingen beïnvloeden de distributie en klaring van slaapmiddelen en beïnvloeden op deze manier de farmacologie van deze intraveneus toegediende slaapmiddelen (in dit geval propofol); en (2) de abrupte blokkade van aanvoerende en neergaande signalen door CNB naar het centrale zenuwstelsel leidt tot een

nieuwe balans van hersennetwerken en hersengebieden die betrokken zijn bij pijnregulering. Dit zijn belangrijke observaties die verdere evaluatie verdienen en meegenomen moeten worden in de klinische behandeling van patiënten. Het effect van de hemodynamische effecten op de farmacokinetiek van slaapmiddelen wordt bijvoorbeeld niet meegenomen in klinische infusiemodellen van propofol. Verbeterde infusiealgoritmen die wel rekening houden met de gemeten hemodynamische effecten van CNB kunnen de kans op het optreden van bijwerking, zoals een te diep niveau van anesthesie/sedatie of hypotensie, verminderen.

Eerdere studies concludeerden dat het versterkte sedatieve effect van neuraxiale blokkade tijdens sedatie of anesthesie verband houdt met deafferentiatie. De in dit proefschrift gepubliceerde resultaten komen niet overeen met deze conclusie, aangezien wij aantoonde dat niet deafferentiatie, maar de hoogte van de verdoving en de daardoor ontstane veranderingen in de farmacokinetiek verantwoordelijk zijn voor hogere bloedconcentraties van propofol dan verwacht, waardoor er een schijnbaar dieper niveau van anesthesie (verminderde arousal) ontstaat. Verdere studies zijn nodig om na te gaan of andere verdovingsmiddelen of hypnotica, zoals dexmedetomidine en remimazolam, op soortgelijke wijze worden beïnvloed door neuraxiale blokkade.

Het bovenstaande betekent niet dat deafferentiatie zonder farmacodynamische effecten is. Blokkade van afferente en efferente input naar het brein heeft wel degelijk een effect op verschillende hersennetwerken. Er zijn voldoende klinische aanwijzingen dat na deafferentiatie veranderingen in de hersenen optreden, bijvoorbeeld na een acute beroerte of na een ruggenmergletsel. Hier laten we zien dat ook pijnperceptie wordt beïnvloed tijdens CNB door veranderingen in verschillende hersennetwerken. Pijn is een complexe sensatie met verscheidene factoren die de perceptie ervan beïnvloeden. Factoren zoals genetica, neurodegeneratie, cognitie, context, sensibilisatie, emotie, stemming, veerkracht, geslacht en eerdere ervaringen zijn enkele van de factoren die betrokken zijn bij de persoonlijke pijnperceptie. Zelf-gerapporteerde pijnintensiteit wordt beschouwd als de gouden standaard voor pijnmeting in de klinische praktijk, maar de betrouwbaarheid van deze subjectieve metingen kan gemakkelijk worden beïnvloed door de fysiologische en psychologische toestand van de patiënt en door de vooringenomenheid van de beoordelaar (arts, verpleegkundige of onderzoeker). Daarom is er een toenemende behoefte aan een instrument dat de pijn kan objectiveren. Meta-analyses van diverse studies naar pijnverwerking in de hersenen tonen consistent de betrokkenheid van specifieke hersengebieden bij pijnverwerking. Er zijn ook studies die deze betrokkenheid gekwantificeerd hebben als functie van de pijnintensiteit. Onze fMRI-studies hebben een aantal aspecten van de complexiteit van acute pijnverwerking en pijnperceptie verhelderd, maar dan in vrijwilligers zonder onderliggend pijnprobleem. Andere studies tonen dat de fMRI niet goed in staat is om afwijkende breinactiviteit bij patiënten met chronische pijn aan het licht te brengen. Mogelijk bestaan er alleen subtiele en diffuse ruimtelijk verschillen binnen het pijnnetwerk of is fMRI meer gevoelig voor nieuwe

experimentele (acute) pijn dan langer bestaande chronische pijn. Het is duidelijk dat verdere studies nodig zijn, bijvoorbeeld met gebruikmaking van deep learning van fMRI-gegevens, die de opsporing van specifieke fMRI-gerelateerde biomarkers voor pijn mogelijk maken.

## Conclusies

Uit het gepresenteerde onderzoek kunnen de volgende conclusies worden getrokken:

1. Postoperatieve pijncontrole van een epidurale anesthesie/opiaat combinatie wordt voornamelijk bepaald door het toegediende opioïd;
2. Epidurale anesthesie heeft een significante interactie met de farmacokinetiek van propofol wat leidt tot een afname van de propofol klaring en een daarmee gepaard gaande verhoogde propofol plasma concentratie;
3. Er is geen farmacodynamische interactie tussen epidurale anesthesie en intraveneus toegediend propofol;
4. Spinale anesthesie induceerde significante veranderingen in een van de tien bekende functioneel verbonden hersennetwerken in rusttoestand, het sensorisch motorische netwerk;
5. Spinale anesthesie vermindert de offset analgesia respons, een teken dat spinale deafferentatie de endogene modulatie van pijn beïnvloedt;
6. Spinale anesthesie leidt tot een verhoogde pijngevoeligheid in niet verdoofde huidgebieden en verandert de activatie in hersengebieden die betrokken zijn bij de sensorisch-motorische en cognitieve verwerking van thermische pijnprikkels.



# *Addenda*

## **Curriculum vitae, List of Publications, Abbreviations**

## Curriculum vitae

Elske Sitsen is geboren op 26 oktober 1970 in Harderwijk, Nederland. Zij volgde het Atheneum op College Groevenbeek in Ermelo en zij behaalde haar eindexamen in 1989. In 1990 startte zij met haar studie geneeskunde en studeerde in 1998 af aan de Rijksuniversiteit van Utrecht. Na een aantal maanden als AGNIO gewerkt te hebben in het Lucas-Andreas ziekenhuis startte zij in 1999 als arts-assistent op de afdeling Anesthesiologie in het LUMC waar zij haar opleiding tot Anesthesioloog in 2006 voltooide. In dat zelfde jaar werd zij aangenomen als staflid op de afdeling Anesthesiologie in het LUMC. Zij werkt sindsdien als algemeen anesthesioloog met expertise in de regionale anesthesie en zij maakt deel uit van het levertransplantatie team. Haar onderzoeksproject startte in de eindfase van de opleiding en werd in 2010 verder uitgewerkt onder begeleiding van Albert Dahan wat heeft geleid tot dit proefschrift. Sinds 2017 zit zij als medisch manager in het managementteam van het OK-centrum, en sinds 2018 is zij verantwoordelijk voor de pre-operatieve polikliniek. Buiten deze taken neemt zij deel aan diverse commissies en stuurgroepen binnen het LUMC, en zit zij sinds 2022 in het bestuur van het stafconvent. Zij is getrouwd met Paul Hedeman Joosten, vaatchirurg, en zij hebben samen 4 kinderen, Bente, Boas, Noor en Jonathan, geboren tussen 2001 en 2006.

## List of Publications

Sitsen, E.; Bax, N. M.; van der Zee, D. C., Is laparoscopic pyloromyotomy superior to open surgery? *Surg Endosc* 1998, 12 (6), 813-5.

Sitsen, M. E.; Ho, G. H.; Blankensteijn, J. D., Deformation of self-expanding stent-grafts complicating endovascular peripheral aneurysm repair. *J Endovasc Surg* 1999, 6 (3), 288-92.

Sitsen, E.; van Poorten, F.; van Alphen, W.; Rose, L.; Dahan, A.; Stienstra, R., Postoperative epidural analgesia after total knee arthroplasty with sufentanil 1 microg/ml combined with ropivacaine 0.2%, ropivacaine 0.125%, or levobupivacaine 0.125%: a randomized, double-blind comparison. *Reg Anesth Pain Med* 2007, 32 (6), 475-80.

Sitsen, E.; van Poorten, F.; Jansen, G.; Kuijpers, R.; Dahan, A.; Stienstra, R., A comparison of the efficacy of levobupivacaine 0.125%, ropivacaine 0.125% and ropivacaine 0.2%, all combined with sufentanil 0.5 microg/mL, in patient-controlled epidural analgesia after hysterectomy under combined epidural and general anesthesia. *Acta Anaesthesiol Belg* 2012, 63 (4), 169-75.

Niesters, M.; Sitsen, E.; Oudejans, L.; Vuyk, J.; Aarts, L. P.; Rombouts, S. A.; de Rover, M.; Khalili-Mahani, N.; Dahan, A., Effect of deafferentation from spinal anesthesia on pain sensitivity and resting-state functional brain connectivity in healthy male volunteers. *Brain Connect* 2014, 4 (6), 404-16.

Sitsen, E.; Olofsen, E.; Lesman, A.; Dahan, A.; Vuyk, J., Epidural Blockade Affects the Pharmacokinetics of Propofol in Surgical Patients. *Anesth Analg* 2016, 122 (5), 1341-9.

Okkerse, P.; Hay, J. L.; Sitsen, E.; Dahan, A.; Klaassen, E.; Houghton, W.; Groeneveld, G. J., Pharmacokinetics and pharmacodynamics of intrathecally administered Xen2174, a synthetic conopeptide with norepinephrine reuptake inhibitor and analgesic properties. *Br J Clin Pharmacol* 2017, 83 (4), 751-763.

Sitsen, E.; van Velzen, M.; de Rover, M.; Dahan, A.; Niesters, M., Hyperalgesia and Reduced Offset Analgesia During Spinal Anesthesia. *J Pain Res* 2020, 13, 2143-2149.

Jaap Vuyk, E. S., Marije Reekers, Intravenous Anesthetics. In *Miller's Anesthesia*, Michael A. Gropper, MD,, Lars I. Eriksson, MD, Lee A. Fleisher, MD, Jeanine P. Wiener-Kronish, MD, Neal H Cohen, MD and Kate Leslie, MD. 2019, Chapter 23.

Meijer, T. S.; Geus-Oei, L. F.; Martini, C. H.; Tijl, F. G. J.; Sitsen, M. E.; Erkel, A. R. V.; Meer, R. W. V.; Kapiteijn, E.; Vahrmeijer, A. L.; Burgmans, M. C., Embolization of variant hepatic arteries in patients undergoing percutaneous hepatic perfusion for unresectable liver metastases from ocular melanoma. *Diagn Interv Radiol* 2019, 25 (6), 451-458.

Sitsen, E.; Olofsen, E.; Dahan, A.; Vuyk, J., Effect of lumbar epidural blockade and propofol on mean arterial pressure, cardiac output and bispectral index: A randomised controlled and pharmacodynamic modelling study. *Eur J Anaesthesiol* 2021, 38 (Suppl 2), S121-S129.

Elske Sitsen MD, Najmeh Khalili-Mahani PhD, Mischa de Rover PhD, Albert Dahan MD PhD, Marieke Niesters MD PhD. Effect of spinal anesthesia-induced deafferentation on pain processing in healthy male volunteers: a task-related fMRI study. Accepted for publication November 2022 *Frontiers in Pain Research*.



## Abbreviations

CNS	Central Nervous System
CNB	Central Neuraxial Blockade
fMRI	functional Magnetic Resonance Imaging
CV	cardiovascular
NONMEM	non-linear mixed-effects modeling software
PCEA	Patient Controlled Epidural Anesthesia
MLAC	Minimal Local Anesthetic Concentration
MLSB	Maximum Level of Sensory Block
MBS	Motor Block Scores
NRS	Numerical Rating Scale
TFD	Time to First Demand
SD	Standard Deviation
ASA	American Society of Anesthesiologists Physical Status
PONV	Postoperative Nausea and Vomiting
MDPE	Median Performance Error
MDAPE	Median Absolute Performance Error
NBS	Number of Blocked Segments
TCI	Target Controlled Infusion
BMI	Body Mass Index
BIC	Bayesian Information Criterion
MVOF	Minimum Value of Objective Function
BLN	Baseline effect
$E_{MAX}$	Maximum Predicted Effect
$C_{50}$	Concentration of a drug that gives 50% of maximal effect
$C_E$	Effect-site Concentration
$t_{1/2keo}$	blood-effect site equilibration half-life
$\gamma$	parameter defining the steepness of the $E_{max}$ curve
$\alpha$	interaction parameter characterizing the influence of epidural blocked segments
SEE	standard error of the estimate
$\omega^2$	between-subject variability
ROPI	Ropivacaine Dose
eVAS	electronic Visual Analogue Scale
PNOI	Predefined Network Of Interest
AUC	Area Under the Curve
SCI	Spinal Cord Injury
MRI	Magnetic Resonance Imaging
RS-fMRI	Resting-State functional Magnetic Resonance Imaging
fMRI	functional Magnetic Resonance Imaging

TR	Repetition Time
TE	Echo Time
FSL	FMRIB's Software Library
FEAT	FMRI Expert Analysis Tool
MCFLIRT	Motion Correction by FMRIB's Linear Image Registration Tool
BET	Brain Extraction Tool
FWHM	Full Width at Half Maximum
FILM	FMRIB's Improved Linear Model
T2W	T2 weighted
T1W	T1 weighted
HRF	Hemodynamic Response Function
MNI152	Montreal Neurosciences Institute; MNI 152 is the averaging of 152 3DT1 coming from 152 different peoples
GEE model	generalized estimating equations model
GLM	General Linear Model
BOLD	Blood Oxygenation Level Dependent
COPE	Contrast Of Parameter Estimate
IPL	Inferior Parietal Lobule
MCC	midcingulate cortex
ACC	anterior cingulate cortex
SII	Secondary Somatosensory cortex
DMN	Default Mode Network
MPFC	Medial Prefrontal Cortex
S1	Primary Somatosensory cortex
M1	primary Motor cortex







